Lehrstuhl für Raumfahrttechnik
Prof. Prof. h.c. Dr. Dr. h.c. Ulrich Walter

Technische Universität München

Master Thesis

RT-MA 2019/23

Critical Parameter Management in Model-Based Systems Engineering

Author: Alexandre Luc

AIRBUS

TUM Supervisor: Daniel Pütz
Institute of Astronautics
Technical University of Munich

Airbus Supervisor: Simon Krüger
Solution Architect
TZIEA Airbus Defence&Space

Starting Date: 27/06/2019

Submission Date: 27/01/2020

Acknowledgments

This thesis becomes a reality thanks to the great support of many individuals. I wish to thank all the people whose assistance was a milestone in the completion of the project.

Foremost, thanks to **Lilian**, who made this internship possible, and whose sympathy and vision have deeply inspired me.

I wish to express my sincere gratitude to my research supervisor, **Daniel**, whose door was always open when I had questions about my research.

This work would not have been successful without the knowledge and the expertise of **Richard** and **Simon**, who were involved throughout the thesis.

My sincere thanks also go to **Hans** and **Dirk**, who facilitated my integration into the team and showed a daily interest in my work, and to **Ilya**, for his insights and his help to fix my model.

Thanks to **Airbus Defence&Space** for this great adventure. I enjoyed delving into topics that will shape the future of the aeronautics and aerospace industry.

Finally, I am grateful to the **Technische Universität München** for the quality of the teaching during my two years of master's degree.

Abstract

Aeronautical industry faces the increase of system complexity and reliability-based constraints, and in the meantime tries to reduce costs, to maximize the system performance and to improve the safety. The recent development of MBSE facilitates the transfer of models and enables to simulate the system behavior early in the development phase. In this context, the thesis aims to shape a collaborative and adaptive software environment to carry out uncertainty management on multidisciplinary aeronautical systems. Case Studies examine the implementation of a systematic CPM throughout the design process of a new commercial aircraft. This work raises the point of uncertainty-based optimization complexity and investigates different solutions to face this issue.

Most of the analytical models tackled in the thesis derive from a set of regressions suited to an Airbus commercial aircraft. While Cameo Systems Modeler supports a modular modeling, ModelCenter bridges the gap between descriptive and analytical models while ensuring a great traceability. The multi-levels simulation enabled by ModelCenter helps identifying the critical parameters from the early steps of the design process. This holistic and data-driven approach drives the product development process by eliminating non-value-added activities. The variety of sensitivity analysis tools suits any type of system complexity.

The software environment supports the implementation of an uncertainty-based multidisciplinary optimization. Non-dominated Sorting Genetic Algorithm NSGA-II highlights the tradeoff between performance optimization and cost reduction and its influence on the optimal design. Reliability-based constraints reduce the solution space and affects the final design of the aircraft by shifting the Pareto-front away from the best objective values. ModelCenter provides effective tools to face the high level of complexity of optimization under uncertainty. While the parallelization of simulations on virtual machines enhances the computational performance, DOE screening enables reducing the design space by eliminating irrelevant inputs. The conversion of multi-objective into single objective function focuses the search for optimal on a part of the global Pareto-front and significantly shortens the computing time. However, this solution requires setting up a hierarchy between the objectives and thus leaves behind non-dominated design solutions.

Although the results show the ability of this software environment to design complex systems under uncertainty, it is difficult to extrapolate a general uncertainty-based multidisciplinary design optimization workflow for various aeronautical systems at Airbus. Each design under uncertainty depends on the model complexity, the size of the design space as well as the available computational resources. Improvements of the Case Studies models are possible by refining both performance and cost functions. While models linking them to the design parameters are difficult to set up, a precise definition may capture the complete product life cycle in the design process under uncertainty.

Zusammenfassung

In der Luft- und Raumfahrtbranche steigen die Ansprüche in Bezug auf die Komplexität, die Verfügbarkeit und die Sicherheit der Systeme enorm, einhergehend mit großem Kostendruck. Jüngste Entwicklungen von MBSE-Methoden erleichtern die Kommunikation durch Modelle und simulieren das Systemverhalten bereits in frühen Entwicklungsphasen. Diese Arbeit führt ein Unsicherheitsmanagement mit der Konzeption einer kollaborativen und adaptiven Softwareumgebung an einem multidisziplinären Luftfahrtsystem durch. Anhand von Fallstudien wird die Implementierung eines systematischen CPM während des gesamten Entwicklungsprozesses eines Verkehrsflugzeuges untersucht. Dazu wurde die Komplexität unsicherheitsbasierter Optimierung mit verschiedenen Lösungsansätzen untersucht und gelöst.

Die Mehrheit, der auf Verkehrsflugzeuge von Airbus bezogenen Modelle, leiten sich aus einer Reihe mathematischer Regressionen ab. Cameo Systems Modeler unterstützt eine modulare Systemmodellierung, ModelCenter überbrückt die Lücke zwischen deskriptiven und analytischen Modellen mit hoher Nachweisbarkeit. Die Multiebenensimulation von ModelCenter ermöglicht die Identifizierung der kritischen Parameter in frühen Entwicklungsphasen. Dieser datengetriebene und integrative Ansatz eliminiert im Produktentwicklungsprozess nicht wertschöpfende Aktivitäten. Vielfältige Sensitivitätsanalysewerkzeuge eignen sich für jede Art der Komplexität.

Die Softwareumgebung unterstützt die Implementierung einer unsicherheitsbasierten Optimierung. Der NGSA-II Algorithmus zeigt ein Trade-Off-Verhältnis zwischen Leistungsoptimierung und Kostenreduzierung auf, was zu einen optimalem Produktdesign führt. Zuverlässigkeitsbasierte Randbedingungen schränken den Lösungsraum ein und wirken sich auf den Flugzeugentwurf aus, indem die Pareto-front von der objektiv besten Lösung weg verschoben wird. Während die Parallelisierung von Simulationen auf virtuellen Maschinen die Rechenleistung verbessert, ermöglicht das DOE-Screening eine Reduzierung des Entwurfsraumes durch Eliminierung irrelevanter Eingangsdaten. Die Konvertierung von Multi-Objekt-Funktionen in Einzelzielfunktionen schränkt die Suche nach dem Optimum auf einen Teil des Entwurfsraums ein und verkürzt somit erheblich die Rechenzeit. Allerdings erfordert diese Lösung die Festlegung einer Hierarchie zwischen Optimierungszielen und hinterlässt somit nicht-dominierte Lösungsansätze zur Flugzeugauslegung.

Obwohl die Softwareumgebung die Fähigkeit hat, komplexe Systeme mit Unsicherheit zu designen, bleibt es schwierig generell einen optimierten, auf Unsicherheit basierenden Arbeitsablauf für verschiedene multidisziplinäre fliegende Systeme bei Airbus zu extrapolieren. Jedes Design mit Unsicherheit hängt von der Komplexität und Größe des Modells, sowie von der verfügbaren Rechnerleistung ab. Verbesserungen des Fallstudienmodells können durch Verfeinerung der Leistungs- und Kostenfunktion erreicht werden. Während das Anbinden von Designparametern an Leistungs- und Kostenfunktion komplex ist, könnte eine präzise Definition dieser Funktionen den unsicherheitsbasierten Designprozess verbessern.

Table of Content

List of Figures

List of Figures

List of Tables

Symbols

ρ	Density	kg/m³
μ	Mean value of respective symbol	
σ	Standard deviation of respective symbol	
σ^2	Variance of respective symbol	
Λ	Angle	rad
Δ	Difference	
$\boldsymbol{g}$	Constraint vector	
$\boldsymbol{P}$	Preference matrix	ø
$\boldsymbol{p}$	Vector of system parameters	
$\boldsymbol{R}$	Reliability vector	ø
$\boldsymbol{x}$	Vector of input variables	
A	Area	m²
b	Wingspan	m
BPR	ByPass Ratio	ø
c	Chord	m
c_i	Cost factor	ø
C_p	Process capability	ø
C_{pk}	Process capability index	ø
C_z	Lift coefficient	ø

d	Distance	km
$f(\boldsymbol{x}, \boldsymbol{p})$	Objective function	
h	Height	m
L	Length	m
l	Width	m
L_{SL}	Lower Specification Limit	
M	Mass	kg
Ma	Mach number	ø
MC	Motor Characteristic	ø
min	Minimize	
p_F	Probability of failure	ø
$P(x)$	Probability mass	ø
q_i	Cost factor	ø
R	Reliability	ø
r	Correlation coefficient	ø
T	Thrust	N
t	Temperature	°C
U_{SL}	Upper Specification Limit	
V	Volume	m³
w	Weight factor	ø
Z	Altitude	m

Subscripts

amb	ambient
Fus	Fuselage
Htp	Horizontal tail plane
ini	initial
Nac	Nacelle
TO	Takeoff
Vtp	Vertical tail plane

Superscripts

L	Lower limit
U	Upper limit

Abbreviations

AMV	Advanced Mean Value
ANOVA	Analysis of Variance
BDD	Block Definition Diagram
BIC	Best In Class
BPR	ByPass Ratio
CP	Critical Parameter
CPM	Critical Parameter Management
DAKOTA	Design Analysis Kit for Optimization and Terascale Applications
DBSE	Document-Based Systems Engineering
DFSS	Design For Six Sigma
DMAIC	Define, Measure, Analyze, Improve and Control
DMADV	Define, Measure, Analyze, Design and Verify
DOC	Direct Operating Costs
DOE	Design Of Experiments
Eq.	Equation
GA	Genetic Algorithm
GUI	Graphical User Interface
I-A-M	Identify-Analyze-Mitigate
INCOSE	International Council on Systems Engineering
ISA	International Standard Atmosphere
KC	Key Characteristic

LHS	Latin Hypercube Sampling
LSL	Lower Specification Limit
MBSE	Model-Based Systems Engineering
MDO	Multidisciplinary Design Optimization
MTOW	Maximum Takeoff Weight
NACA	National Advisory Committee for Aeronautics
NSGA	Non-dominated Sorting Genetic Algorithm
OWE	Operational Weight Empty
PDF	Probability Density Function
PLC	Product Life Cycle
PPMCC	Pearson’s Product Moment Correlation Coefficient
RBDO	Reliability-Based Design Optimization
RBO	Robust Design Optimization
RSM	Response Surface Modeling
SA	Sensitivity Analysis
SLS	Sea Level Standard
SOI	System Of Interest
s.t.	subject to
SysML	Systems Modeling Language
TOFL	Takeoff Field Length
UMDO	Uncertainty-based Multidisciplinary Design Optimization
USL	Upper Specification Limit
WIC	Worst In Class

1 Introduction

1.1 Motivation

In recent years, Systems Engineering has undergone major changes. The development of new IT tools, types of modeling, and the desire to standardize processes, have contributed to the development of Model-Based Systems Engineering (MBSE). This approach can replace Document-Based Systems Engineering (DBSE). Popularized by the International Council on Systems Engineering (INCOSE) in 2007, the MBSE methodology focuses on the maturation of standardized models to simplify the collaborative work between engineers working on a common project.

In the modern world, quick growth of new technologies and rising system complexity create new challenges. In order to overcome challenges like flexibility, modularity and automation, the manufacturing industry must change. Thus, the design process of new systems must be optimized in an environment with numerous and conflicting constraints, while ensuring a certain level of quality, robustness and reliability. While performance indicators must be optimized, particular attention should be paid to reducing development and operating costs. Most current development methods are based on basic safety factors for uncertainty modeling. This approach results in designs that meet the requirements but remain conservative and therefore tends to be overdesigned and expensive solutions.

The new MBSE standards for traceability improvement over complex system architectures seem to be suited to identify the critical design parameters leading to performance variation, especially in the aeronautics field. The better understanding of the uncertainty propagation is a prerequisite for performing reliable and robust multi-objective optimization. The monitoring of uncertainty during the development phase of new complex systems might drive to noticeable cost reductions.

1.2 State of the art

The topic of variation and uncertainty that are linked to the manufacturing and assembly of complex technical systems is not a new one. Indeed, starting with Toyotism in the mid-20th century (Lupan et al. 2005), companies have been seeking to increase the quality of manufactured products, and thus reduce waste.

Progressively, specification limits have been introduced for components parameters such as mass or geometrical characteristics (Choudri 2004). The standard deviation of the design parameters must be controlled to ensure that the manufactured components fall within the specification interval. Specific statistical tools and methods are implemented to illustrate the production characteristics and quantify the manufacturing uncertainty. The functional distribution of the design parameters is commonly approximated by a Gaussian statistical model (Thornton 2003).

Design methods like Design For Six Sigma (DFSS) aim to certify the final quality of the product (Bubevski 2018) and many procedures such as Define, Measure, Analyze,

Improve and Control (DMAIC) (Shahin 2008) or Define, Measure, Analyze, Design and Verify (DMADV) (Feo and Bar-El 2002) are emerging to help reach high production standards. Companies like Raytheon, Motorola and General Electrics played a central role in the advancement of the DFSS in the industry during the last decade (Mackertich et al. 2017; Lupan et al. 2005: 724).

In recent years, the transition from DBSE to MBSE has helped to centralize information in a single document (Friedenthal 2015) and thus facilitated data transfer between working teams (NDIA 2011). This modeling configuration facilitates the simulation of complex systems and therefore the mastering of uncertainty propagation by ensuring traceability of the variables across the system levels (Friedenthal et al. 2009).

Estefan (2008) provides some examples of successful MBSE methodologies in the industry such as IBM Telelogic Harmony-SE and Vitech MBSE Methodology. In the context of ESA-Airbus cooperation, Estable et al. (2017) set up a new MBSE process called “Federated and Executable Models”. This method intends to contribute to the development of a multi-disciplinary process to standardize the design phase of new systems with a holistic approach. INCOSE's Vision 2025 foresees an improved integration of stakeholders in MBSE processes and an expansion into new areas (Beihoff et al. 2014; INCOSE 2014).

Furthermore, Critical Parameter Management (CPM) seeks to identify and control key characteristics, the variation of which leads to risks in terms of performance, costs or safety for the global system (Thornton 2003; Narayanan and Khoh 2008). This new variation management method is highly successful in the industrial world, and increases the reliability and robustness of new systems (Shahin 2008; Vrinat 2007). Increasing computational resources, as well as investments coming from the involved companies, encourage the refinement and progress in this research subject (Koch et al. 2004).

However, this methodology is most effective when implemented early in the design phase of a new product, but access to models and data is relatively complicated at this stage of development (Thornton 2003). Furthermore, the global uncertainty does not derive only from the variation in production, but also from the model, the equations and the simulation approximations during the analytical processing. The uncertainty propagation remains a very complex field, difficult to extrapolate on further models and highly dependent on the systems under study and their specific uncertainties (Zaman et al. 2011; Du 2002).

Finally, the sensitivity analysis (SA) methods are essential to perform Uncertainty-based Multidisciplinary Design Optimization (UMDO). Different mathematical models exist to perform Reliability-Based Design Optimization (RBDO) as well as Robust Design Optimization (RDO) (Yao et al. 2011; Keane and Nair 2005). Krüger et al. (2015) propose a method to deal with multiple functions optimization. While mathematical systems of equations to perform UMDO are common (Yao et al. 2011), the computational complexity and the lack of acceptation in the community slow down its implementation in companies (Zang et al. 2002). Zang et al. (2002) insist however

on the necessity to seek uncertainty based design methods for the development of new aerospace vehicles.

1.3 Research questions

Regarding the state of the art and Airbus expectations, a list of research questions is defined for the project:

- Is it possible to use the critical parameter management in a multi-level sensitivity analysis to define which elements in the system decomposition need an improved modeling or which parameters need to have a tight tolerance?
- How can uncertainty quantification and sensitivity studies drive the product development process with the goal of reducing overall lead-time by eliminating non-value-added activities?
- Is there a suitable remedy to overcome computational resource limitations affecting the uncertainty-based multidisciplinary design optimization?
- Is it possible to come up with a generic approach of CPM and uncertainty-based multidisciplinary optimization for various aerospace and aeronautical projects at Airbus?

1.4 Structure of the work

Chapter 2 focuses on the theoretical background regarding Critical Parameter Management, Sensitivity Analysis and design under uncertainty, in order to introduce the required tools and methods for the thesis.

After describing the software used in the thesis as well as the interaction between Cameo Systems Modeler and ModelCenter, Chapter 3 shapes a collaborative software package to carry out design under uncertainty. Different flowcharts are developed in order to implement CPM and UMDO in the software environment at successive steps of the product life cycle.

Case Studies of Chapter 4, 5 and 6 rely on the process flowcharts defined in Chapter 3 to design a reliable commercial aircraft system. While Chapter 4 carries out a systematic CPM process to drive the design of the new aircraft from the early steps of the development process, Chapters 5 and 6 analyze the influence of the reliability-based constraints on the aircraft design optimization. These concrete examples afford to compare the SA methods identifying the critical parameters on ModelCenter and to find out solutions to handle multidisciplinary system complexity. For each Case Study, the system modeling and analysis is performed while keeping in mind the following aim: evaluate the viability of integrating this collaborative package to more complex aeronautical systems.

Figure 1-1 summarizes the different steps of the thesis.

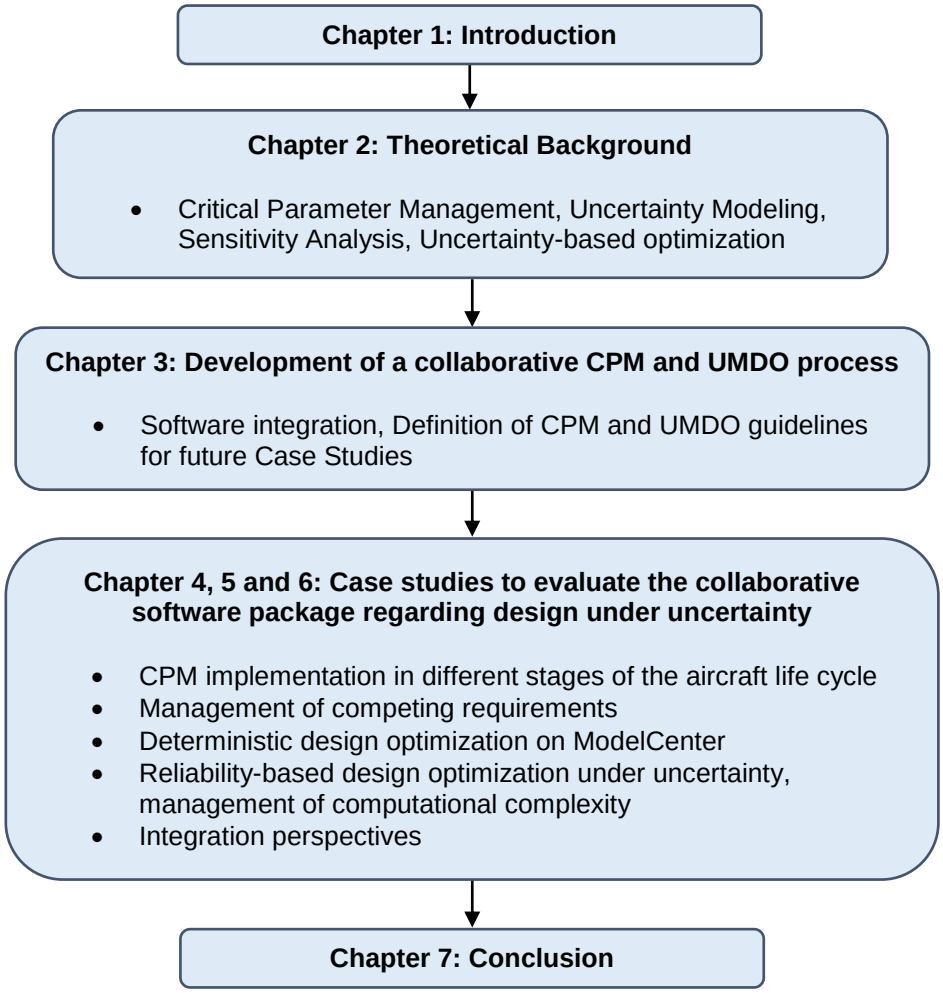

Figure 1-1: Structure of the work

2 Theoretical Background

This chapter introduces the different technical tools that will be useful to implement a CPM process in the Case Studies of the following chapters.

After briefly presenting the CPM methodology, this section emphasizes the uncertainty modeling tackled in the literature, provides a review of the sensitivity analysis methods and finally focuses on the uncertainty-based design optimization.

2.1 Critical Parameter Management

2.1.1 Necessity of Variation Monitoring

While quality control methods such as the Six Sigma Standard exist in the context of the DFSS, companies seek to go further in the monitoring of variation management (Choudri 2004). DFSS aims to shift the knowledge about the system toward earlier steps of the development process, when the design configuration is still flexible (Figure 2-1). This shifting may help reducing the lead-time and therefore saving costs during the product development phase (Figure 2-2) (Cao et al. 2018: 3055).

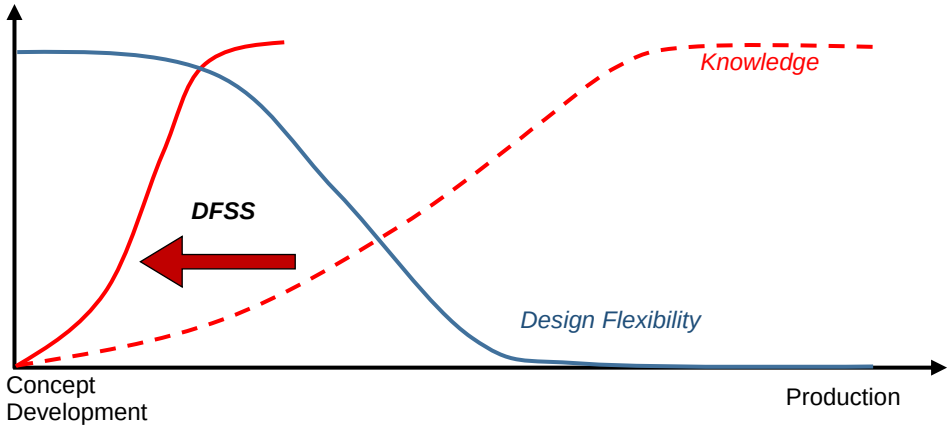

Figure 2-1: Shifting System Knowledge toward earlier steps of Product Design Process (Choudri 2004)

In his review of DFSS implementation in world-class companies, Shahin (2008) insists on the key idea of shifting from a reactive to a proactive management of uncertainties. Several standardized methodologies and approaches are proposed by the industry to reach the Six Sigma Quality Standard and ensure the production of a reliable and robust system, among which CPM. The structural and analytical modeling of the system allows the management of uncertainty propagation impacting the top-level performances (Vrinat 2007).

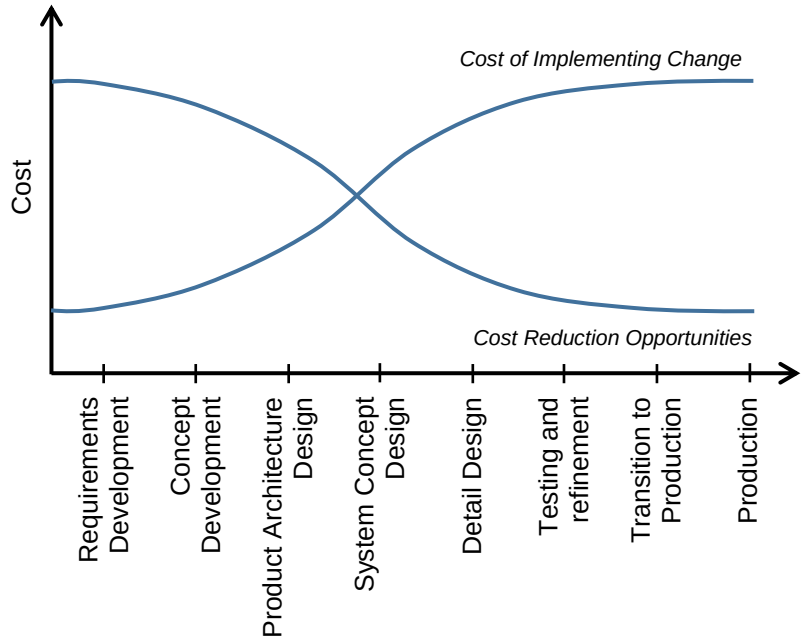

Figure 2-2: Representation of the cost of change and of the cost reduction opportunities throughout the product development (Thornton 2003: 6)

2.1.2 Key Characteristics

CPM aims to identify the critical parameters (CP) that contribute to variation in customer requirements. CP are called Key Characteristics (KC) in the literature too. Thornton (2003) provides the following definition:

«A key characteristic is a quantifiable feature of a product or its assemblies, parts, or processes whose expected variation from target has an unacceptable impact on the cost, performance or safety of the product.» (Thornton 2003: 35)

The list of KC evolves along the product development. As soon as the impact of a KC on the system performance is monitored, the parameter is removed from the list (Whitney 2004). Parameters from different system levels may contribute to variation in system performances. The CPM therefore requires breaking down the structure of the system to the component level.

2.1.3 Flowchart Critical Parameter Management

Literature sources agree about the classic flowchart of a CPM implementation. Vrinat (2007) and Mackertich and Kraus (2012) describe a two-step modeling of the system: the creation of the structural tree in a first step and then the creation of the analytical tree.

The CPM analysis starts with the structural decomposition of the system. This work begins with an exhaustive requirement analysis in order to formalize the Voice of Customer (Du et al. 2012). Then, the structural tree is created, breaking down the global system into sub-systems to the component level. From the top-level requirements derive technical requirements as well as product specifications on the

different levels of the structural tree (Narania et al. 2008: 1076). This top-down process may be difficult to carry out, as it requires anticipation and imagination when the system is new (Whitney 2004).

In a second time, the analytical tree is progressively built up by defining the transfer functions between lower and upper system levels, starting with the component level. The flowchart of Figure 2-3 illustrates the modeling process. X stand for the input parameters of the analytical tree, while Y represent outputs which derive from the input values. The statistical flow-up of uncertainties coming from the design, the manufacturing and the assembly reveals both risks and opportunities of the system.

Information about previously designed and manufactured products can facilitate the modeling process of the CPM (Whitney 2004).

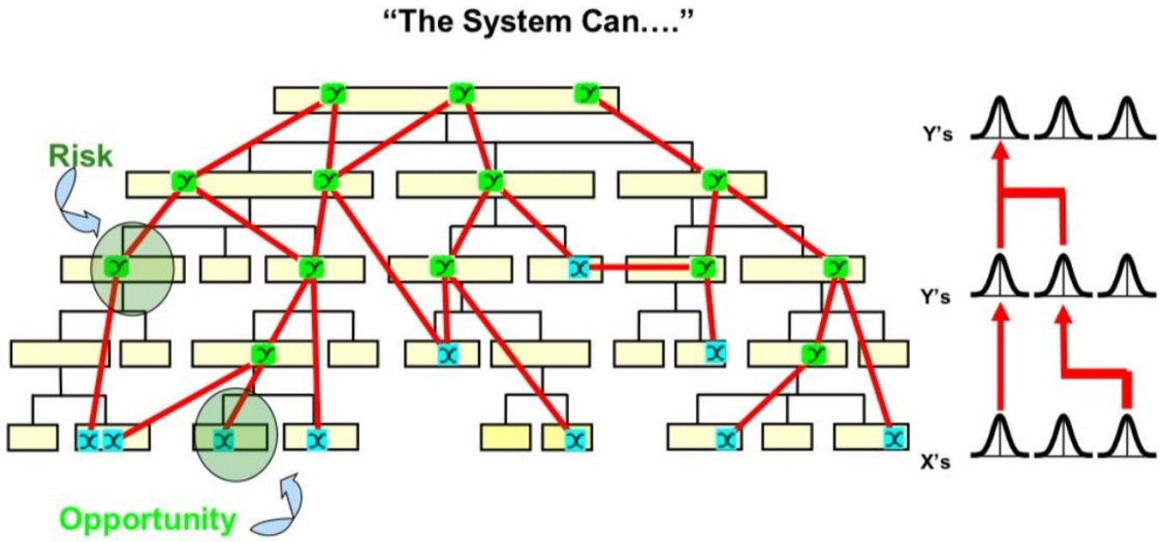

Figure 2-3: Statistical Flow-Up of Design and Manufacturing Uncertainties revealing both Risks and Uncertainties (Mackertich and Kraus 2012)

Once the modeling is complete, the variation management can begin. Thornton (2003) and Narania et al. (2008) describe an Identification, Assessment and Mitigation (I-A-M) process that can be applied to systems in production as well as proactively to systems in early steps of the development process. The flowchart involves the identification, ranking and updating of the KC list and the search for solutions to ensure the correct functioning of the system.

Different key concepts are relevant while implementing CPM to a system. The CPM process must be:

- Holistic: The study must analyze the influence of the parameter variations on the global system in terms of performance, cost and safety, and not only just on a part of it. The propagation of uncertainties across system levels and their combination must be studied (Thornton 2003).

- Traceable: In the context of MBSE, CPM must ensure the traceability of the components and of the variables between the different models of the descriptive

and analytic structures (Ramos et al. 2012). This property is essential to perform multi-levels simulations and have a direct interaction between the requirement definition, the system design and the requirement validation simulations.

- Data driven: The assessment of critical parameters during the sensitivity analysis requires quantifiable results to compare and rank the contribution of inputs to the system variation (Vrinat 2007). Therefore, the uncertainty modeling must introduce parameters and variables to quantify the variation occurring on the different system levels. Data coming from previous systems may help ensuring the data driven property of the CPM applied to new systems.

Finally, CPM requires a data-driven uncertainty modeling of the system to propagate the design and manufacturing variations through the analytical tree and gain in knowledge about the KC. However, the lack of data about the system limits the assessment detail in the early steps of the product development (Figure 2-4). CPM perspectives aim to mitigate risks from the beginning of the design phase despite limited knowledge about the system (Narania et al. 2008).

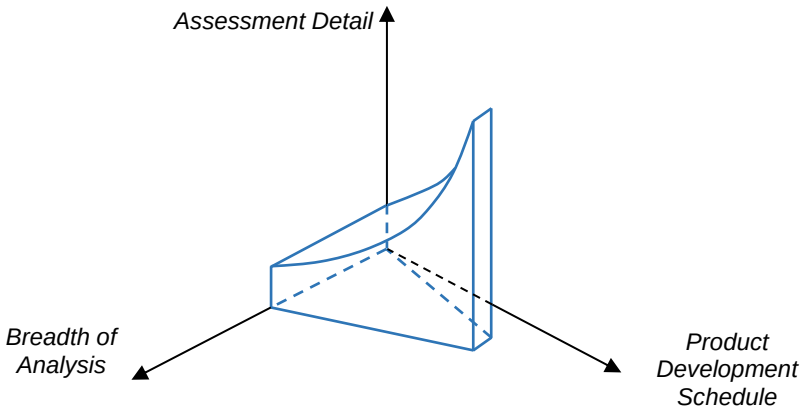

Figure 2-4: Assessment breadth and detail in product development (Thornton 2003: 22)

2.2 Uncertainty Management

In order to propagate the variation coming from design and manufacturing during the CPM, an uncertainty model must be defined beforehand. The definition of the uncertainty concept varies in the literature depending on the engineering field. While DeLaurentis and Mavris (1970) propose a functional definition specific to the aerospace engineering, Yao et al. (2011) define it from the perspective of systems engineering and consider the whole Product Life Cycle (PLC) of the system. According to them, uncertainty is «the incompleteness in knowledge and the inherent variability of the system and its environment.» (Yao et al. 2011: 452)

2.2.1 Types of Uncertainty

There are two main categories of uncertainties. While statistical uncertainties cannot be avoided, systematic uncertainties can be reduced thanks to a better understanding of the system (Yao et al. 2011; Zaman et al. 2011).

One of the sources of complexity in the study of a multidisciplinary system is the diversity of the sources of uncertainties involved and coming from different engineering fields (Du 2002). According to different literature sources, a non-exhaustive list is drawn up:

- Manufacturing Variation: «Variation is a physical result of manufacturing processes: Parts and assemblies that are supposed to be identical actually differ from each other and from what we want them to be.» (Whitney 2004: 112) Unit-to-Unit variation arise in each component production. Manufacturing and assembly processes introduce a statistical uncertainty into the system structure (Thornton 2003).

- External noise factors: Environmental conditions such as temperature influence the system performance (Zaman et al. 2011). The effects can be minimized but not totally suppressed. The manufacturer can however notify the customer not to use the product under certain external conditions in order to prevent situations that might be risky for the system.

- Modeling Uncertainty: By definition, a model is a simplified representation of the reality. The conversion of the real world system into a virtual one leads to approximations and systematic uncertainties in the system model (Yao et al. 2011; Du 2002).

- Computing Uncertainty: In simulation-based designs, approximations and discretization errors may occur while computing the transfer functions (Yao et al. 2011: 455). The consideration of several disciplines in the context of multidisciplinary system design amplifies this kind of uncertainty, as outputs of one discipline are inputs for other ones (Du 2002: 546).

2.2.2 Uncertainty Modeling

Since the CPM must be data-driven, the system requires a mathematical uncertainty modeling. Du (2002) brings the uncertainty into the analytic model as follows: the output result sums up the simulated output and an epsilon function which captures the modeling uncertainty (Eq. (2-1)):

$$z = F(\boldsymbol{x}) + \epsilon(\boldsymbol{x}) \qquad \textbf{Eq. (2-1)}$$

z is the output, $\boldsymbol{x}$ the input vector, $F(\boldsymbol{x})$ the simulated output and $\epsilon(\boldsymbol{x})$ the modeling uncertainty.

Zang et al. (2002) introduce three models to describe the uncertainty of the parameters at stake in the system model (Figure 2-5). Interval bound, membership function and Probability Density Function (PDF) provide increasing information about a parameter uncertainty. Mathematical formalism of PDF is explained by Blitzstein and Hwang (2015) (p.196).

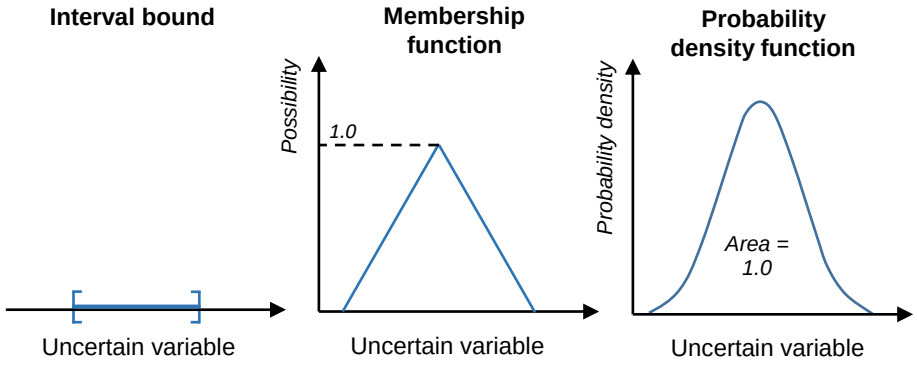

Figure 2-5: Uncertainty description of input parameters (Zang et al. 2002: 7)

Most of the time, PDF describes parameter uncertainty. Mean and standard deviation values provide good indications about the uncertainty coming from a parameter.

The Gaussian distribution is the most common PDF to model variations coming from the design, the manufacturing and the assembly. Parameters are more likely to take values nearby the mean, the greater the distance between a value and the mean, the lower the probability for the parameter to equal it (Blitzstein and Hwang 2015).

Appendix B.1 describes the PDF implemented in the thesis.

2.2.3 Uncertainty Analysis Tools

Specification limits are thresholds delimiting the valid space of a parameter (Figure 2-6). LSL and USL refers to Lower Specification Limit and Upper Specification Limit, respectively. «Tolerance refers to the amount of variation that we can tolerate in a part or assembly.» (Whitney 2004: 112) It corresponds to the size of the interval between LSL and USL. A part which dimension lies outside the allowable tolerance is called defect.

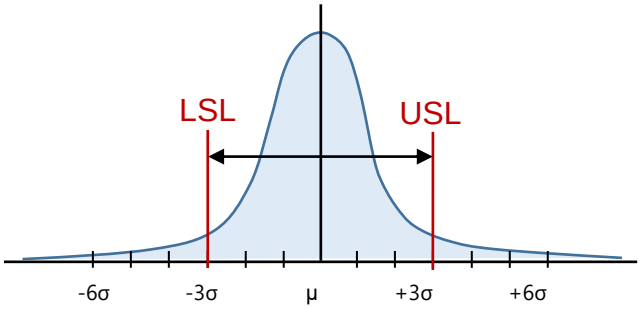

Figure 2-6: Normal distribution, 3-σ design (Koch et al. 2004: 238)

The Six Sigma Quality Standard of DFSS stands for six standard deviations between the mean of the distribution of the produced part and the closest specification limit, either USL or LSL. For information, such confidence interval represents only 3 defects every million parts produced (Lupan et al. 2005).

From the definition of the specification limits of a parameter and its PDF characteristics, i.e. its mean and standard deviation, it is possible to control the parameter uncertainty and to assess the production quality (Narayanan and Khoh 2008).

The process capability C_p and the process capability index C_{pk} (Eq. (2-2) and Eq. (2-3)) depend on the part specifications, mean value and standard value. It measures how well the manufacturing creates parts falling inside the specification interval (Bubevski 2018: 1–2). C_{pk} is an adjustment of C_p for the effect of non-centered distributions.

$$C_p = \frac{U_{SL} - L_{SL}}{6 \cdot \sigma} \qquad \textbf{Eq. (2-2)}$$

$$C_{pk} = \min\left(\frac{U_{SL} - \mu}{3 \cdot \sigma}, \frac{\mu - L_{SL}}{3 \cdot \sigma}\right) \qquad \textbf{Eq. (2-3)}$$

C_p and C_{pk} can evaluate both short and long term capabilities (Bubevski 2018; Maass and McNair 2010). Short-term capability evaluates the quality of a manufacturing process under control over a short period of time. Long-term capability considers several manufacturing process shifts. Distribution function may change throughout the production due to machine breakdown for instance. The process capability decreases then (Figure 2-7). According to DFSS, long-term process capability index can be calculated by adding a 1.5σ mean shift to the PDF (Thornton 2003).

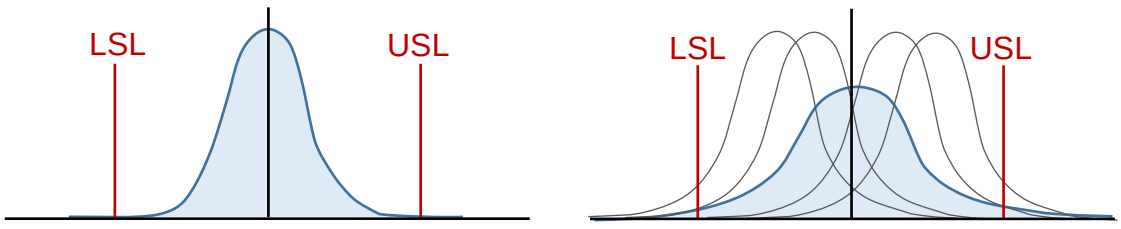

Figure 2-7: Short-Term and Long-Term Capability (Thornton 2003: 31)

Probability of failure p_f is defined from the reliability function R and represents the fraction of products which do not fall within the tolerance (Eq. (2-4) and Eq. (2-5)) (Yao et al. 2011).

$$R = \int_{L_{SL}}^{U_{SL}} P(x) \cdot dx \qquad \textbf{Eq. (2-4)}$$

$$p_f = 1 - R \qquad \text{Eq. (2-5)}$$

2.2.4 Uncertainty Propagation

Once the PDF of input parameters are defined, the transfer functions of the analytic model can propagate the uncertainty toward upper levels of the analytical tree. A probabilistic analysis allows assessing the PDF of the top-level performances. Several types of probabilistic analysis exist and Part 2.3 tackles some of them.

The input parameters interact with each other and the combination of their variation leads to uncertainty of the output. Design under uncertainty aims to chose a design for its reliability-level, and not only its mean performance (Figure 2-8) (Yao et al. 2011).

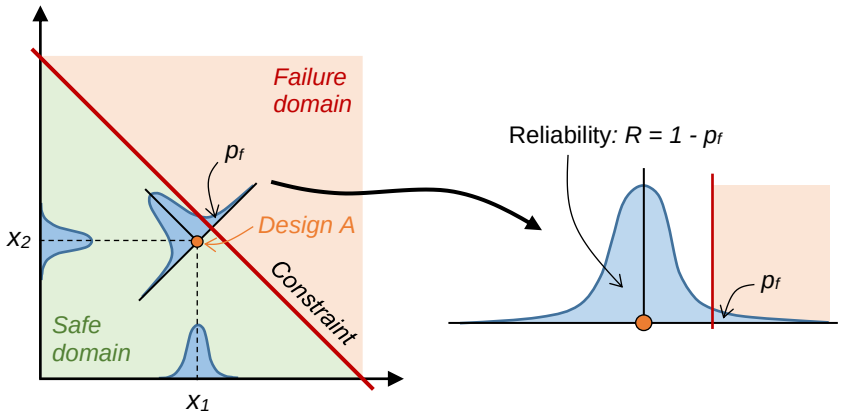

Figure 2-8: Graphical representation of uncertainty propagation and reliability analysis (Yao et al. 2011)

In manufacturing, since the assembly relies on the relative positioning of the different parts which commonly follow a Gaussian distribution, the Central Limit Theorem states that the distribution of the assembly component will tend to a normal distribution (Rohatgi and Saleh 2015: 321; Whitney 2004).

2.3 Sensitivity Analysis

Sensitivity analysis aim to investigate the influence of the input parameters on the output variations. They are implemented in the CPM process once the structural and analytical models as well as the uncertainty model of the system are established. Lots of SA tools exist, the choice of the method depends directly on the complexity and the properties of the system (Bilal 2016).

2.3.1 Goals Sensitivity Analysis

In a SA, the objective function linking inputs and outputs is considered as a black box (Morio 2011). Probabilistic analysis as well as Design Of Experiments (DOE) are statistical tools performing SA and providing information about this black-box.

Brevault et al. (2013) enumerate the goals of performing SA:

- Highlight the critical parameters, variation of which affects the output reliability.
- Identify parameters that have no significant influence on the output.
- Evaluate interactions between different input parameters.
- Identify the input configurations maximizing the variation of the output.

The assessment detail of SA methods depends on the goal of the analysis. On the one side, screening methods aim to reduce the dimensionality of the problem. Parameters that have no influence on the output variation are removed from the probabilistic analysis (Narania et al. 2008). On the other side, characterization methods seek to identify KC and the relevant parameter interactions (Khan 2013) and need more function evaluations than the screening methods.

2.3.2 Sampling Methods

The sampling method of a SA defines the process of selection of input vectors for which the output is calculated. The most commonly used sampling methods are:

- Random sampling: The input samples are totally random and the value of each input parameter derives from its PDF (Mckay et al. 1979). The Monte Carlo simulation method uses random sampling to study properties of systems with components that behave in a random fashion. The idea is to simulate the behavior of a system by randomly generating the input parameters according to their PDF. Quasi Monte Carlo is a low discrepancy method based on the Monte Carlo method but proposing a more uniform sampling of the design space (Lemieux 2009).

- Stratified sampling: The stratified sampling involves the decomposition of the sample space into sub-spaces called strata. This method ensures the populating of each strata during the sampling and also samples more uniformly the design space (Mckay et al. 1979).

  The Latin Hypercube Sampling (LHS) method stratifies the sampling spaces of all random variables (Figure 2-9). Ba and Joseph (2011) propose an extension of the LHS to perform a more efficient sampling method.

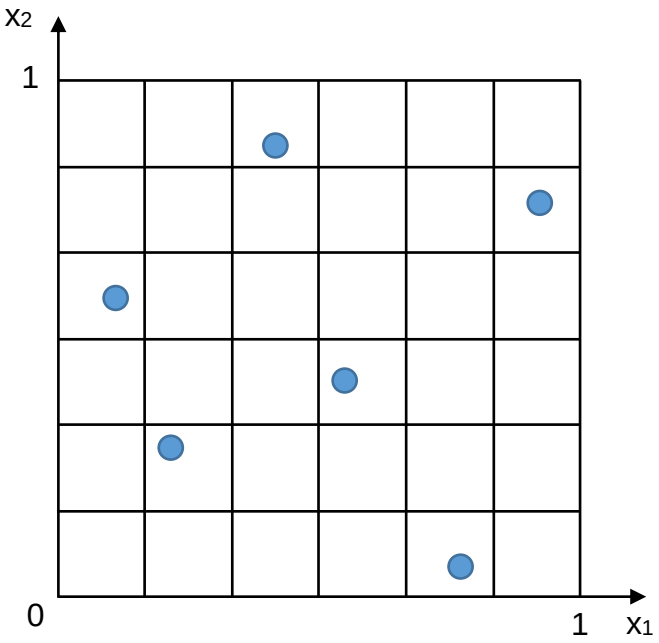

Figure 2-9: A Latin Hypercube Sample with two random variables distributed uniformely on [0;1] and a sampling of six input vectors (Stein 1987: 144)

- Non-probability sampling: Sampling technique, which is not random-based. The input samples are chosen. Full factorial design confers several levels to each input variable and evaluates the output of all combinations between the levels of each variable (Khan 2013: 408–9). Most of the time, the higher and lower levels of variables are defined by the values +1 and -1, respectively.

  While full fractional design provides a good understanding about the main effects and the interactions between the variables, the complexity is exponential and the implementation is not suited for systems with too many variables.

  Fractional factorial design reduces the complexity of the full fractional design by evaluating only a subset of the samples (Figure 2-10). Confounding occurs because several combinations of the full factorial design are not studied, the analysis of variables interactions is limited (Barton 1999: 55).

  Hirsch et al., eds. (2019) delve deeper into the non-probability sampling with the Polynomial Chaos Expansion and Levy and Steinberg (2010) develop new space filling designs to improve the DOE screening.

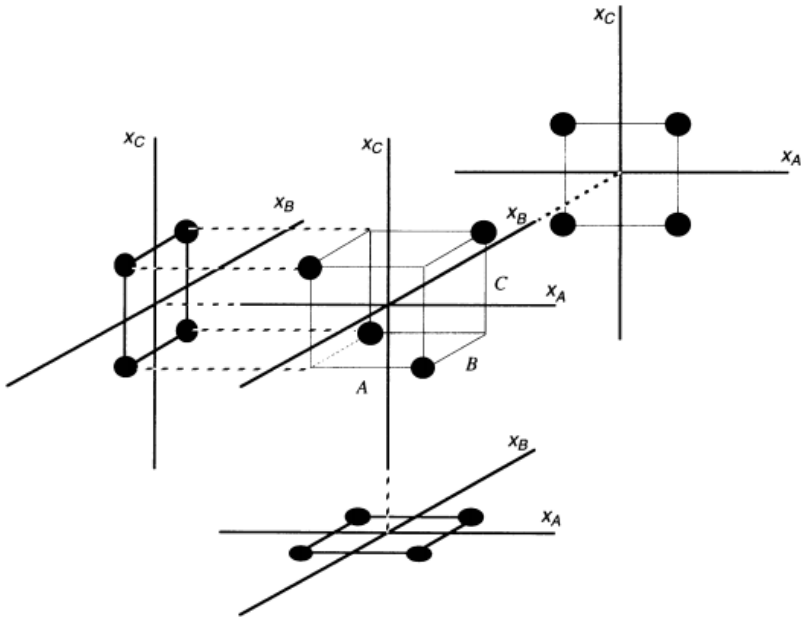

Figure 2-10: 2^{3-1} fractional factorial design, projection of each effect on the remaining factors, resulting in 3 full factorial designs (Barton 1999: 65)

The choice of the sampling method depends on the system complexity and on the expectations of the SA. While Monte Carlo provides the most accurate results, the method requires a great number of runs. LHS and Fractional Factorial Design may require less runs but only provide a screening of the design space. For complex systems with many variables, a screening method like fractional factorial design can extract a rough group of KC and reduce the complexity of the system. A characterization method like Monte Carlo can then refine the list of KC.

2.3.3 Sensitivity Analysis Methods

Brevault et al. (2013) compare different sensitivity analysis methods for aerospace vehicle optimal design. Several sensitivity indices definitions exist, depending on the implemented SA method. The following categorization of SA methods is proposed:

- Variance decomposition methods: Different sensitivity calculations arise from the ANOVA (Analysis of Variance) decomposition of variance (Archer et al. 1997: 103–7). ANOVA by Sobol approach introduces Sobol sensitivity indices which quantify the contribution of each input variation on the output variance (Lamboni et al. 2012; Dimov et al. 2013). ANOVA by DOE approach is suited for discrete input factors.

- Differential Analysis: Differential Analysis is a local SA assessing the effect of a small shift of an input variable from its initial value on the output (Morio 2011). Morris method is based on the one Factor At a Time method and assesses the impact of single variable variation on the output (Alam et al. 2004).

- Linear relationship measures: A linear function approximates the transfer function. Sensitivity measures directly derive from the coefficients of the Standardized Regression and assess the contribution of the input variables on the output variation (Brevault et al. 2013).

Table 2-1 captures the strengths and weaknesses of the SA methods tackled by Brevault et al. (2013):

Table 2-1: Comparison and evaluation of diverse SA methods (Brevault et al. 2013)

	Linear Functions	Non Linear Functions	Quantitative analysis	Input factors interaction	Computational effort	Sample size until convergence	Ease of implementation
ANOVA by Sobol approach	🟢	🟢	🟢	🟢	🔴	🔴	🔴
ANOVA by DOE	🟢	🟢	🟢	🟢	🟡	🔴	🟢
Standardized Regression Coefficients	🟢	🔴	🟢	🟡	🟢	🟢	🟢
Morris	🟢	🟢	🔴	🟡	🟢	🟢	🟡

In addition to the sensitivity analysis results, providing insights about the variation propagation across the system, correlation coefficients may be useful to assess the dependency between system variables, either two inputs or one input and one output. The correlation scale differs between the domains and the models. There is no absolute valuation of the correlation, but the relative comparison between the coefficients provide useful results about the interactions (Akoglu 2018).

Pearson's Product Moment Correlation Coefficient (PPMCC), Spearman's rho and Kendall's tau are the common statistical tools to illustrate the dependency between two random variables. Eq. (2-6), Eq. (2-7) and Eq. (2-8) define these three coefficients (Xu et al. 2010). Coefficients fall within the interval [-1 ; 1], 1 and -1 correspond to a positive and negative linear correlation between the random variables, respectively. The higher the dependency between two random variables, the greater the correlation coefficient. Kendall's tau and Spearman's rho are more robust than PPMCC against outliers (Abdullah 1990; Xu et al. 2010).

Pearson's product moment correlation coefficient r_P:

$$r_P(X_i, Y_i) := \frac{\sum_{i=1}^{n}(X_i - \bar{X}) \cdot (Y_i - \bar{Y})}{[\sum_{i=1}^{n}(X_i - \bar{X})^2 \sum_{i=1}^{n}(Y_i - \bar{Y})^2]^{1/2}} \quad \textbf{Eq. (2-6)}$$

Spearman's rho r_S:

$$r_S(X_i, Y_i) := 1 - \frac{6\ \sum_{i=1}^{n}(P_i - Q_i)^2}{n(n^2 - 1)} \quad \textbf{Eq. (2-7)}$$

Kendall's tau r_K:

$$r_K(X_i, Y_i) := \frac{\sum_{i \neq j=1}^{n} sgn(X_i - X_j) \cdot sgn(Y_i - Y_j)}{n(n-1)} \quad \textbf{Eq. (2-8)}$$

$\{(X_i, Y_i)\}_{i=1}^{n}$ stands for n independent and identically distributed data pairs drawn from a bivariate population with continuous joint distribution. P_j is the rank of X_j among $X_1, \dots, X_n$ and Q_j is the rank of Y_j among $Y_1, \dots, Y_n$. $\bar{X}$ and $\bar{Y}$ represent the arithmetic mean values of X_i and Y_i. $sgn(.)$ returns +1 if the argument is positive, and -1 otherwise.

Finally, the multiple sensitivity measures, DOE analysis, correlation coefficients and process capabilities form a pool of useful tools to assess the KC. Figure 2-11 summarizes the different steps of a global SA (Idriss et al. 2018).

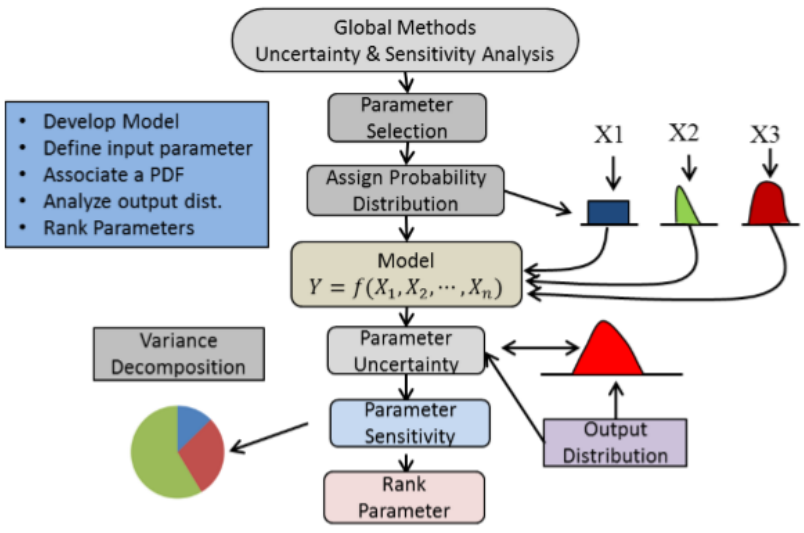

Figure 2-11: Schematic for global sensitivity analysis according to Idriss et al. (2018)

2.3.4 Mitigation Strategies

The Mitigation phase is the last step of the I-A-M process to implement a CPM and aims to reduce parameter variation or its impact on the top-level performances of a system.

In some cases, several KC are in conflict: the improvement of one KC automatically leads to the deterioration of another one (Whitney 2004: 224). In this configuration, Thornton (2003) proposes to set up a hierarchy between the performances and the requirements evaluated. The mitigation of KC related to the less reliable performances is prioritized over the others. The mitigation strategy is much easier when the KC are independent.

The process capability knowledge as well as the results of the statistical analysis drive to the assignment of new tolerances for the key characteristics, in order to lower the risks in terms of performance, safety and costs (Mackertich and Kraus 2012).

Figure 2-12 illustrates two mitigation strategies for increasing the reliability of a performance: The shift of the PDF away from the specification limit and the shrink of the PDF (Koch et al. 2004: 247). To achieve such changes, engineers can decide to improve the accuracy of the model and of the production for instance, or change the design and the technical solutions of the system if it does not drive to high investment costs.

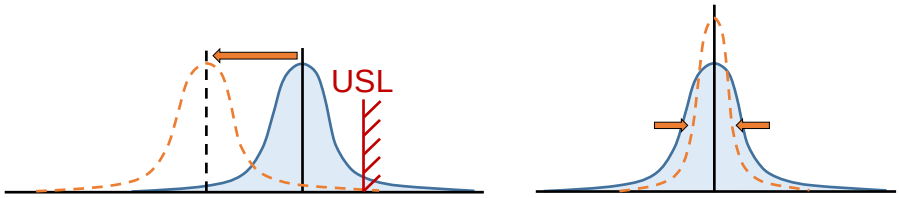

Figure 2-12: Mitigation strategies (Koch et al. 2004: 238)

2.4 Uncertainty-Based Multidisciplinary Design Opitimization

During the development process of a new system, engineers seek to optimize the performance and minimize the costs. However, the complexity of aerospace systems makes the optimization process difficult (Brevault et al. 2013). Multidisciplinary Design Optimization (MDO) intends to improve a system regarding all the domain fields concerned (Yao et al. 2011).

«[…] optimization algorithms tend to search for “peak” solutions, ones for which even slight changes in design variables and uncontrollable, uncertain parameters can result in substantial performance degradation. In this case the “optimal” performance is misleading: worst-case performance could potentially be much less than desirable and failed designs could occur.» (Koch et al. 2004: 235)

In order to achieve reliable systems, the optimization process should not consider optimal performance as the only objective while seeking to optimal design, but also examine the reliability of the solution. Therefore, in the context of CPM and DFSS,

uncertainty propagation across the system needs to be tackled during the optimization process. UMDO refers to Uncertainty-based Multidisciplinary Design Optimization.

2.4.1 Robust and Reliability-Based Design Optimization

In their review of UMDO for aerospace vehicles, Yao et al. (2011) tackle the concepts of robustness and reliability. On the one side, robustness characterizes the ability of a system to perform great despite small variations of the system parameters or of the environment. On the other side, the reliability regards the extreme behaviors of the system in performance. A reliable system performs consistently great despite the various sources of uncertainty affecting it.

The reliability and robustness concepts are easily transposable to optimization studies. While RBDO stands for Reliability-based Design Optimization, RDO refers to Robust Design Optimization. Figure 2-13 illustrates the difference between a deterministic optimization and a RDO.

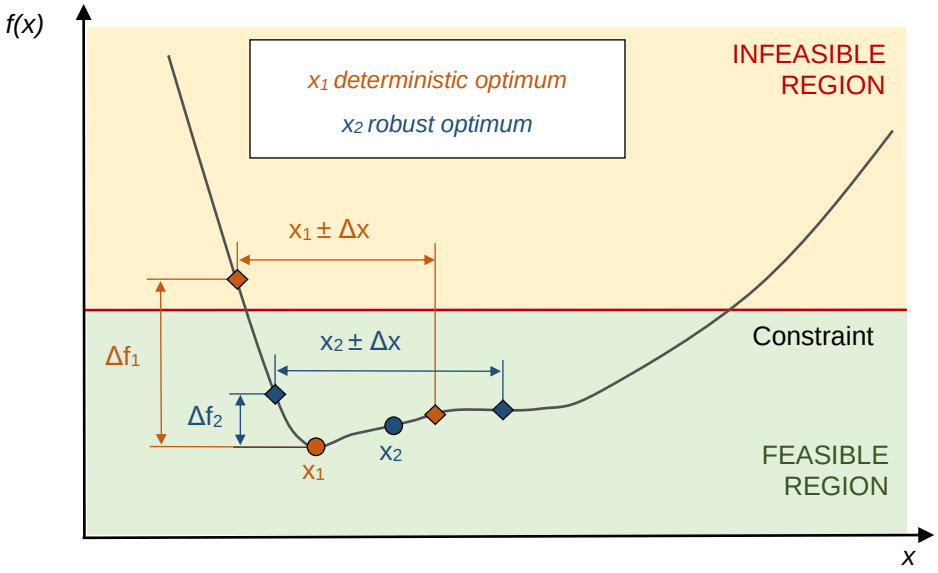

Figure 2-13: Graphical representation of RDO (Yao et al. 2011: 453)

In opposition to a standard deterministic optimization system (Eq. (2-9) to Eq. (2-11)), the RDO system introduces the uncertainty in the definition of the objective function (Eq. (2-12) to Eq. (2-14)). The robustness of the system becomes in this way a decisive factor in the search for the optimal design. The RBDO converts the deterministic constraint into a reliability-based constraint (Eq. (2-15) to Eq. (2-17)) The reliability vector $\boldsymbol{R}$ is introduced to fix reliability thresholds for the different constraints of the problem. Under the consideration of uncertainty, a design is feasible if the probability of the system to satisfy the constraint is greater than a certain level. Padmanabhan et al. (2006) provide more details about RBDO as well as efficient methods to implement it based on Monte Carlo simulations.

Deterministic optimization system:

$$\min_{\boldsymbol{x}} f(\boldsymbol{x},\boldsymbol{p}) \qquad \textbf{Eq. (2-9)}$$

$$subject\ to\ (s.t.)\quad \boldsymbol{g}(\boldsymbol{x},\boldsymbol{p}) \leq \boldsymbol{0} \qquad \textbf{Eq. (2-10)}$$

$$\boldsymbol{x}^L \leq \boldsymbol{x} \leq \boldsymbol{x}^U \qquad \textbf{Eq. (2-11)}$$

$\boldsymbol{x}$ and $\boldsymbol{p}$ are the array of design variables and of parameters, respectively. f is the objective function and $\boldsymbol{g}$ the constraint vector. $\boldsymbol{x}^L$ and $\boldsymbol{x}^U$ delimit the range of the design space for the variables.

RDO system:

$$\min_{\boldsymbol{x}} F\left(\mu_f(\boldsymbol{x},\boldsymbol{p}), \sigma_f(\boldsymbol{x},\boldsymbol{p})\right) \qquad \textbf{Eq. (2-12)}$$

$$s.t.\quad \boldsymbol{g}(\boldsymbol{x},\boldsymbol{p}) \leq \boldsymbol{0} \qquad \textbf{Eq. (2-13)}$$

$$\boldsymbol{x}^L \leq \boldsymbol{x} \leq \boldsymbol{x}^U \qquad \textbf{Eq. (2-14)}$$

F is the objective functions of the RDO. μ_f and σ_f stand for the mean and the standard deviation of objective function f defined in Eq. (2-9). For the other variables see Eq. (2-9).

RBDO system:

$$\min_{\boldsymbol{x}} \mu_f(\boldsymbol{x},\boldsymbol{p}) \qquad \textbf{Eq. (2-15)}$$

$$s.t.\quad P(\{\boldsymbol{g}(\boldsymbol{x},\boldsymbol{p}) \leq 0\}) \geq \boldsymbol{R} \qquad \textbf{Eq. (2-16)}$$

$$\boldsymbol{x}^L \leq \boldsymbol{x} \leq \boldsymbol{x}^U \qquad \textbf{Eq. (2-17)}$$

2.4.2 Multi-Objective Optimization

In the context of UMDO implementation, the optimization system contains several objective functions to optimize. Two solving methods exist in this case. On the first hand, the problem can be converted into a standard single objective optimization problem by summing up the objective functions. On the other hand, multi objective optimization algorithms determine a set of design solutions, called Pareto-front (Teich 2001). All design configurations of the front are valid, non-dominated by the other design points and therefore candidates to be the best solution. The determination of the optimal design requires the definition of a relative weighting between the objectives (Keane and Nair 2005: 166–7).

The situation of conflicting goals is common in UMDO, since performance and costs optimization pull the system design in different trajectories.

2.4.3 Implementation of Uncertainty-Based Design Optimization

While the UMDO process is barely gaining acceptance in the industry, its application for aerospace vehicle design faces a main issue, the computational complexity of the UMDO algorithms (Yao et al. 2011). Indeed, the UMDO process requires much more computational resources than standard deterministic design optimization method. The reliability of each design studied must be evaluated, which increases the complexity of the process. Evolutionary algorithms like genetic algorithms (GA) are often used in order to determine the Pareto-front without having to calculate any gradient. Nevertheless, the complexity of multidisciplinary systems often requires to take measures to handle it.

First of all, the conversion of the multi-objective problem into a single objective problem focuses the search for optimal in a reduce area of the global Pareto-front (Krüger et al. 2015). This method determines a sub-part of the non-dominated solutions of the design space.

Furthermore, Teich (2001) and Jin and Branke (2005) propose to introduce an approximation of the objective functions. This solution reduces the computation time but brings uncertainty in the objective function definition. The influence of the approximation on the Pareto front can be controlled.

Finally, the implementation of sensitivity analysis upstream of the UMDO can reduce the complexity of the problem by gaining knowledge about the uncertainty propagation across the system. Flowchart of Figure 2-14 illustrates this idea, the general UMDO process is split up into two stages: Uncertain system modeling first, and then the optimization under uncertainty (Zang et al. 2002).

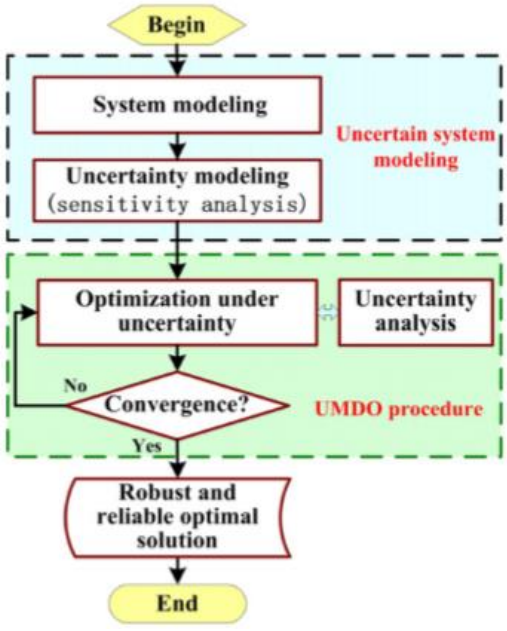

Figure 2-14: General flowchart of UMDO according to Zang et al. (2002)

3 Development of a collaborative MBSE software environment

3.1 Problem definition

On the one hand, the development of new MBSE software and the widely use of SysML, a standard modeling language, are encouraging the creation of a collaborative software environment to carry out CPM. Unfortunately, on the other hand, the diversity of software used by different engineers to develop a new complex system is problematic. In this regard, Airbus seeks to go further in the development of MBSE, by working on a collaborative software package tackling the different phases of the product life cycle, from the requirement analysis to the validation of the final design (Figure 3-1). The idea is to automate the synchronization of the requirement definition in the SysML models and to have a feedback of the analysis and validation processes on the customer level. Flexibility, traceability and modularity properties are the key stones of this project. In this perspective, the customer will gain knowledge about the evolution of system design and performances along the product development.

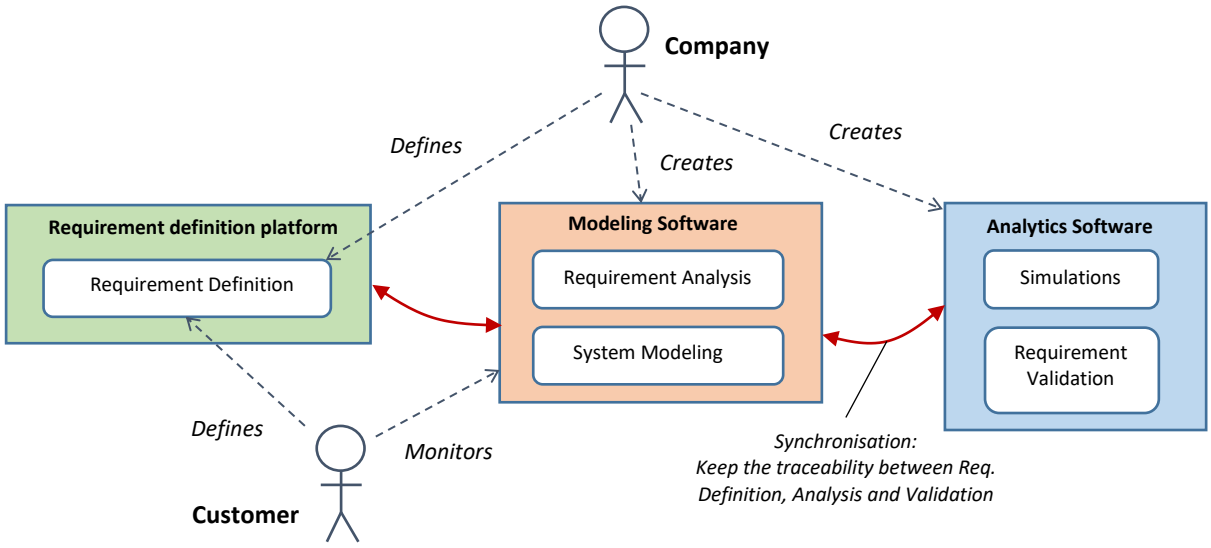

Figure 3-1: Scheme of the workflow desired by Airbus to improve the flexibility and the traceability in the design process of a new complex system

As part of a project between Airbus and ESA on the e.Deorbit Space Debris Removal Mission (Flohrer and Schmitz, eds. 2017), Estable et al. (2017) and Romand (2017) worked on the maturation of the designs and on the dependencies between the different system architectures of the product. They came up with an agile development process, improving the communication between the engineers and the customer. This thesis falls within the extension of this preceding work.

There are two main categories of software supporting model creations, the descriptive and the analytical ones. On the one hand, descriptive software capture the structure, functions, components and interfaces of a system. They are often written in SysML and can provide a good support to keep the traceability along the development of a complex system. On the other hand, analytic software are mathematically-based and consistent with the architecture model. Their goal is to run some simulations and trade studies, to assess the feasibility of a given design and to evaluate its performance and its robustness (NDIA 2011).

3.2 Cameo Systems Modeler

Cameo Systems Modeler is a cross-platform MBSE environment. This software enables storing the important information of a system regarding its structure, functions and logical architecture using System Modeling Language.

Figure 3-2 represents the main window of Cameo Systems Modeler. Block Definition Diagrams (BDD), Requirement Diagrams, Parametric Diagrams and other components and values are stored into the containment tree on the left. The window on the right represents the diagrams modeling the system. The graphical SysML representation and the user-friendly interface offer a better visibility of the system structure.

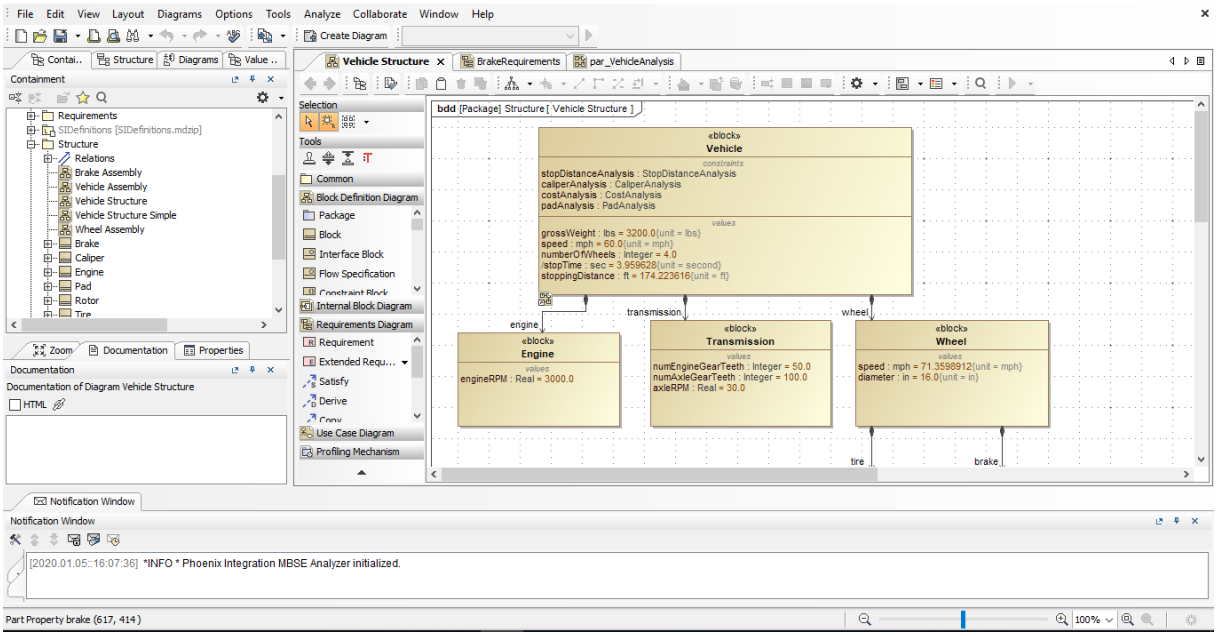

Figure 3-2: Screenshot of the main window of Cameo Systems Modeler

Cameo Simulation Toolkit is an add-on of the Cameo Suite, which can execute parametric models and logical state diagrams as state machine or activity models. While this analytical add-on can validate basic model requirements, it is not suited for the uncertainty propagation analysis across complex systems. The system designs built up in Cameo therefore require the use of external analytics software to assess their performance and validate the configuration.

3.3 ModelCenter

ModelCenter is a software produced by Phoenix Integration. It plays a key role in the development of a collaborative software package in MBSE. This section is inspired by the book of knowledge of the software (Phoenix Integration 2018).

3.3.1 Software description

Despite the progressive replacement of DBSE by MBSE and the recent advances in the domain, the connection between descriptive and analytical models is still complex to configure. The variety of analytics software and programming languages slows down the simulation process. It is also difficult to ensure the link between the inputs and outputs of the different models and thus preserve the traceability property of the global system.

ModelCenter proposes a platform to bridge the gap between the system engineering descriptive models and the analytic models coded on different software (Figure 3-3). ModelCenter performs simulations and trade studies to validate the requirements and analyze the sensitivity of the system.

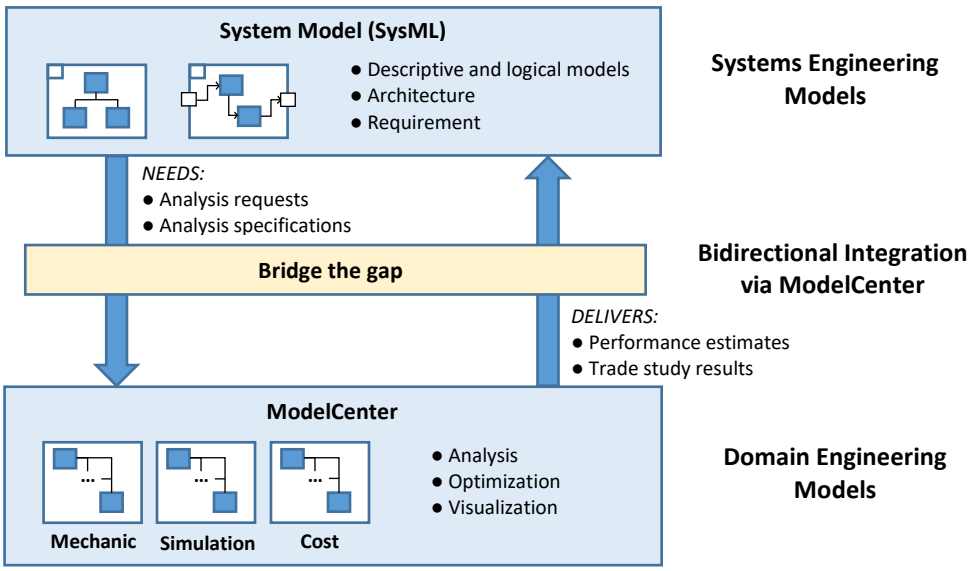

Figure 3-3: Bidirectional Integration of Systems Engineering and Domain Engineering Models via ModelCenter (Simmons et al. 2018)

A ModelCenter process is a chain containing models, components and trade study tools. While trade studies are directly implemented on ModelCenter, the software requires several Plug-Ins to integrate analytic models into the process (Part 3.3.2).

ModelCenter Integrate tool regroups basic simulation and analysis tools to execute the workflow and to run basic trade studies like probabilistic analysis (Simmons et al. 2018).

3.3.2 Analysis Server and Software Plugins

Analysis Server plays a central role in the unification of the analytic models into a single workflow. The app configures a link between the workstation and the ModelCenter model. Analytic models must be wrapped and saved on the workstation to be accessible from ModelCenter.

The integration of specific software files into a ModelCenter process requires the installation of the software plugin on ModelCenter. An easy drag-and-drop of the files from the Server browser window to the workflow process adds the analytic file to the chain (Figure 3-4). ModelCenter automatically detects the inputs and outputs variables of the new file and displays their characteristics in the Component Tree.

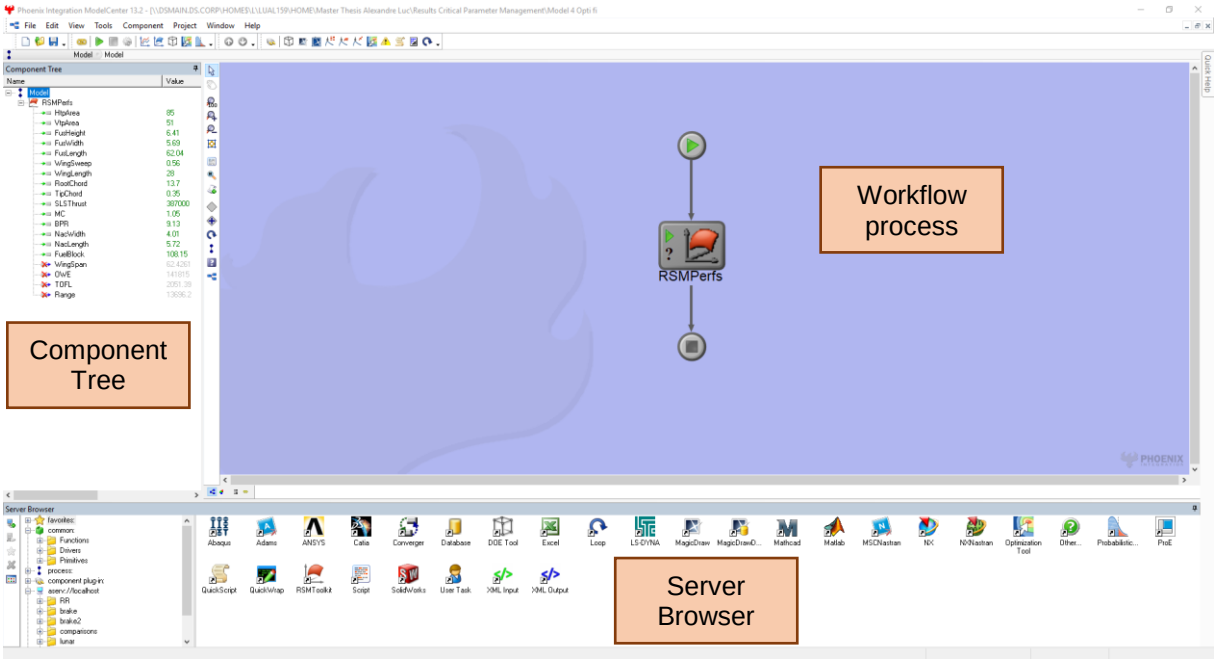

Figure 3-4: Main window ModelCenter

An Analysis Server component is similar to a black box. ModelCenter gets only access to the input and output variables of the model. As soon as the inputs of the Analysis Server component change, ModelCenter transfers the new set of inputs to Analysis Server. The native software of the model is opened in background, calculates the new outputs and transfers the results back to the ModelCenter workflow through Analysis Server (Figure 3-5).

The clustering of different analytic models on a single simulation workflow simplifies the analysis of uncertainty propagation across complex systems. Link Editor manages the linkage between the input and output variables of the different components and ensures the traceability property. A specific attention must be drawn on the name nomenclature and the type of the variables since ModelCenter detects and automatically creates a connection between variables having the same name.

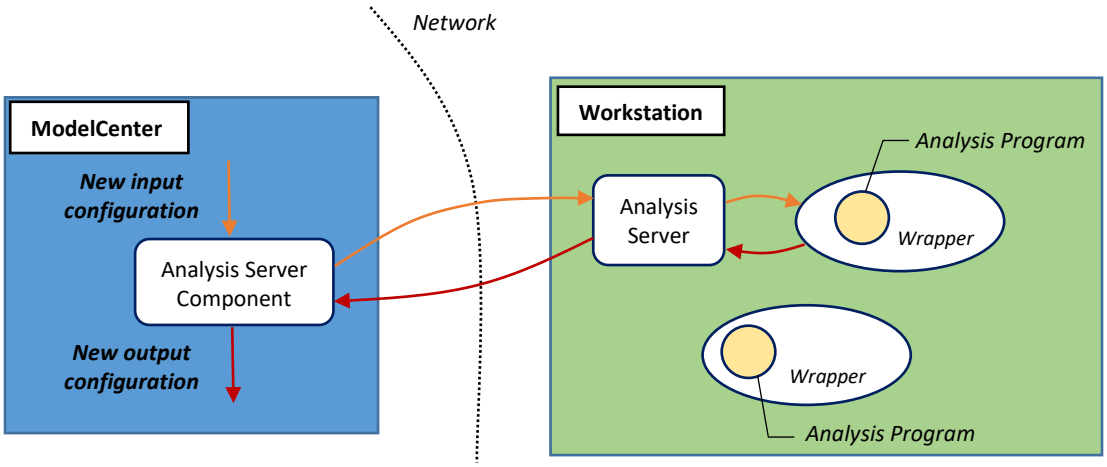

Figure 3-5: Representation of the connection between Analysis Server Components on ModelCenter, Analysis Server app and the targeted wrappers

3.3.3 MBSE Pak

MBSE Pak is a suite of software tools that ensures the link between descriptive SysML models and analytic models on ModelCenter. It consists of MBSE Analyzer and MagicDraw Plug-In. MBSE Analyzer is available on Cameo Systems Modeler and directly interacts with the descriptive and logical models of the descriptive software. As for the wrapped analytic models, the integration of Cameo files into a ModelCenter process requires the upstream installation of MagicDraw Plug-In. Figure 3-6 displays the configuration menu of MBSE Analyzer and illustrates the different capabilities of the plugin.

MBSE Analyzer enables to:

- Create new constraint blocks on Cameo
- Establish a connection between constraint blocks and Analysis Server wrappers
- Proceed to a requirement analysis to validate a design
- Run DOE without opening any ModelCenter process
- Automatically create a workflow to compute the constraint blocks and export it to ModelCenter.

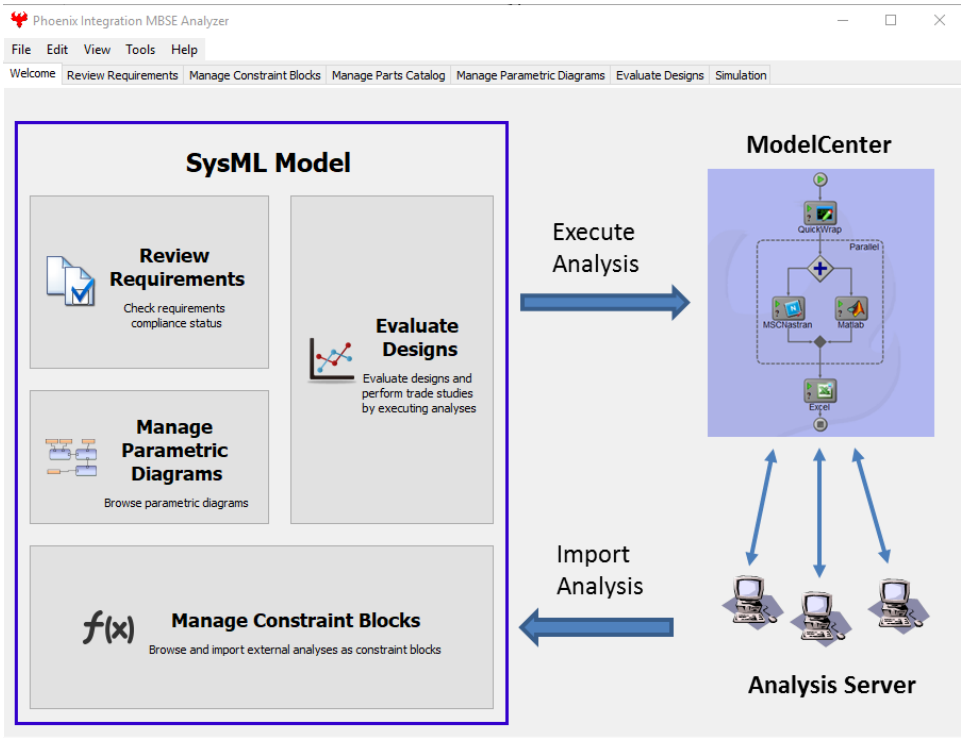

Figure 3-6: Main window of MBSE Analyzer

MBSE Analyzer handles the computation of parametric diagrams and the requirement validation of basic system designs. However, the combination with ModelCenter Integrate is necessary to perform trade studies on complex systems and analyze the propagation of uncertainty across the model. The MagicDraw Plug-In makes possible to import the created Cameo workflow into a ModelCenter process, where detailed Trade Studies can be carried out.

Through this connection and assuming a modular architecture on Cameo, ModelCenter can run simulations linking component levels to system levels in a single workflow. ModelCenter also bridges the gap between descriptive and analytic models by performing a bidirectional integration. Data Explorer table stores the results of the trade studies, which can be exported back to the Cameo Systems Modeler file.

3.3.4 ModelCenter advantages

The following lists summarizes the advantages of ModelCenter to achieve the development of a collaborative MBSE software environment:

- Centralization of the analytical models: no more time loss or information deformation while transferring the input and output parameters between engineering teams for performing different studies. Clustering of all analytics models in a unique file.

- Traceability: easy monitoring of the variable connections between the models. The linkage is partially automated. Link Editor represents physical links between the parameters, which can help finding modeling errors.

- Flexibility: User-friendly interface, add components from different software by a simple drag and drop. The program wrapped on the Analysis Server can therefore be run on their “native platform”.

- Diversity of the analytical models: While MatLab is widely used by engineers to compute complex algorithms, Excel suits to develop simple cost models or work with macros. Nastran and Abaqus support mechanic thermal analysis and finite element analysis whereas Catia and Solidworks Plug-Ins enables the integration of CAD designs in ModelCenter processes. This description presents a non-exhaustive list of the software models that can be integrated into ModelCenter files and shows the diversity of the studies that ModelCenter can carry out.

- Connection to the descriptive models: import of the workflow based on Cameo parametric diagrams through MBSE Pak and its MagicDraw plugin. ModelCenter runs the workflow and can perform trade studies to gain in knowledge about the system. ModelCenter sends back the results to Cameo and ensures the traceability between the descriptive and the analytical models.

3.4 Guideline for CPM along the product life cycle

CPM is a key methodology in the management of uncertainty for complex systems. The earlier the identification of KC takes place in the product life cycle of a system, the easier it is to control the system variation. However, the poor knowledge of the system and the lack of concrete data make the CPM implementation difficult in the early steps of the design process. The new MBSE standards facilitate the knowledge transfer from previous projects and might help introducing the CPM process from the early design steps onwards.

Two generic CPM flowcharts are created in this section, based on the literature reviews of Chapter 2, and serve as a reference for the Case Studies of the next chapters. The CPM follows the 3-step I-A-M structure proposed by Thornton (2003) and Narayanan and Khoh (2008).

3.4.1 Step-by-step CPM during the design phase of a new system

At the beginning of the design process, the system architecture is not decided yet. Components as well as technical solutions still might change. The analytical models are not complete and accurate.

The workflow of Figure 3-7 puts forward a step-by-step iteration of the CPM from the earliest steps of the PLC to understand the uncertainty propagation across the system.

In the identification step, requirement analysis breaks down the top-level requirements. A top-down procedure decomposes the System of Interest into sub-levels. The transfer knowledge from previous system modeling helps creating preliminary analytical models. The definition of a precise and realistic data-driven uncertainty model is a key

stone to implement CPM successfully from the very beginning of the PLC of a new system.

Then, in the assessment phase, SA afford gaining knowledge about the parameters driving the variations of the top-level performances of the system. Transfer knowledge from similar projects about KC helps reducing the complexity of the SA by reducing the number of the assessed design parameters.

Finally, the mitigation stage intends to reduce the variation of the top-level performances. The reduction of the modeling uncertainty as well as the final choice of a component design are possible mitigation solutions.

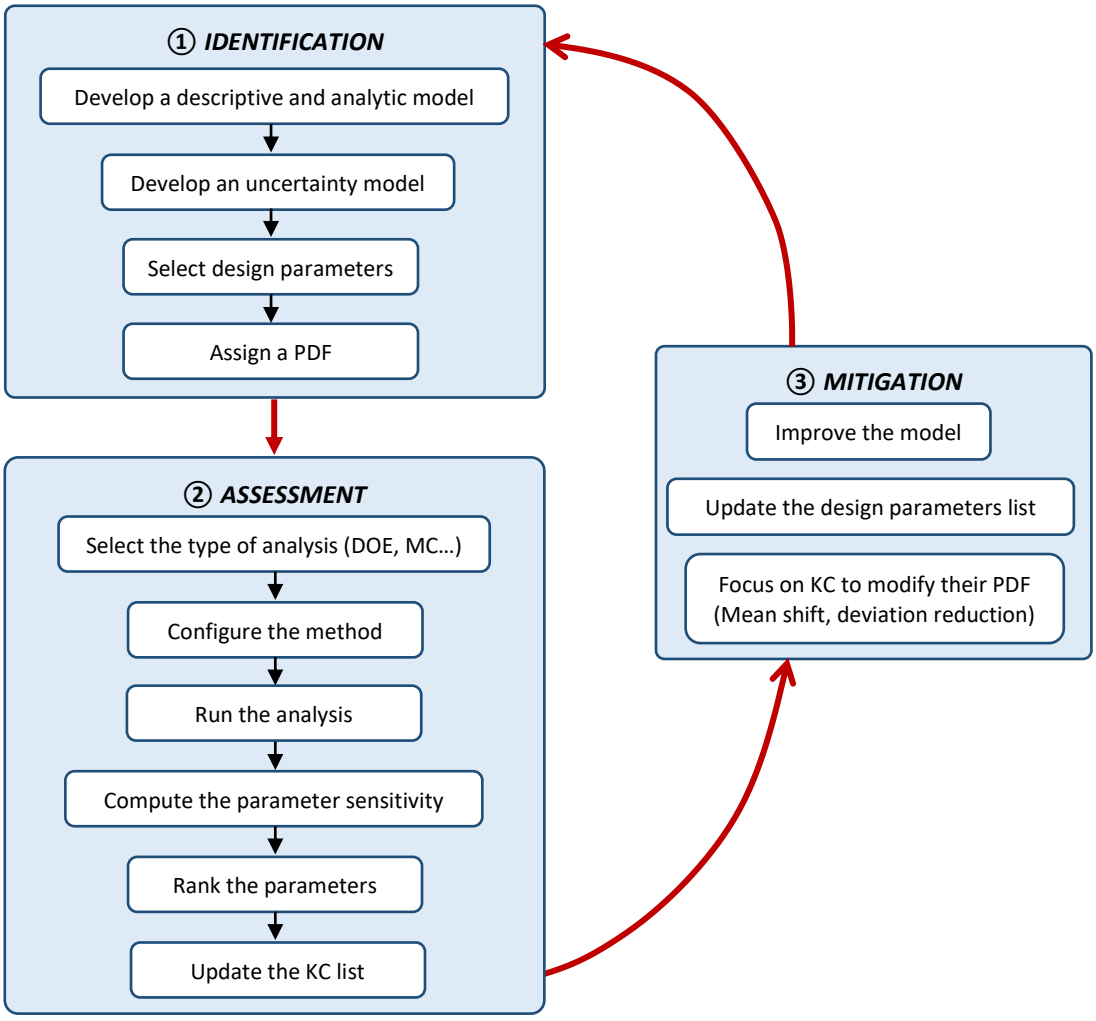

Figure 3-7: Guideline for a step-by-step CPM during the design phase of a new system

3.4.2 CPM for a system in production

The problem is different when implementing CPM for a system entering in production or already into production stage. The final design is established, the model is accurate

and precise specifications are defined down to the component level in order to control the quality of the manufacturing and assembly processes.

Flowchart of Figure 3-8 develops a CPM process specific for systems in production. Actual data from factories provides current results about the manufacturing quality. The set of mean values and standard deviations coming from the production enables to update the value of the process capability. This analysis highlights parameters which manufacturing quality is too poor and therefore require quality enhancement.

Mitigation strategies are fewer than in the earlier steps of the PLC, because the design is fixed and each modification drives many additional costs. Solutions rather focus on the improvement of manufacturing quality to ensure great values of long-term process capability indexes.

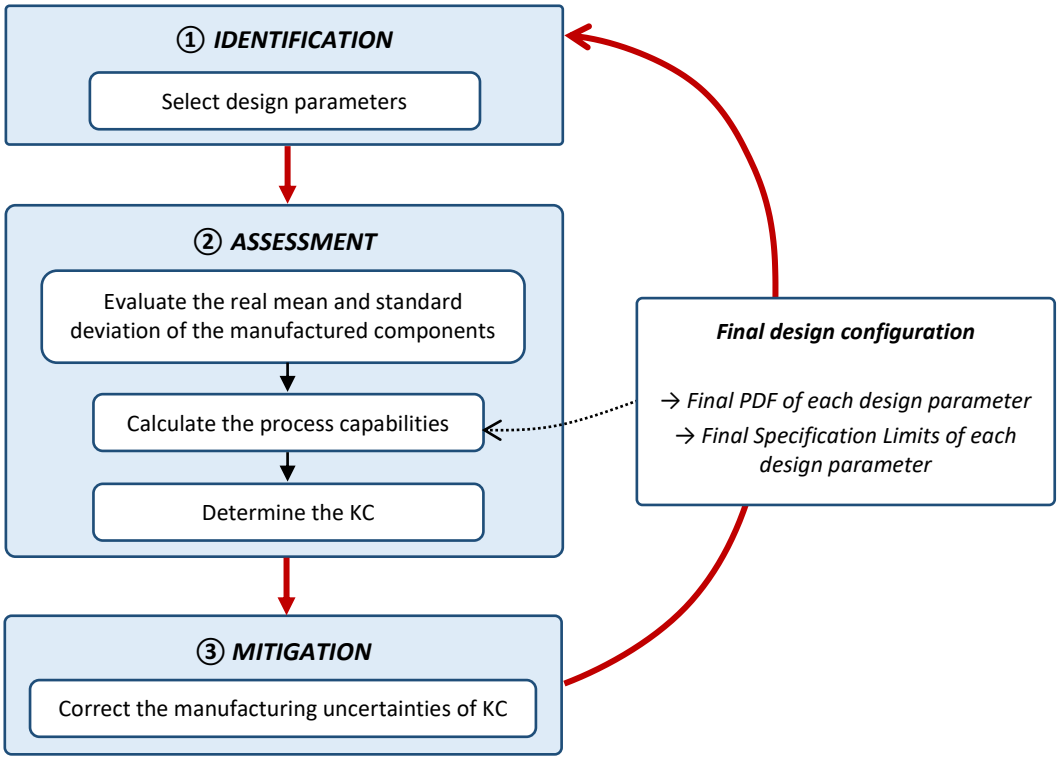

Figure 3-8: Guideline for CPM for a system in production

3.5 Guideline for UMDO during the design phase of a new system

Since the thesis also addresses the topic of UMDO, Figure 3-9 describes a guideline for its implementation during the design phase of a new system. Part 2.4.3 underlines the complexity of the UMDO process. Orange blocks on the flowchart denote implementation steps that directly influence the complexity and the feasibility of the optimization process. In that respect, their configuration will be tackled in detail in the Case Study of Chapter 6.

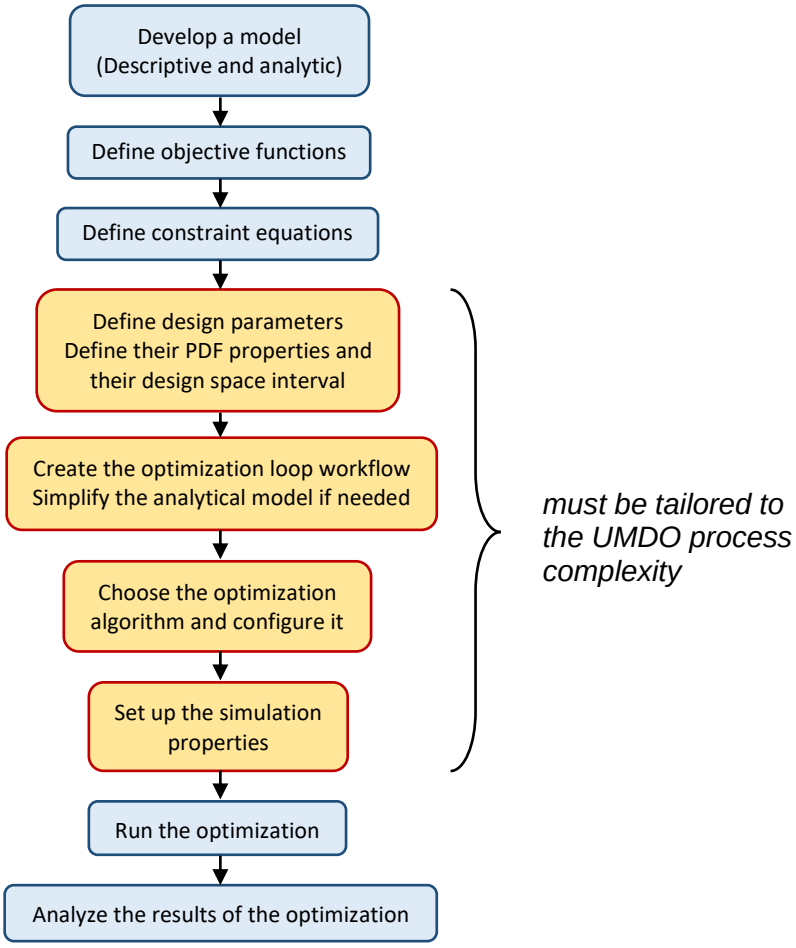

Figure 3-9: Guideline for UMDO during the design phase of a new system

3.6 Software Integration to conduct CPM and UMDO process

This part describes some of the tools of ModelCenter to run sensitivity analysis and optimizations. The theoretical chain of interaction between Cameo Systems Modeler and ModelCenter sets up the connections between the descriptive and analytic software and will serve as a basis to implement the CPM and the optimization process. Case Studies of Chapters 4, 5 and 6 will assess the feasibility of the implementation of the CPM flowcharts (Figure 3-7, Figure 3-8) and of the UMDO flowchart (Figure 3-9) in the collaborative software environment revolving around the ModelCenter/Cameo couple.

3.6.1 Sensitivity Analysis

ModelCenter Explore provides additional design space exploration tools to supply the basic simulation tools of ModelCenter Integrate (Simmons et al. 2018).

For each DOE or probabilistic analysis implementation, ModelCenter helps picking the most suited method. A Selection Wizard asks a series of questions regarding system complexity and characteristics of the analytic model to guide the user in selecting an appropriate method. A table summarizes the evaluation of the different methods

regarding their accuracy and the required number of function evaluations to perform the analysis.

In addition to the standard DOE and probabilistic analysis mentioned in Chapter 2, such as Monte-Carlo, LHS, Full and Fractional Factorial Design, ModelCenter provides the NESSUS probabilistic analysis tool (Southwest Research Institute 2012). NESSUS was developed by the Southwest Research Institute for the NASA several years ago and performs reliability analysis. Most of the NESSUS methods compute the most probable point (Southwest Research Institute 2012: 6; Yao et al. 2011: 462) and then approximate the performance function by a polynomial function. These analytical methods require far fewer function evaluations than a standard Monte Carlo probabilistic analysis to assess the reliability but deliver less accurate results.

3.6.2 Optimization Algorithms

In a similar way that Method Selection Wizard for DOE and probabilistic analysis selection, ModelCenter helps the user in selecting the appropriate optimization algorithm. Table 3-1 describes the diversity of algorithms implemented on ModelCenter. While Non-dominated Sorting Genetic Algorithm NSGA-II (Deb et al. 2002; Han et al. 2014), Darwin algorithm and DAKOTA Multi-objective Genetic Algorithm (DAKOTA 2017) are evolutionary algorithms carrying out multi-objective optimizations, Design Explorer, OPTLIB Gradient Optimizer and DAKOTA OPT++ are gradient-based and convert the multi-objective optimizations into single-objective problems. The robustness against system complexity is also an important characteristic to consider while picking the optimization algorithm.

Table 3-1: Description and evaluation of ModelCenter optimization algorithms

Algorithm Characteristics / ***Name of the Algorithm***	Model Speed	Smooth Responses	Design Constraints	Multiple objectives	Population based	Gradient based	Genetic Algorithm	Local / Global optimum	Approximations
Design Explorer	🟢	🟢	🟢	🔴	Yes	Yes	No	Global	Yes
DAKOTA Multi-objective Genetic Algorithm	🟡	🟢	🟢	🟢	Yes	No	Yes	Global	No
Darwin algorithm	🟡	🟢	🟢	🟢	Yes	No	Yes	Global	No
NSGA-II	🟡	🟢	🟢	🟢	Yes	No	Yes	Global	No
OPTLIB Gradient Optimizer	🟢	🟡	🟢	🔴	No	Yes	No	Local	Yes
DAKOTA OPT++ Finite differences Newton	🟢	🟡	🟢	🔴	No	Yes	No	Local	Yes

Design Explorer stands out by its hybrid character: This gradient method is population-based and finds out global optimum in a limited time. Moreover, the efficiency of the NSGA II algorithm driving to the Pareto-front determination makes it one of the most widely used algorithms in the industry (Squillero and Burelli, eds. 2016: 110–6; Ye and Huang 2015).

Finally, the choice of the algorithm used in Chapters 5 and 6 will be based on the characteristics of the system, such as the number of objective functions and the complexity of the analytical workflow.

3.6.3 Schematic implementation of the Cameo/ModelCenter integration

In this thesis, the structure of the collaborative MBSE software environment revolves around the Cameo/ModelCenter couple (Parts 3.2 and 3.3). Figure 3-10 describes the chain of interactions between the two software tools to carry out the CPM as well as the UMDO. MBSE Pak, Analysis Server and the multiple component Plug-Ins on ModelCenter support the bidirectional integration of descriptive and analytical models. ModelCenter hosts the final process workflow and can perform both optimization and SA, such as probabilistic analysis or DOE. Trade Study Files gather the simulation results, which can be exported to Cameo.

This chain acts as reference point for carrying out CPM and optimization process in Chapters 4, 5 and 6. The Case Studies intend to evaluate the feasibility of implementing a CPM and a reliability-based optimization in the so defined collaborative software environment.

During all the steps of this implementation, attention is drawn on ensuring the traceability of components and variables (Link editor of ModelCenter, Parametric equation wizard on Cameo), the structural modularity of the models and the data-driven aspect of the analysis.

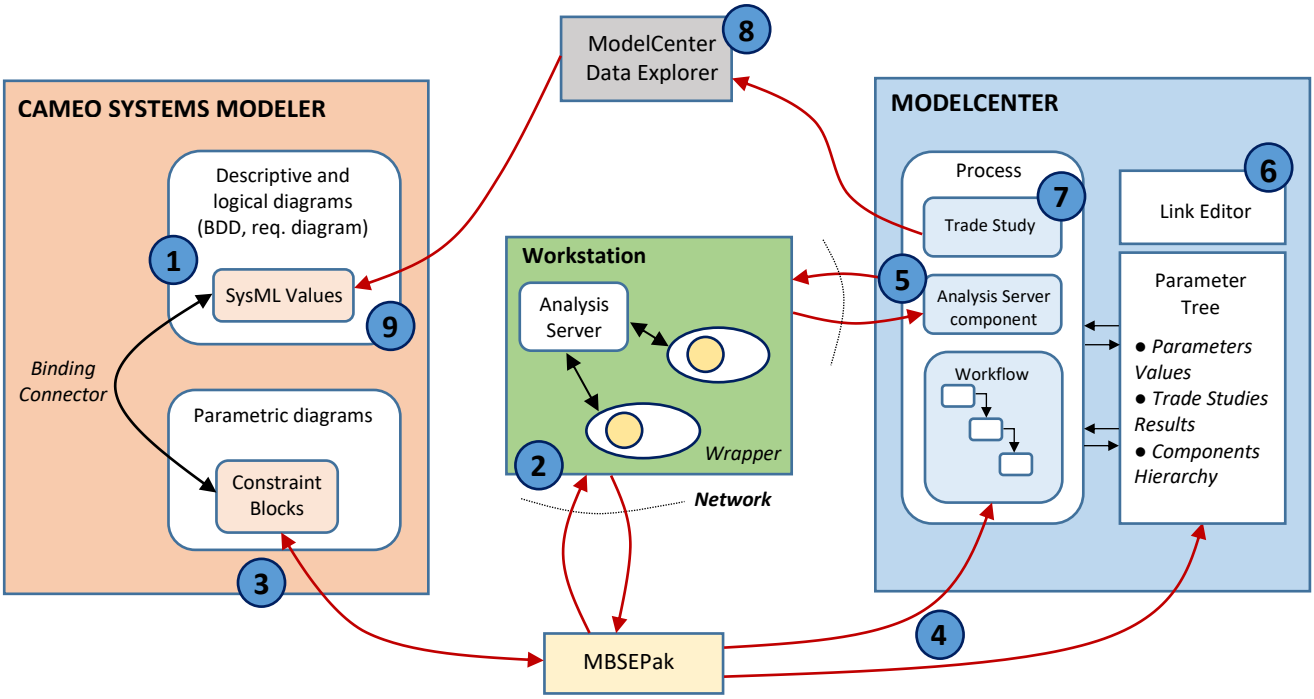

1. *Create descriptive and logical diagrams on Cameo Systems Modeler*
2. *Create new Analysis Server Scripts via MBSE Pak*
3. *Create new constraint blocks on Cameo through MBSE Pak*
4. *Create and export the workflow associated to parametric diagrams to ModelCenter*
5. *Bring analytical models into the process via component plugins and Analysis Server*
6. *Edit the link between the variables to keep the traceability property*
7. *Configure DOE, Probabilistic Analysis or optimization (Select design variables, PDF, select the algorithm, configure the simulation and run the trade study)*
8. *Analyze the results on the Data Explorer Table, assess the KC and find out mitigation strategies in case of a CPM process or identify the best design in case of an optimization*
9. *Export the results back on Cameo Systems Modeler*

Figure 3-10: Description of the chain of interactions between Cameo and ModelCenter to carry out CPM and UMDO studies

4 Implementation of the CPM process for an aircraft model

This section deals with a concrete implementation of the CPM flowcharts described in the previous chapter (Figure 3-7, Figure 3-8) using the Cameo/ModelCenter connection (Figure 3-10). The Case Studies evaluate the feasibility of implementing a CPM in this software environment, assess the different analysis tools and functionalities of ModelCenter and raise the issues that engineers will have to face during the CPM. Much attention is drawn to the future integration of this CPM procedure to more complex aeronautical systems.

The first Case Study tackles the CPM of a commercial aircraft system entering into production. The gain of knowledge about the uncertainty propagation in the aircraft system and its key characteristics supports the implementation of the CPM in the early development process of a new aircraft in Case Study 2. Finally, Case Study 3 focuses on the competing requirements issue and the various solutions to overcome it.

4.1 Initial situation

An analytical data model of an Airbus commercial aircraft provides the initial set of equations to carry out a CPM process. A set of regressions establishes the analytical relations between several design parameters of the aircraft and the performance indexes, such as the range, the Operational Weight Empty (OWE) and the Takeoff Field Length (TOFL) for instance. Here, the aircraft is considered entering into the production phase. Its parameters are already set up and the analytical model is accurate. This first example offers a short introduction to the critical parameter identification methods for a system in production.

The knowledge transfer about the analytical equations, key characteristics and uncertainty propagation for this type of commercial aircraft will then serve as a basis for the design of a new aircraft in Case Study 2.

4.2 Case Study 1: Aircraft in production

4.2.1 Requirement definition

In this first example, four requirements drive the design of the system: the TOFL, the range, the wingspan and the OWE. Figure 4-1 illustrates the requirements' properties. The TOFL must be less than 2500 m, the range greater than 17 500 km, the wingspan smaller than 73.5 m and the operational weight empty lower than 176 000 kg.

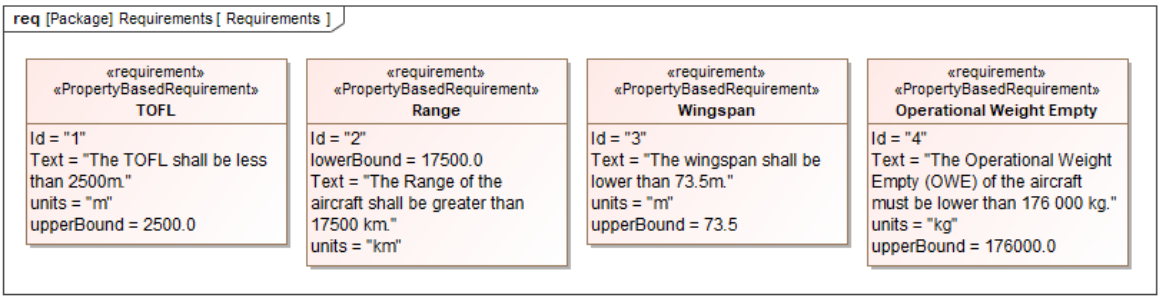

Figure 4-1: Requirement diagram of the aircraft in production

4.2.2 System modeling

Due to model property protection, the regression equations are not described here. A black box replaces the entire analytical model linking the design parameters inputs to the final performance outputs. MatLab plugin supports the integration of the MatLab analytic model in ModelCenter. The execution of this workflow evaluates the TOFL, the range, the wingspan and the OWE of the aircraft under study.

Fifteen design parameters form the set of inputs of the model. The Sea Level Standard Thrust T_{SLS}, the motor characteristic MC and the Bypass Ratio BPR describe the engine bloc and the wing sweep Λ_{Sweep} , the wing length L_{Wing}, the root and tip chords c_{Root} and c_{Tip} express the geometry of the wings. h_{Fus}, l_{Fus} and L_{Fus} stand for the fuselage dimensions, whereas A_{Htp} and A_{Vtp} characterize the tails area. l_{Nac} and L_{Nac} describe the geometry of the nacelle and $V_{FuelBlock}$ stands for the volume of the block fuel.

Table 4-1 describes the PDF associated to the design parameters to carry out the probabilistic analysis in this Case Study. Specification levels have already been set in the design process to monitor the quality level of the manufacturing and the assembly.

Table 4-1: PDF and specifications of the design parameters in Case Study 1

Design Parameters	Symbol	Unit	Distribution Type	μ	σ (% of μ)	LSL	USL
Horizontal Tail Area	A_{Htp}	m²	Normal	103	0.19	101.97	104.03
Vertical Tail Area	A_{Vtp}	m²	Normal	61.8	0.18	61.18	62.42
Fuselage Height	h_{Fus}	m	Normal	7.24	0.25	7.17	7.31
Fuselage Width	l_{Fus}	m	Normal	7.52	0.23	7.44	7.60
Fuselage Length	L_{Fus}	m	Normal	75.3	0.18	74.55	76.05
Wing Sweep	Λ_{Sweep}	rad	Normal	0.56	0.20	0.55	0.57
Wing Length	L_{Wing}	m	Normal	28	0.25	32.87	33.53
Root Chord	c_{Root}	m	Normal	17.4	0.25	17.23	17.57
Tip Chord	c_{Tip}	m	Normal	0.40	0.25	0.40	0.40
SLS Thrust	T_{SLS}	N	Normal	496000	0.17	491040	500960
Motor Characteristic	MC	ø	Normal	1.2	0.24	1.19	1.21
Bypass ratio	BPR	ø	Normal	11.1	0.21	10.99	11.21
Nacelle Width	l_{Nac}	m	Normal	4.61	0.16	4.56	4.66
Nacelle Length	L_{Nac}	m	Normal	6.3	0.16	6.24	6.36
Fuel Block Volume	$V_{FuelBlock}$	m³	Normal	125	0.22	123.75	126.25

4.2.3 Probabilistic analysis

A Monte Carlo statistical analysis with 50 000 runs simulates the distribution properties of the outputs. Figure 4-2 represents the histogram of the Range output with the final set of design parameters. The Range performance is robust and reliable as no runs have failed to overcome the lower bound limit of 17 500 km. The other performances also succeed the requirement and have a reliability of 100%.

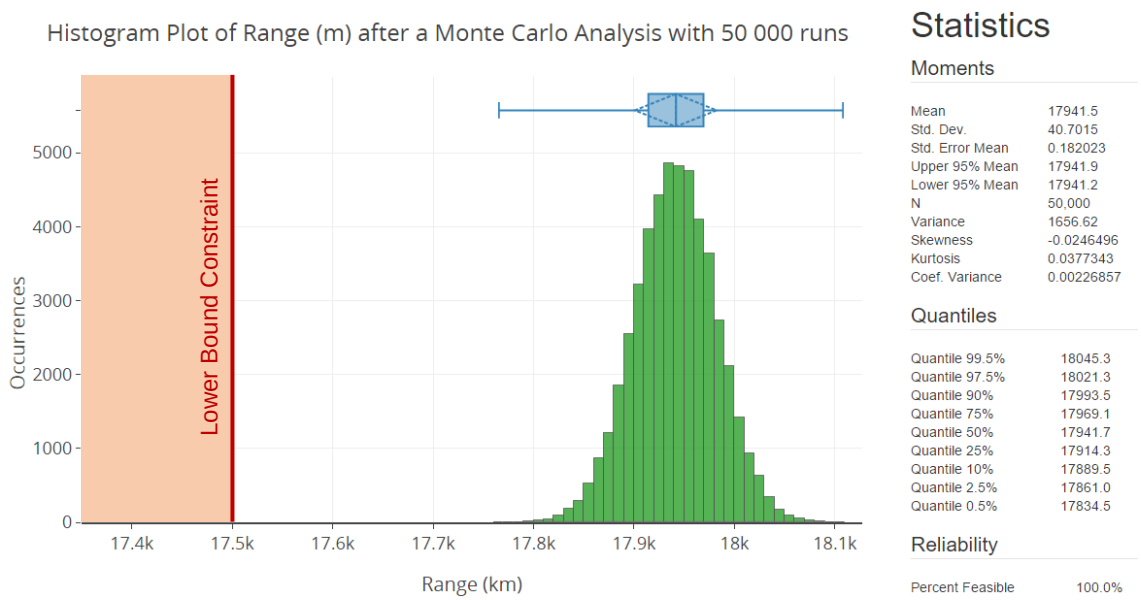

Figure 4-2: Histogram representing the range distribution of the aircraft under study after running a Monte Carlo probabilistic analysis with 50 000 runs

The process capability index C_{pk} defined in Eq. (2-3) provides a measure of the production quality and serves for the assessment of the KC, as described in the CPM flowchart for systems in production (Figure 3-8). The histogram of Figure 4-3 depicts the short-term process capability index C_{pk} of the design parameters, based on the Monte Carlo simulation results. Each short-term capability index overcomes the 1.33 threshold, common boundary of a good manufacturing uncertainty management (Mackertich and Kraus 2012).

However, process capability may get worse over manufacturing shifts (Thornton 2003). Long-term capability indexes must also be calculated to anticipate the deterioration of the production quality. Since there is no information coming from the factories about the real manufacturing characteristics yet, as the system just enters in production, the Six Sigma method recommends adding a mean shift of 1.5 standard deviations to the simulated means to forecast the long-term capability index of the design parameters (Thornton 2003: 30). The height and the width of the fuselage, the length of the wings and the tip and root chords present a long-term capability C_{pk} lower than 1.0 and are also the critical parameters to monitor during the manufacturing of the components.

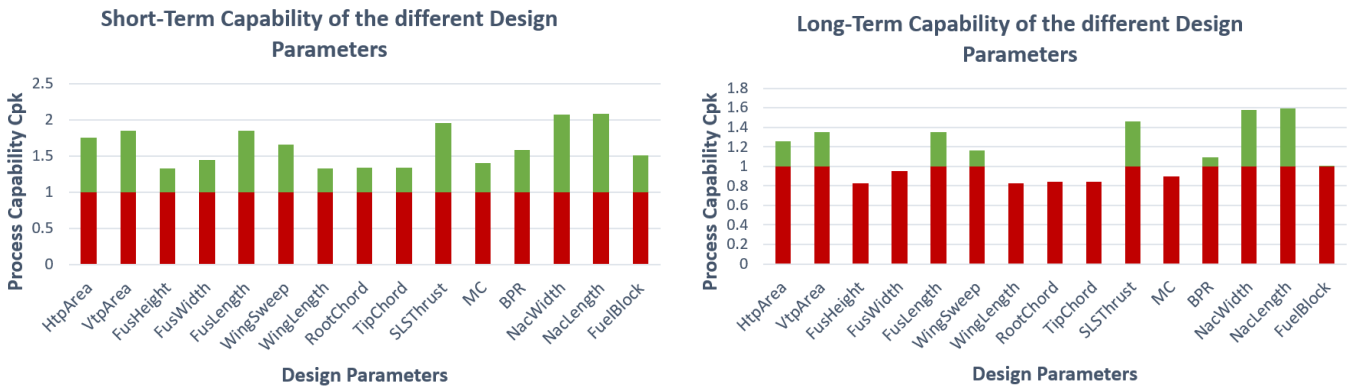

Figure 4-3: Representation of the short-term (left) and long-term (right) process capability index for the aircraft in production

Later in the product life cycle, information coming from the manufacturing may provide a better understanding of the manufacturing characteristics. The refinement of the long-term capability indexes calculation will ensure a better monitoring of the critical parameters of the system.

4.2.4 Discussion

When a new system is brought into production, the analytical model is very accurate, and the propagation of uncertainty is controlled. ModelCenter probabilistic analysis tools are useful to validate the final design and assess the short- and long-term capabilities of the design parameters. Statistical analysis can forecast the parameters that might become critical later in production. However, only the analysis of data coming from the manufacturing will allow identifying the real critical parameters. Statistical tools and DOE may have a key role to play earlier in the development process of new complex systems to handle the uncertainty propagation affecting the top-level performances.

4.3 Case Study 2: Aircraft in design phase

ModelCenter supports the model unification promoted by the MBSE and can run multi-level simulations from the early stages of system development. This feature breaks with the commonly used V-Model in which global simulations are carried out only at the end of the development process (Vaneman 2016) and is in line with agile development methods (Balaji and Sundararajan Murugaiyan 2012). The study of uncertainty propagation across the different levels of the analytical tree can therefore be applied systematically throughout the development of the new system, following the flowchart defined in Chapter 3 (Figure 3-7).

In this Case Study, a fictive situation is conceived in which communication process is set up with the engineers working on the design, model and architecture of the system. At each step considered in the design phase, the engineers deliver a set of descriptive, analytical and uncertainty models to characterize the preliminary design of the system.

The goal is then to identify and assess the CP, and to propose mitigation solutions to the designers.

4.3.1 Initial situation

As the understanding about the system is poor in the early design steps, this analysis tackles the possible transfer of knowledge from previous similar systems. Some brunches of the analytical tree of Case Study 1 connecting design parameters to the top system level remain. The analytical regressions of the previous Case Study provide a basis approximation of the system performances.

Since the system is still in the design stage, there is no data from manufacturing to monitor production quality (Thornton 2003). Furthermore, the specification limits of the individual components are not set up yet, so it is not possible to evaluate the process capability index C_{pk} like in Case Study 1.

The step-by-step CPM implementation over the development process follows the I-A-M flowchart built up in Figure 3-7. For each step, the goal is to analyze the model, extract the critical parameters and provide some advice to the designers to improve the performances and meet the requirements with a certain level of reliability at the end.

4.3.2 Requirement definition

For the sake of clarity, this Case Study will consider only one requirement out of the four described previously in Part 4.2. The upper bound of the TOFL performance is set to 2950 m for this new system, for a takeoff altitude included between 0 and 2000 m and an initial temperature between -5 and 35 °C (Figure 4-4).

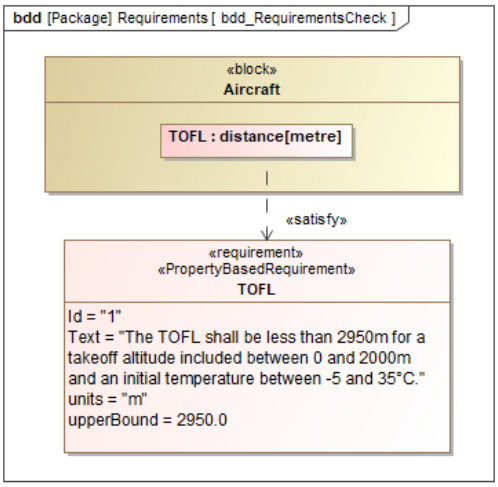

Figure 4-4: Requirement diagram of the aircraft in design phase

This definition of the TOFL requirement allows introducing two external parameters in the study of the system performance: the take-off altitude Z_{TO} and the ambient temperature during takeoff t_{amb}. External noise factors have a great influence on the aircraft performances indeed. This case study explores how a systematic CPM starting

from the early design phase of a new aircraft system can drive to a design which reliability is greater than 97.5% regarding the TOFL requirement.

4.3.3 Uncertainty modeling

The characterization and the management of the different categories of uncertainties is essential to implement uncertainty-based design methods. The following list describes the uncertainty categories tackled in the Case Study 2, based on the literature review of Part 2.2:

- Design parameter uncertainty: Since the component's design is not decided yet, a statistical uncertainty adds up to the random uncertainty of the design parameters. A probabilistic uncertainty modeling groups the statistical and random uncertainties together and associates a PDF to each design parameter. The design parameters have a Normal distribution in this model.

- Modeling uncertainty: The poor knowledge about the system in the early steps of the design process leads to approximations in the transfer functions. However, analytical models become more precise throughout the design process. A design decision concerning a technical aspect or the choice of a component improves directly the accuracy of the model.

  In this Case Study, an equation uncertainty factor, noted U_Y, captures the model uncertainty coming from the different analytic equations (Eq. (4-1)). An interval boundary (Figure 2-5) centered around 1 defines the range in which the parameter can evolve. The more accurate the equation to which the uncertainty factor refers, the narrower the boundary interval. The equation uncertainty factor is equal to 1 when the equation is 100% accurate.

$$Y = U_Y \cdot f(X_1, X_2, X_3) \qquad \textbf{Eq. (4-1)}$$

  X and Y represent the input and the output of the transfer function f, respectively. The equation uncertainty factor U_Y characterizes the uncertainty associated to the transfer function f.

- Computing uncertainty: The analytical model is based on a set of regressions, so the computing complexity is low and many runs can be performed during the sensitivity analysis. Monte Carlo analysis performs great in these conditions and provides accurate results. Therefore, the computing uncertainty is negligible compared to the others and is not modeled in this Case Study.

- External Perturbations: Since it is not possible to forecast the takeoff temperatures and altitudes in the life cycle of this aircraft, a uniform distribution describes the variations of these two external parameters. The boundaries of the distributions directly derive from the Requirement diagram definition (Figure 4-4).

4.3.4 System modeling

This part explains the different modeling steps on Cameo and ModelCenter introduced in Figure 3-10 to come up with performance and reliability analysis of the new aircraft, while ensuring the traceability between the different software and models.

A BDD (Block Definition Diagram) configures a basic aircraft structure for the CPM analysis (Figure 4-5). The model could be broken down into additional sublevels, but the study does not intend to go into as much detail.

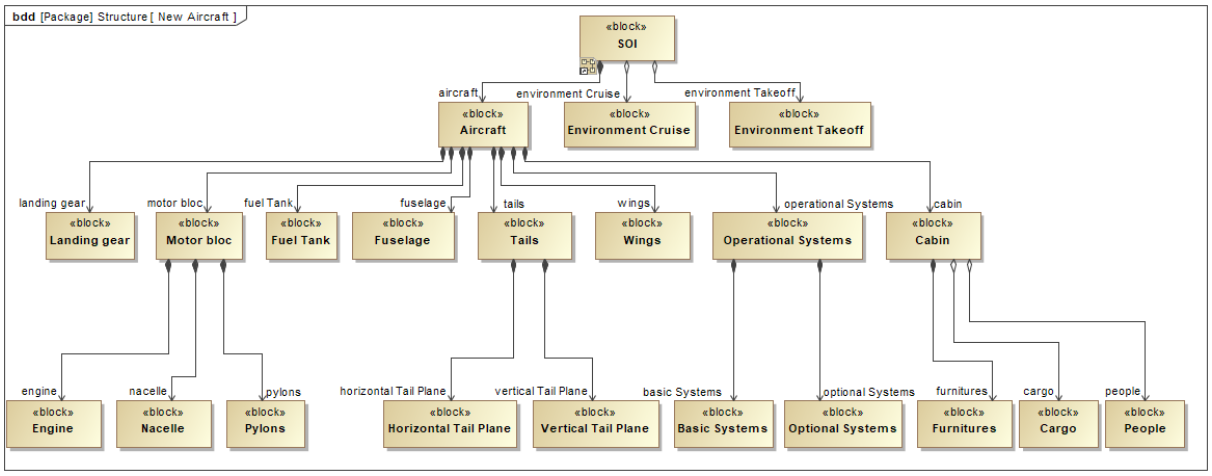

Figure 4-5: Creation of the BDD of the new aircraft on Cameo Systems Modeler

Cameo supports the connection between the system performance variables and the requirement properties, important for the reliability analysis later on ModelCenter. Therefore, the “satisfy” connection is created between the TOFL variable and the TOFL requirement block on Cameo (Figure 4-4).

MBSE Analyzer implements the analytical equations and ensures the traceability of variables between the descriptive and the analytical models. The plugin offers the possibility to create new constraint blocks using Analysis Server Scripts and JavaScript Scripts. In addition to the units and the initial value of each variable of the Script, the user must define the type of the variable: either an input or an output (Figure 4-6). This characteristic is essential for ModelCenter to create a valid workflow computing all the equations assessing the aircraft performances.

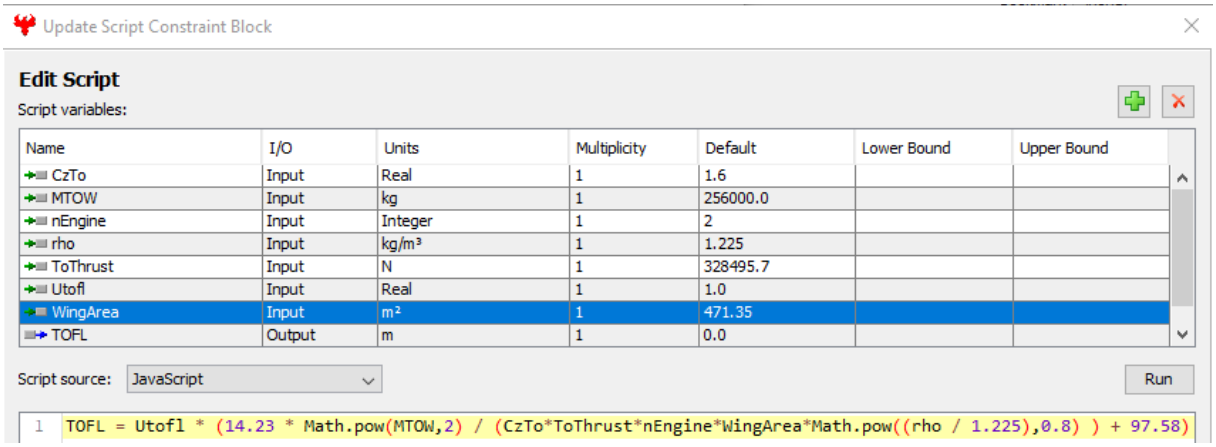

Figure 4-6: Creation of a constraint block on MBSE Analyzer

MBSE Analyzer automatically exports the equations to the descriptive model on Cameo. A parametric diagram is built on the System Of Interest (SOI) level, a simple drag and drop of the equations into the parametric diagrams adds a new constraint block (Figure 4-7). The Parametric Diagram Automation links the variables of the analytical model to the Cameo variables and ensures therefore a great traceability between the different models (Figure 4-8).

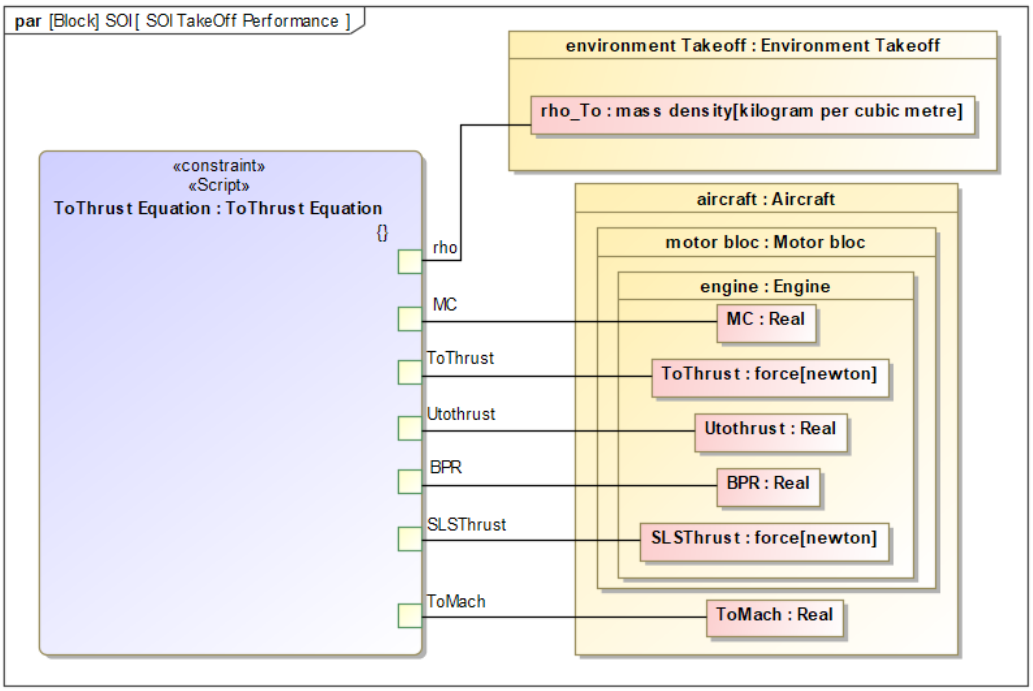

Figure 4-7: Creation of a constraint block on Cameo Systems Modeler based on a MBSE Analyzer Script

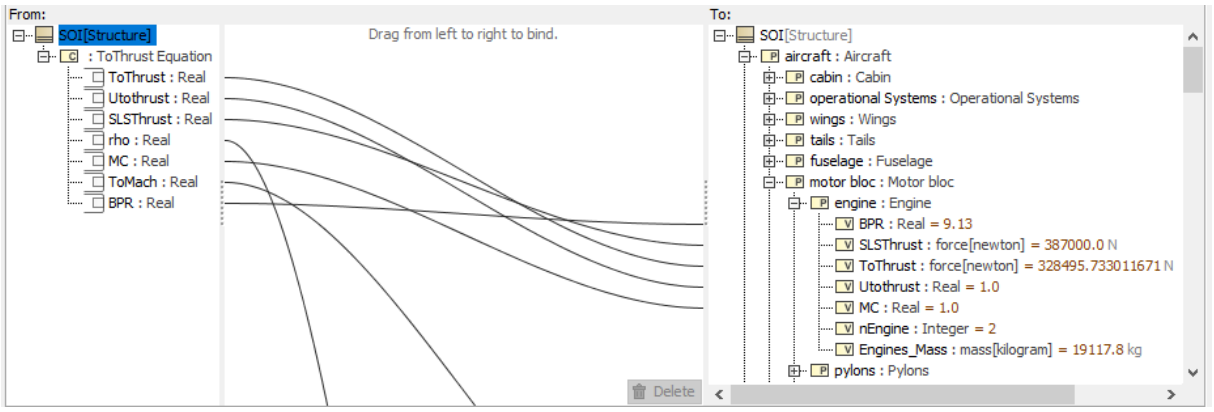

Figure 4-8: Parametric Diagram Automation tool ensures the traceability property between the variables of Cameo Systems Modeler (right) and of the analytic model (left)

MBSE Analyzer automatically creates a valid workflow enabling to compute the constraint blocks and get access to the TOFL performance. MagicDraw Plug-In ensures the integration of the created worklow in a ModelCenter process (Figure 4-9). Statistical analysis tools are then available to carry out Trade Studies, evaluate the reliability of the performances and identify the KC. Next section implements probabilistic analysis and provides an overview of the analysis tools of the software.

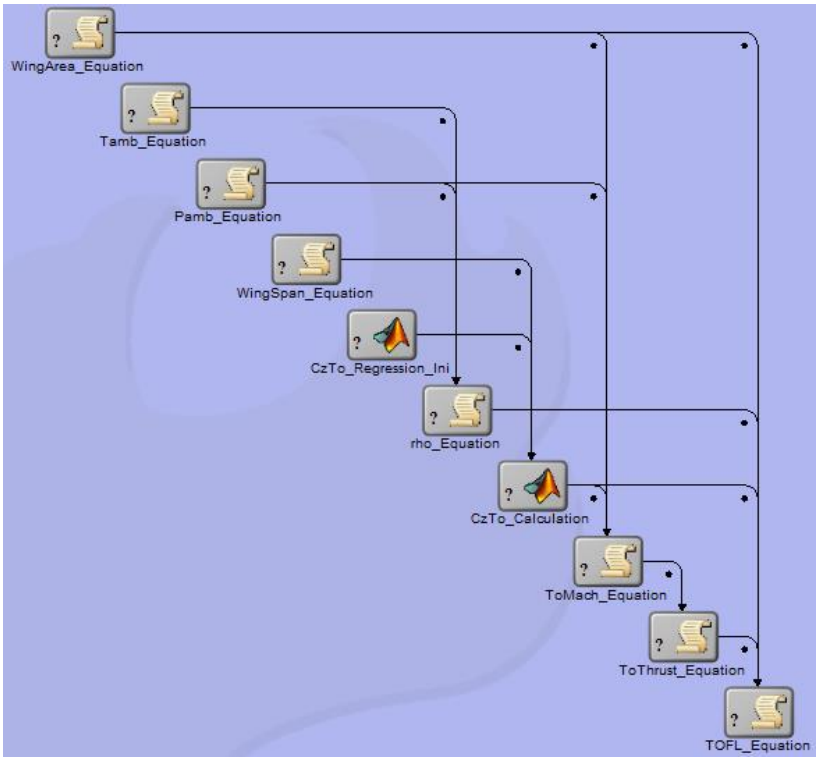

Figure 4-9: Workflow export from MBSE Analyzer to ModelCenter

4.3.5 Step 1 CPM in design phase

This section addresses the first implementation of the CPM in the design process of the new aircraft. Table 4-2 lists the input parameters and their probability density

function at this Step of the design process. The initial configuration has been obtained by interpolation of the design characteristics of the commercial aircraft in Part 4.2.

Δt_{ISA} represents the difference between the ambient temperature and the standard temperature under International Standard Atmosphere (ISA).

Table 4-2: List of input parameters and their PDF at Step 1 of the design phase

		List of input parameters		Distribution Type	Lower Value	Upper Value	Mean	Standard Deviation
Perturbations		Z_{TO}	m	Uniform	0	2000		
		Δt_{ISA}	°	Uniform	-20	20		
Design parameters	***Wings***	A_{Wing}	m²	Normal			341	5%
		$C_{z,TO}$	ø	Normal			1.60	5%
	Engine	BPR	ø	Normal			9.13	5%
		MC	ø	Normal			1.0	5%
		T_{SLS}	N	Normal			387000	5%
		Ma_{TO}	ø	Normal			0.25	5%
Equation uncertainties		U_{TOFL}	ø	Uniform	0.85	1.15		
		U_{ρ}	ø	Uniform	0.995	1.005		
		$U_{T_{TO}}$	ø	Uniform	0.9	1.1		
		$U_{P_{amb}}$	ø	Uniform	0.995	1.005		
		$U_{t_{amb}}$	ø	Uniform	0.995	1.005		

Figure 4-10 represents the analytical tree at Step 1, some parameters are not decomposed up to the component level, because the design solutions are not decided yet. For instance, the wing design can still evolve. The lift coefficient of the aircraft $C_{z,TO}$ and the wing area A_{Wing} will be inputs in the model, whereas their value actually depend on the geometrical characteristics of the wings, like the root chord and the wing length.

While the blue boxes denote input parameters of the analytic model, white boxes represent output parameters. The arrows refer to an input/output relation between different parameters. As the Case Study tackles the modeling uncertainty (4.3.3), the more the inputs/output relation between variables is precise, the more the model is accurate. While green arrows indicate that the uncertainty associated with the input/output function is close to zero, orange arrows denote a high degree of uncertainty. This illustration matches with the interval bounds set up for the equation uncertainties in Table 4-2.

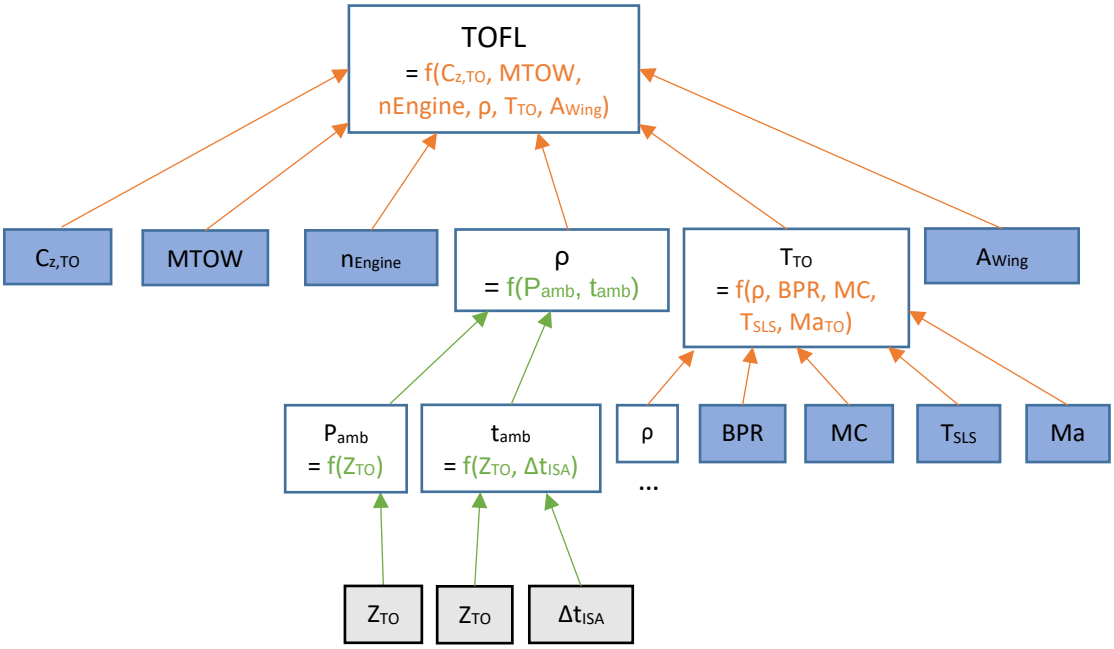

Figure 4-10: Analytical tree and equation uncertainty modeling at Step 1 of the design phase

Since the model complexity is relatively low, a Monte Carlo statistical analysis is carried out with 2000 runs in order to assess the reliability of the TOFL. The probability density of the TOFL seems to follow a Gaussian law, with a mean value around 3249 m (Figure 4-11). The reliability of the TOFL regarding the 2950 m requirement threshold is lower than 33%, far away from the required 97.5%.

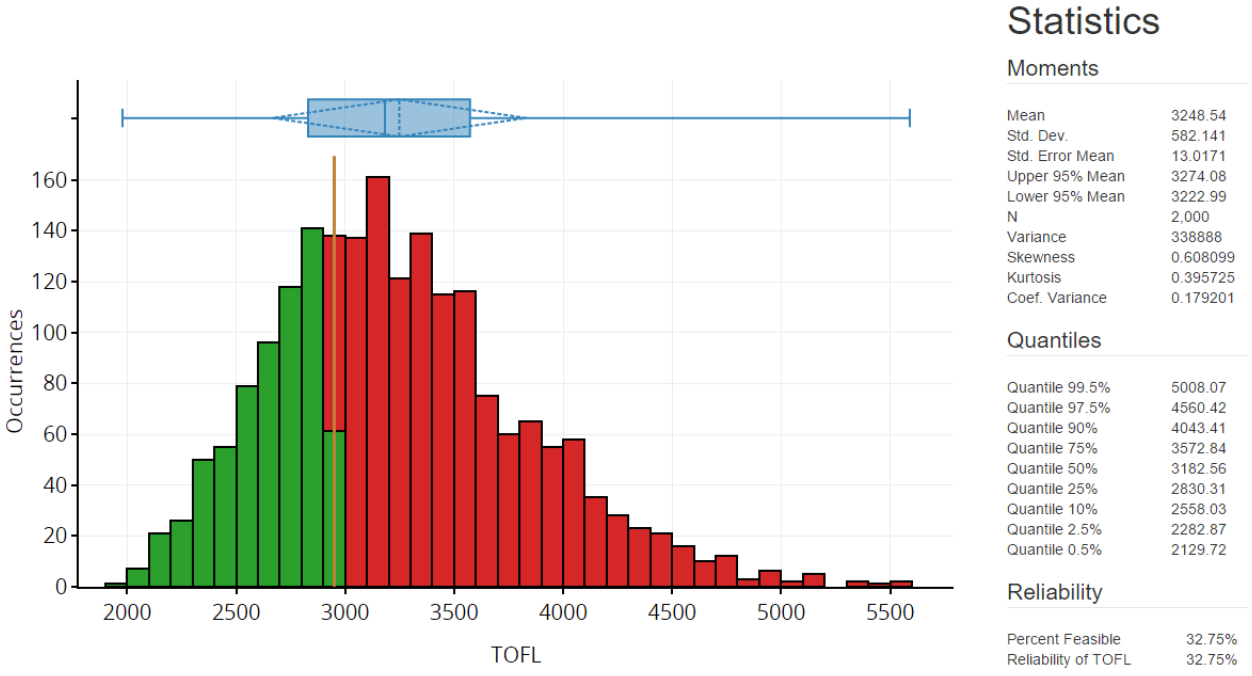

Figure 4-11: Histogram representing the TOFL distribution after running a Monte Carlo statistical analysis with 2 000 runs at Step 1 of the design phase

The study of sensitivity levels based on Pearson and Spearman correlation algorithms shows that the equation uncertainties parameters U_{TOFL} and $U_{T_{TO}}$ and the external noise factors are the most critical parameters. While there is no solution to improve the environmental conditions during the takeoff, a better understanding of the system and the development of a more accurate model can reduce the uncertainty coming from the equations and increase the reliability of the TOFL output.

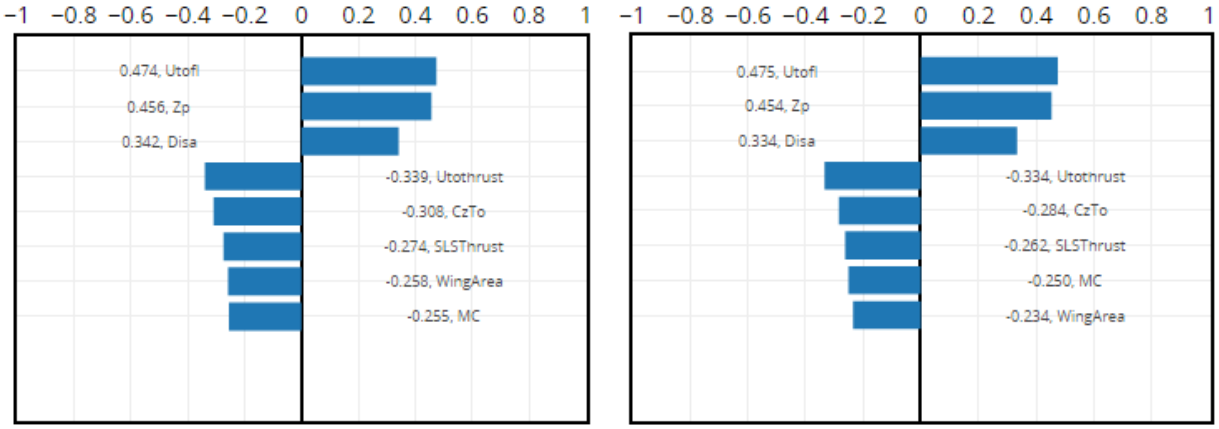

Figure 4-12: Sensitivity Levels based on Pearson (left) and Spearman (right) Correlation Algorithms

Parallel coordinates is a graphical tool representing the design configurations tested during the simulation and their associated output. Figure 4-12 highlights the runs driving to the worst TOFL results in the simulation. It clearly appears that high values of the takeoff altitude and ambient temperature lead to bad performances of the aircraft regarding the TOFL.

Furthermore, the parallel coordinates graph confirms the results of the sensitivity analysis regarding the equation uncertainty parameters. The worst design runs are clustered around the extreme values of U_{TOFL} and $U_{T_{TO}}$ intervals. To avoid these combinations in the future and mitigate the output variation, the variation interval of the parameters U_{TOFL} and $U_{T_{TO}}$ must be narrowed and centered to 1. It therefore requires the improvement of the model accuracy to reduce the equation uncertainties.

$C_{z,TO}$ is the most critical design parameter. It seems interesting to break down this variable by developing an analytical model linking the wings geometrical parameters and the lift coefficient. This decomposition will enable to identify in the next step of the design process the design parameters responsible for the variation of the lift coefficient of the aircraft.

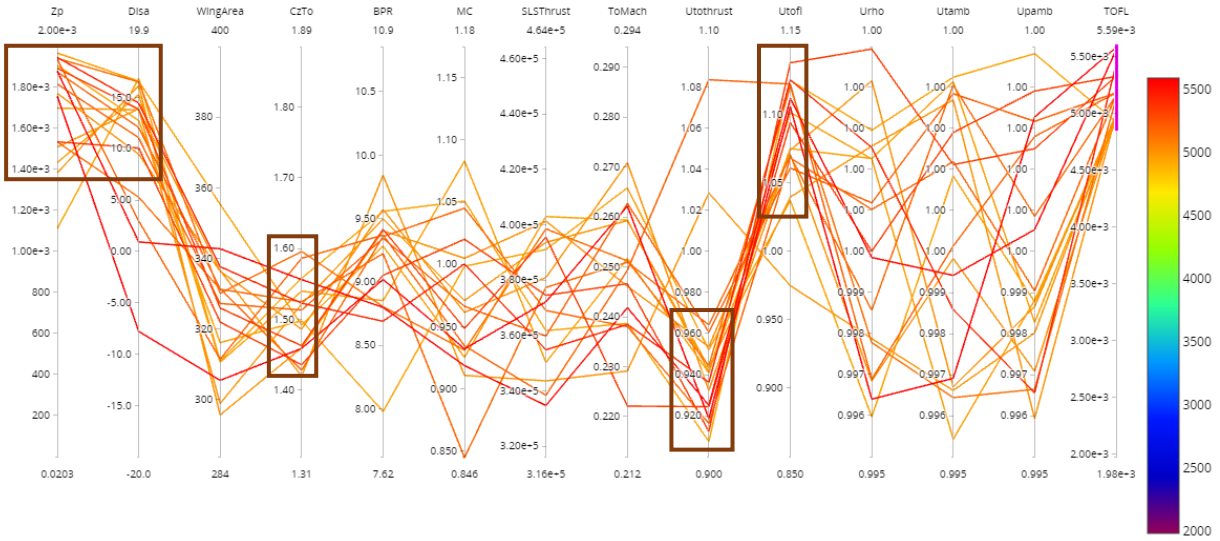

Figure 4-13: Parallel Coordinates graph filtering the worst outputs at Step 1 of the design phase

4.3.6 Step 2 CPM in design phase

Step 2 comes later in the design process of the new commercial aircraft. Engineers come up with a design decision about the aircraft wings: NACA 2412 airfoils profiles will equip the new aircraft. This standard wing design does not require much computational effort to evaluate the wing performances. Keane and Nair (2005) propose a more complex and detailed aircraft wing design (Keane and Nair 2005: 447–80), but the NACA configuration suits better regarding the computational limitations of the computer. The design decision concerning the wings' type increases the accuracy of the aircraft model and introduces new design parameters: the tip and root chords c_{Tip} and c_{Root}, the wing length L_{Wing} and the fuselage width l_{Fus}. $C_{z,TO}$, Ma_{TO} and A_{Wing} are no more input parameters but outputs in the analytical model. Three additional parameters characterize the uncertainty of the new transfer functions (Table 4-3).

Table 4-3: Introduction of new input parameters at Step 2 of the design phase

		List of new input parameters		Distribution Type	Lower Value	Upper Value	Mean	Standard Deviation
Design parameters	***Wings***	c_{Root}	m	Normal			13.7	5%
		c_{Tip}	m	Normal			0.35	5%
		L_{Wing}	m	Normal			23.32	5%
		l_{Fus}	m	Normal			5.69	5%
Equation uncertainties		$U_{C_{z,TO}}$	ø	Uniform	0.94	1.06		
		$U_{Ma_{TO}}$	ø	Uniform	0.97	1.03		
		$U_{A_{Wing}}$	ø	Uniform	0.99	1.01		

Designers also manage to reduce the interval bound of both U_{TOFL} and $U_{T_{TO}}$. The statistical uncertainty of BPR, MC and T_{SLS} is reduced by 2% in the meantime. Appendix B.2 synthetizes the PDF of the input parameters for this Step 2.

The model used to determine the mathematical relation between the wings dimensions and the lift coefficient $C_{z,TO}$ is based on a MatLab program, developed by Divahar (2009), which evaluates the lift coefficient from the wings characteristics. The transfer function linking the geometrical parameters of the wings and the lift coefficient is not directly accessible, but a Graphical User Interface (GUI) offers the possibility to test different design configurations. A full fractional design is manually performed and a MatLab function determines then a linear regression function between the wing chord dimensions, the wingspan and the lift coefficient. Figure 4-14 illustrates the wing model and the root and tip airfoils for the Step 2 of this Case Study. Transfer functions of Case Study 1 are used to establish the relation between the wing parameters, Ma_{TO} and A_{Wing}.

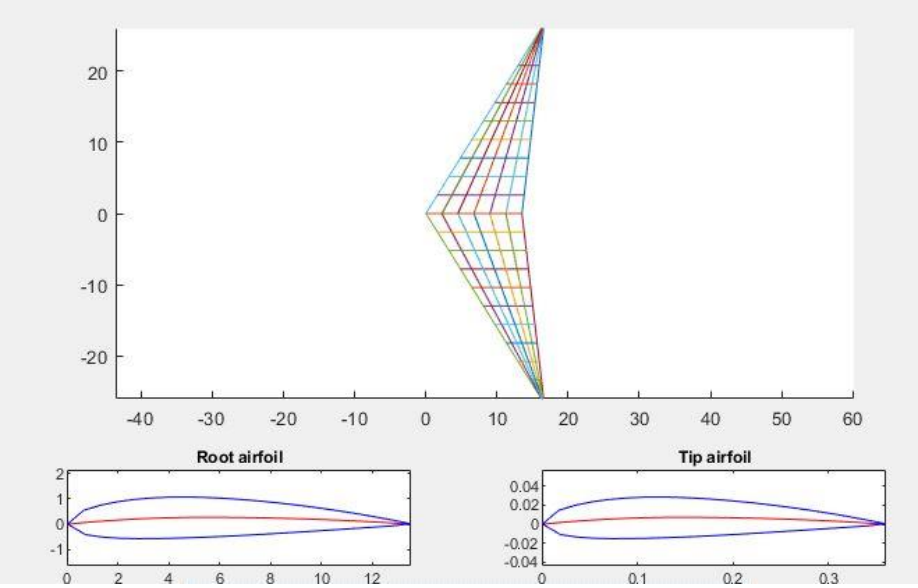

Figure 4-14: Representation of NACA 2412 wing design for both root and tip airfoils

Following the same procedure as previously, the transfer functions establishing the link between $C_{z,TO}$, A_{Wing}, Ma_{TO} and the lower system levels are implemented on MBSE Analyzer and integrated to the ModelCenter workflow. ModelCenter demonstrates a great modularity by the ease to add or remove equations from the workflow.

The work done to refine the analytical model since Step 1 enables breaking down some input parameters of the Step 1 and therefore extends the depth of the analytical tree (Figure 4-15).

A new Monte Carlo statistical analysis with 2000 runs is performed and shows an improvement of both TOFL mean value, from 3249 m to 2950 m, and TOFL reliability, from 33% to 52%.

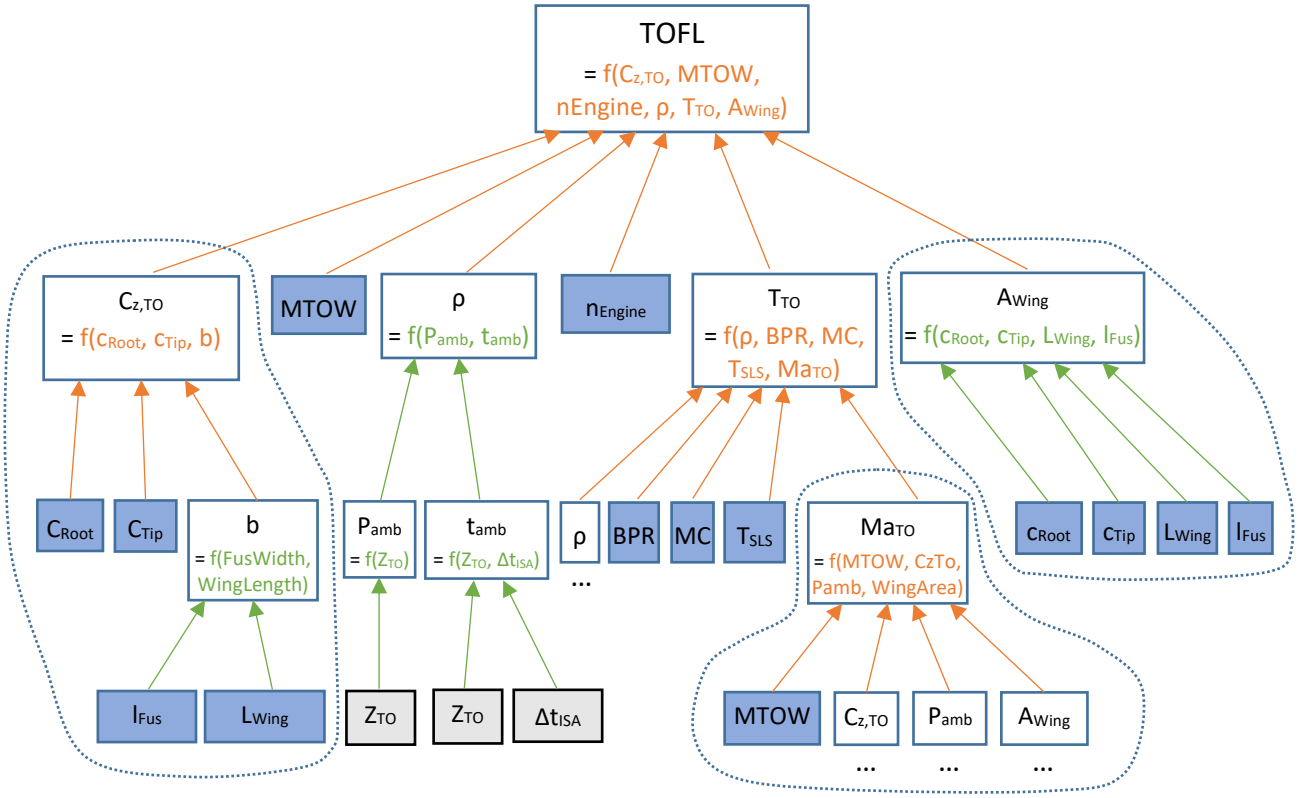

Figure 4-15: Decomposition of $C_{z,TO}$, Ma_{TO} and A_{Wing} in the analytical tree at Step 2 of the design phase

Figure 4-16 illustrates the results of the sensitivity analysis. The influence of U_{TOFL} and $U_{T_{TO}}$ decreases thanks to the work of the designers to enhance the accuracy of the design. The identification and assessment of Key Characteristics during the first step of the design phase proves to be useful to guide the designer's work. Among the input parameters introduced in this Step 2, the wing length and the root chord are the most critical parameters. Their variation must be mitigated before the next CPM implementation.

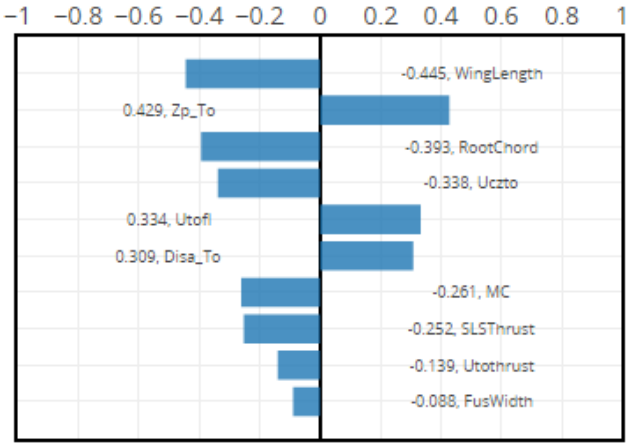

Figure 4-16: Sensitivity Analysis of the TOFL at Step 2 of the design phase, based on Pearson Correlation Algorithm

Parallel coordinates graph of Figure 4-17 filters the design runs having a high value for both L_{Wing} and c_{Root} parameters. These configurations achieve a great TOFL performance, below the requirement threshold. This analysis confirms the results of the sensitivity analysis: Designers should seek to increase the value of both geometrical parameters by the next step of the design process.

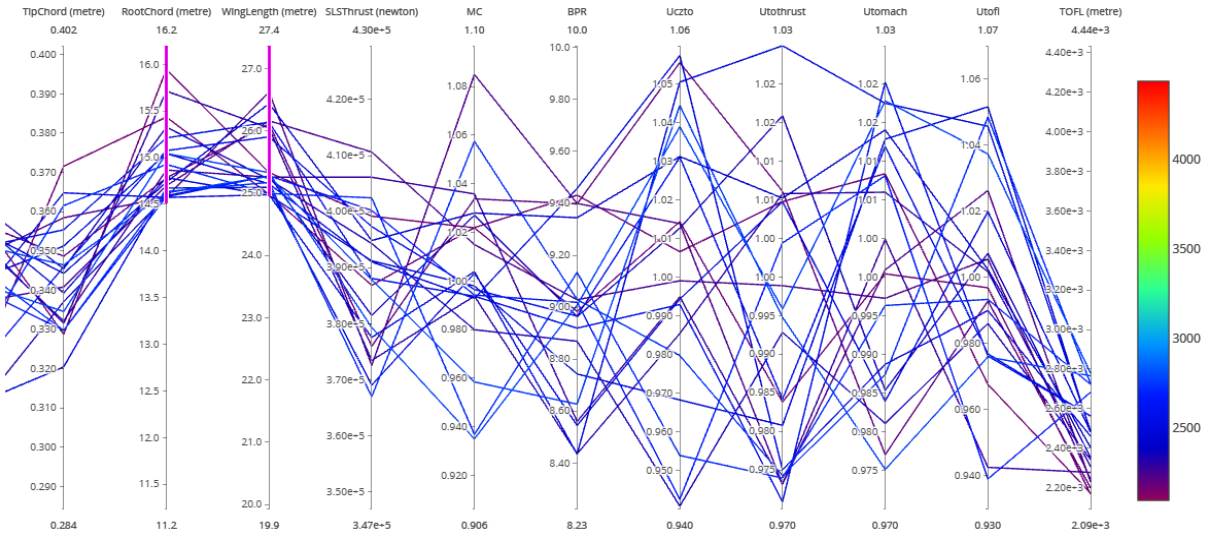

Figure 4-17: Parallel Coordinates graph filtering the high values of c_{Root} and L_{Wing}

Full Fractional Design of Experiments (See Part 2.3.2) illustrates the dependency between the input parameters' mean value and the TOFL. Regarding Prediction Profiler graphs (Figure 4-18), wing length, root chord and SLS thrust are the most critical parameters and their increase directly improves the output. Both sensitivity analysis results and Prediction Profiler graph underline the negligible effects of BPR and tip chord parameters on the TOFL performance. Their variation will no longer be simulated in the trade studies. Equation uncertainty parameters $U_{t_{amb}}$, $U_{P_{amb}}$ and U_b are ignored in the future analysis for the same reason.

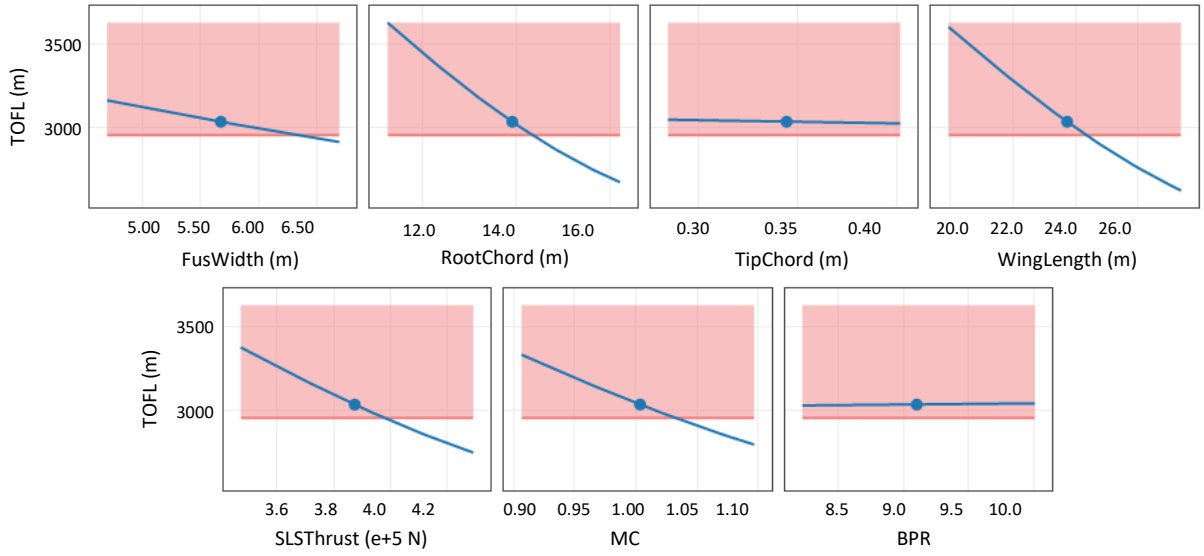

Figure 4-18: Prediction Profiler graph assessing the TOFL reliability at Step 2 of the design phase

4.3.7 Results and discussion

These two first design step analysis deliver a good overview of the tools proposed by MC to perform statistical analysis and DOE and to identify the CP. The next design steps conducting to a TOFL reliability greater than 97.5% are detailed in Appendix B.2. Table 4-4 describes the final configuration of the design parameters overcoming the reliability threshold.

Table 4-4: Final configuration of the input parameters after Step 6 of the design phase, satisfying the 97.5% reliability threshold for the TOFL performance

		Input parameters		Distribution Type	Lower Bound	Upper Bound	Mean Value	Standard Deviation
Perturbations		Z_{TO}	m	Uniform	0	2000		
		Δt_{ISA}	°	Uniform	-20	20		
Design parameters	***Wings***	c_{Root}	m	Normal			14.0	0.5%
		c_{Tip}	m	Normal			0.35	3%
		L_{Wing}	m	Normal			24.0	0.5%
		l_{Fus}	m	Normal			5.69	0.5%
	Engine	BPR	ø	Normal			9.13	0.5%
		MC	ø	Normal			1.04	3%
		T_{SLS}	N	Normal			400000	0.5%
Equation Uncertainties		U_{TOFL}	ø	Uniform	0.99	1.01		
		$U_{C_{z,TO}}$	ø	Uniform	0.99	1.01		
		$U_{T_{TO}}$	ø	Uniform	0.99	1.01		
		$U_{Ma_{TO}}$	ø	Uniform	0.99	1.01		
		$U_{A_{Wing}}$	ø	Uniform	0.99	1.01		

This CPM implementation over the design process demonstrates the quality of the probabilistic analysis tools of ModelCenter. The monitoring of critical parameters and the mitigation strategies proposed at each step of the design process progressively shift the TOFL distribution towards lower values, decrease the standard deviation and thus improve the TOFL reliability (Figure 4-19).

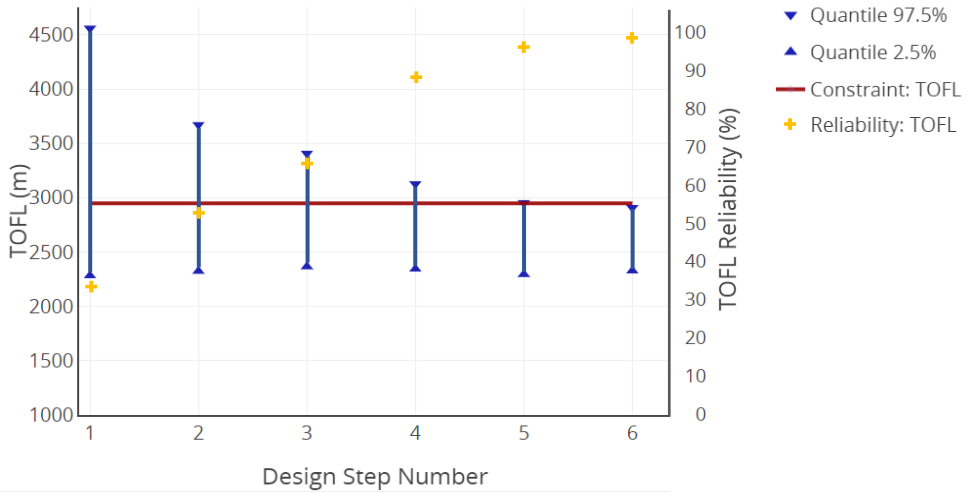

Figure 4-19: Evolution of the TOFL distribution and reliability according to probabilistic analysis over different steps of the design phase

Figure 4-20 represents the results of the Monte Carlo analysis with 2000 runs at Step 1 and Step 6 of the design process regarding the TOFL. The mitigation measures based on the uncertainty analysis of the different design steps contribute to the shift and narrowing of the TOFL density function, thus reducing the proportion of defect systems, represented by red bars in the histogram, and achieving the reliability criteria initially set.

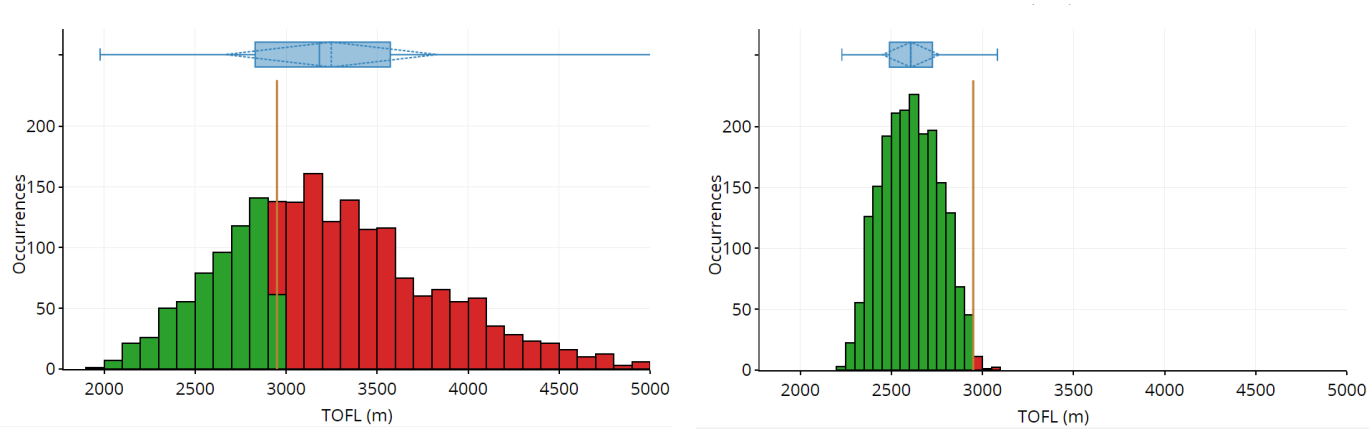

Figure 4-20: Evolution of TOFL distribution between the Step 1 (left) and the Step 6 (right) of the design phase

The Case Study yields interesting insights into Critical Parameter Management in early steps of the PLC and its implementation on ModelCenter:

- Early in the design process, the model uncertainty is high. The equation uncertainty parameters hold the top positions of the sensitivity levels ranking. The uncertainty propagation coming from the design parameters is therefore difficult to analyse. Design decisions and model improvement can reduce equation uncertainties.

- The sensitivity levels ranking, based on Pearson and Spearman correlation algorithms presented in Part 2.3.3, is useful to identify both critical parameters and inputs which variation has no consequence on the output. The latter can be set constant and removed from the Trade Study to reduce the complexity of the analysis.

- DOE are useful to confirm the results of the sensitivity analysis. The Prediction Profiler Profiler interactive tool displays instantaneously the effect of the modification of a design parameter on the output.

- The parallel coordinates graph, which represents the runs of the statistical analysis, provides a good overview of the simulation. In some cases, the application of constraint filters can lead to identify the critical parameters and the range of values causing defects. However, it is sometimes complex to draw conclusions from the parallel coordinates graph.

- The definition of parameters characterizing the environmental conditions during takeoff allows bringing the external noise factors into the probabilistic simulations. The variation of the external parameters is important to consider, even if there is sometimes no mitigation solution to reduce the impact of their variation.

Finally, this CPM implementation from the early steps of the design process proves to be an efficient method to manage the uncertainty and to guide the development of new aircraft systems. This systematic approach reduces the overall development duration by moving the knowledge curve of the system towards earliest steps of the PLC. The collaborative Cameo/ModelCenter software environment handles this CPM process and ModelCenter tools provide interesting insights about the system variation.

4.4 Case Study 3: Competing requirements issue

The previous section introduces the different analysis tools to identify the critical parameters related to one requirement on ModelCenter. However, complex systems have plenty of requirements to meet. The holistic approach of design under uncertainty requires analyzing their dependencies and tackling the CPM of the different outputs all on once. This section therefore addresses the problem of competing requirements.

4.4.1 Initial situation

While the previous CPM implementation focuses on only one output performance, the TOFL, the other performances analyzed in Part 4.2 for the aircraft in production are reintroduced in this section. Figure 4-21 provides the requirements characteristics for this Case Study.

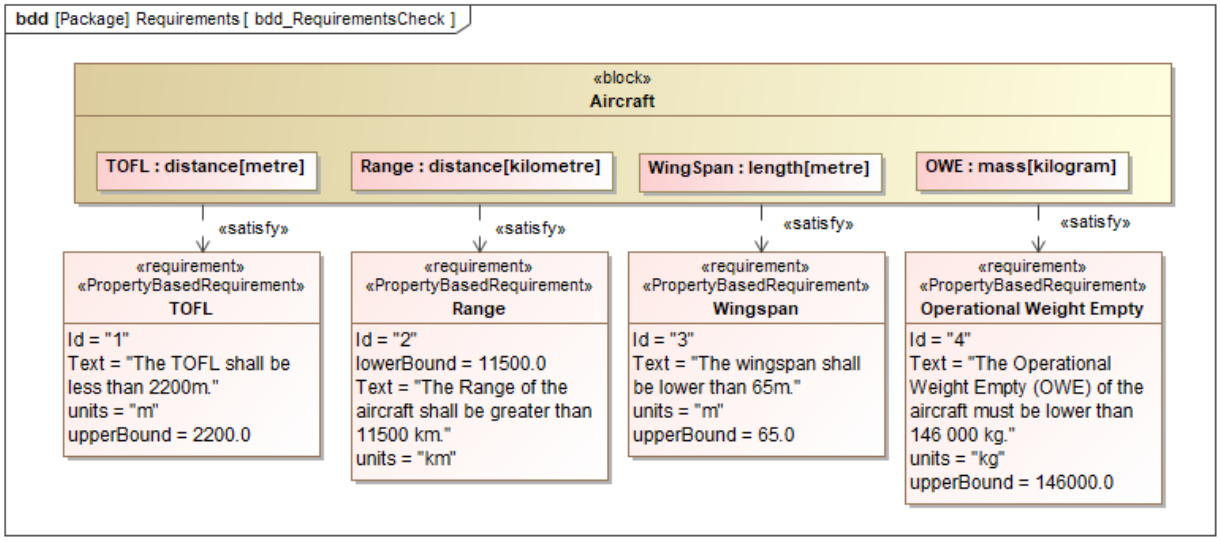

Figure 4-21: Requirement diagram of the aircraft in Case Study 3

For the sake of clarity, the study do not further consider the external perturbation parameters Z_{TO} and Δt_{ISA} and the equation uncertainty parameters U_Y. It is supposed that the takeoff altitude is at mean sea level, the ISA model also attributes the following value to the ambient temperature: $t_{amb} = 15\,°C$.

4.4.2 System modeling

This analysis requires the creation of new variables and equations in Cameo. The modularity of the modeling enables keeping the descriptive and analytical models of Part 4.3. The increase of the number of equations and variables raises the question of the structural organization of the descriptive model. How to configure the parametric diagrams on Cameo Systems Modeler in order to keep clarity and ensure flexibility of the model?

On the one hand, the creation of lots of independent parametric diagrams ensures a great clarity even for complex systems. On the other hand, the use of only one parametric diagram provides an overview of the global system and represents all the dependencies between the variables. As engineering teams work apart on different components and characteristics of the global systems, the use of a unique parametric diagram does not seem to be the best solution regarding model modularity. The equations' folder structure, regrouping the equations by specific categories, serves as a basis for the parametric diagrams' structure, all located on the SOI level and tackling a precise analysis category (Figure 4-22). MBSE Analyzer creates then a workflow on ModelCenter to solve the equations of each constraint block of the parametric diagrams. This clustering of analytical models within a same workflow allows to calculate several aircraft performances in a single simulation process on ModelCenter.

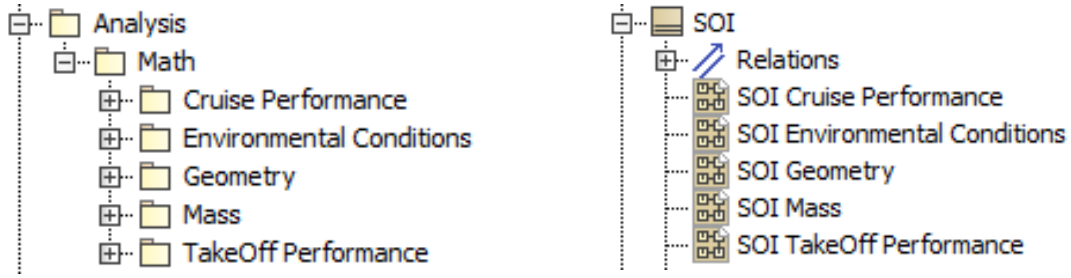

Figure 4-22: Structural modularity and homogeneity of the constraint block equations and of the parametric diagrams on Cameo Systems Modeler

Table 4-5 lists the input parameters for this Case Study and their initial statistical characteristics, namely their mean value and their standard deviation. The design parameters are more numerous than for Case Study 2.

Table 4-5: Initial PDF of the input parameters in the Case Study 3

Input parameters		Distrib Type	Mean Value	Standard Dev.	Input parameters		Distrib Type	Mean Value	Standard Dev.
c_{Root}	m	Normal	13.70	3%	MC	ø	Normal	1.01	3%
c_{Tip}	m	Normal	0.35	3%	T_{SLS}	N	Normal	381900	3%
L_{Wing}	m	Normal	29.17	3%	$V_{FuelBlock}$	m³	Normal	101.05	3%
Λ_{Sweep}	rad	Normal	0.56	3%	A_{Htp}	m²	Normal	85.00	3%
l_{Fus}	m	Normal	5.69	3%	A_{Vtp}	m²	Normal	51.00	3%
h_{Fus}	m	Normal	6.42	3%	L_{Nac}	m	Normal	5.72	3%
L_{Fus}	m	Normal	63.54	3%	l_{Nac}	m	Normal	4.01	3%
BPR	ø	Normal	9.26	3%					

4.4.3 Comparison of sensitivity analysis methods

The analytical workflow gains in complexity, as the number of function evaluations to compute the four aircraft performances increases. It therefore seems interesting to put in perspective the tradeoff between computing time and estimation accuracy for different probabilistic analysis methods on ModelCenter.

Table 4-6 lists the results of four probabilistic analysis methods. As random probabilistic sampling ensures precise results for high number of runs, the 10 000 runs Monte Carlo simulation serves as a reference to evaluate the accuracy of the other methods. The NESSUS probabilistic analysis tool strongly reduces the number of evaluations to estimate the reliability of the different outputs. Southwest Research Institute (2012) gives more information about the NESSUS statistical tool. If Monte Carlo provides a better accuracy with a high number of simulation runs, NESSUS delivers accurate results quickly, which is very important when it comes to the integration to more complex systems.

Table 4-6: Comparison of probabilistic analysis methods in Case Study 3

Method	Number of evaluations	Computing time	Reliability $Range$	Reliability $TOFL$	Reliability OWE	Reliability $WingSpan$
Monte Carlo	10 000	6 h 36’	0.997	0.989	0.838	0.711
NESSUS Mean Value	64	2’	0.996 (-0.1%)	0.995 (+0.6%)	0.841 (+0.4%)	0.709 (-0.3%)
NESSUS AMV+	256	8’	0.997 (-0%)	0.990 (+0.1%)	0.840 (+0.2%)	0.709 (-0.3%)
NESSUS FORM	576	22’	0.997 (-0%)	0.990 (+0.1%)	0.840 (+0.2%)	0.709 (-0.3%)

Because of its efficiency and accuracy, NESSUS Advanced Mean Value (AMV) + supports the reliability analysis in this Case Study. Reliability estimates have indeed a deviation of less than 0.3% from the results of the Monte Carlo analysis, which is good enough to have an order of magnitude of the system reliability in this Case Study. This

small deviation might however have an influence during reliability-based optimization and will need further attention in Chapter 6. In addition, NESSUS AMV+ requires only 256 evaluations to provide a reliability estimate and considerably reduces the computing time compared to a Monte Carlo analysis.

4.4.4 Results and discussion

Figure 4-23 illustrates the results of the NESSUS AMV+ sensitivity analysis regarding the TOFL and the OWE outputs. Several Mean and Standard Value parameters stand out and turn out to be the critical parameters of the aircraft. Whereas the mean value of L_{Wing}, L_{Fus}, l_{Fus}, c_{Root}, T_{SLS} and h_{Fus} must be increased to improve the reliability of the TOFL performance, lower mean value of L_{Wing}, L_{Fus}, T_{SLS} and c_{Root} lead to an enhanced OWE reliability. Regarding the standard deviations, wing length appears to be the most critical parameter for both performances.

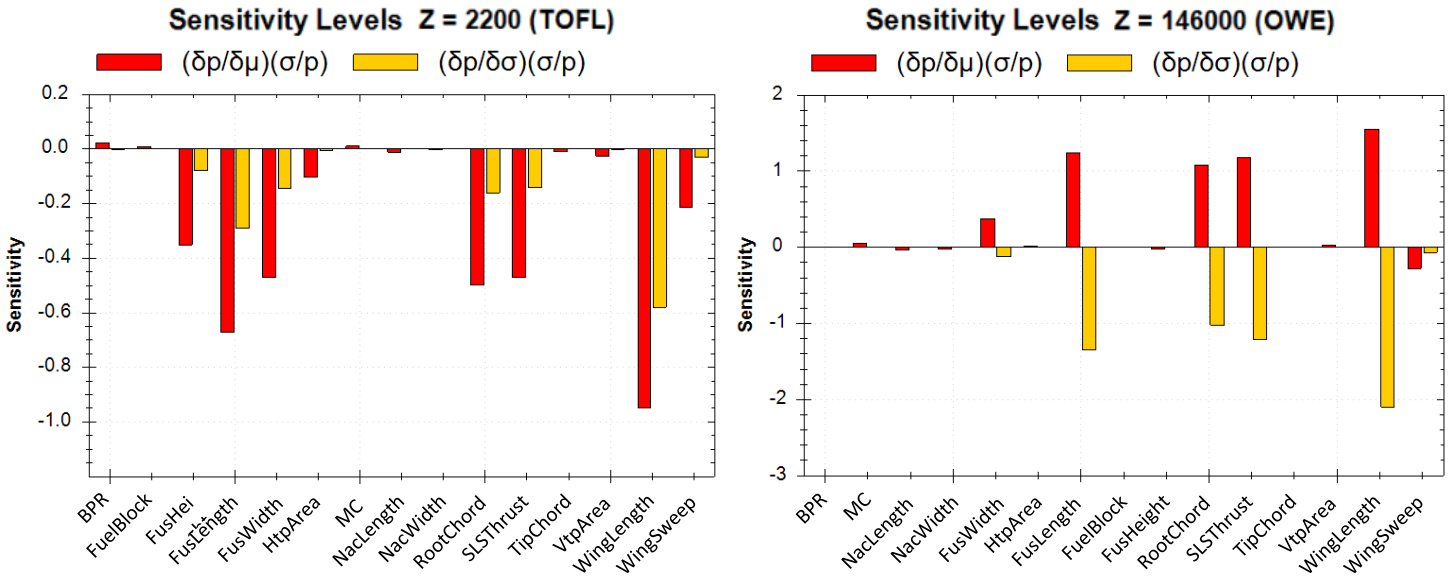

Figure 4-23: Results of the NESSUS AMV+ Sensitivity Analysis of TOFL and OWE outputs

A first review of the results provides a set of design decisions to improve the reliability of both performances. The lower the mean value of the wing sweep, the greater the TOFL and the OWE reliabilities. Furthermore, the shrinking of the standard deviation of the wing length, the fuselage length and the SLS Thrust enhance the global system reliability.

However, most of the time, measures to improve the OWE and the TOFL performances are competing against each other. For instance, a greater mean value of the wing length will lead to a greater TOFL reliability on the one hand, but increases the probability of failure of the OWE requirement on the other hand. It thus requires further studies to draw conclusions and handle this competing requirement issue.

A DOE is set to analyze the relation between the mean and the standard deviation values of each input parameter and the requirements reliability. A combination of Design Orthogonal Explorer and LHS methods is conducted in that respect. Prediction Profilers represent the dependencies between several input parameters. The required reliability threshold splits the Prediction Profiler graph into different areas. The white area shows all the valid design configurations, which meet the reliability-based constraints, while the colored areas correspond to designs that do not reach at least one of the reliability thresholds.

Figure 4-24 investigates the relation between the mean value and the standard deviation value of the wing length parameter regarding TOFL and OWE reliabilities. Two situations are imagined to underline the importance of the reliability constraints on the aircraft design. In the first case, the reliability thresholds of both TOFL and OWE requirements are set to 95%. These threshold are set equal to 99% in the second case. The black point on the graphs represents the standard design configuration. If all other parameters remain constant, the increase of wing length mean value can be sufficient to meet the 95% reliability threshold for both performances. If the design solution aims to ensure a 99% reliability, the standard deviation of the wing length parameter must be reduced too.

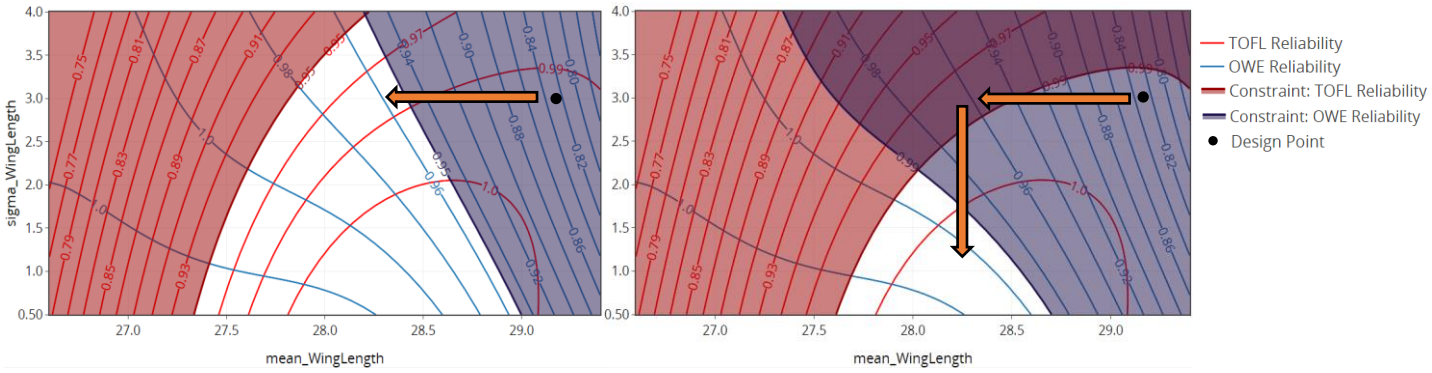

Figure 4-24: Prediction Profiler representing the system reliability regarding TOFL and OWE constraints in function of the mean and the standard deviation values of the wing length in the case of a 95% (left) and a 99% (right) reliability thresholds for both TOFL and OWE

The interaction between different critical parameters is also visible on prediction profiler graphs. Figure 4-25 draws the dependencies between L_{Wing} and T_{SLS} to fall inside the valid space domain. The engineers working on the engine design and those responsible for the wing geometry must therefore collaborate to satisfy the reliability level required by the customer.

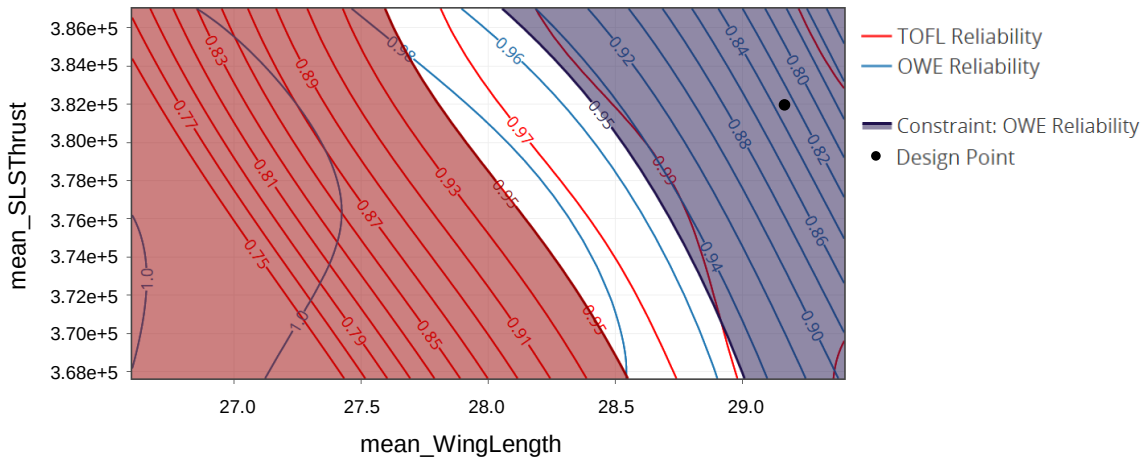

Figure 4-25: Prediction Profiler representing the dependencies between the mean values of wing length and SLS Thrust and the system reliability, in the case of a 95% reliability constraint for both TOFL and OWE

In conclusion, independent Sensitivity Analysis for each performance may not be sufficient to identify the critical parameters of the global system. If there is no competing effect for a given input to improve all requirements' reliabilities, the parameter do not need further study. However, for most of the design parameters, the modification of their PDF have opposite effects on the different performances. The Prediction Profiler graphs put in perspective the dependency between the input parameters and illustrate the design tradeoff due to competing requirements. The graphical representation of the constraints and the feasible domains helps improving the design in such competing requirement situation.

4.5 Conclusion and integration perspectives

In conclusion, the collaborative software environment described in Chapter 3 copes with the implementation of CPM to a basic commercial aircraft model. From the modeling on Cameo with the support of MBSE Pak, to the SA on ModelCenter, the collaborative software environment supports the clustering of descriptive and analytical models into a unique process. SysML ensures the modularity of the Cameo system structure, facilitating the data-transfer and the refinement of existing models (Part 4.4). The partial automation of the linkage between the variables on Cameo and ModelCenter helps ensuring the traceability property.

ModelCenter's ability to perform multi-level simulations affords to implement CPM early in the design phase and to guide the development process of a new product. ModelCenter proposes a wide portfolio of SA methods and DOE. The analysis enables the identification and the assessment of KC, and provides interesting insights about the uncertainty propagation in the system to come up with mitigation strategies.

Furthermore, the last Case Study exhibits some limits of the SA when tackling several requirements. Further studies may be needed to assess the key characteristics in case of conflicting requirements.

The successful implementation of the CPM flowcharts (Figure 3-7 and Figure 3-8) for three real case studies raises the question of the integration to more complex aeronautical systems. This challenge addresses three different topics:

- System Modeling: the Cameo - ModelCenter interaction works great. MBSE Analyzer Plugin sets the connection between Analysis Server and the constraint blocks on Cameo. Analytical models can be integrated to ModelCenter process through Analysis Server App and Component Plug-Ins. ModelCenter can regroup models from different engineering teams relatively easily and ensures the traceability of the variables between the different models.

  The definition of a hierarchy pattern for the parametric diagrams is necessary to ensure the modularity of the descriptive model and the integration to complex aeronautical systems. Part 4.4.2 comes up with a modeling solution.

- Uncertainty modeling: Since the CPM is meant to be data-driven, the biggest issue of the modeling is the lack of knowledge about the system to model. While the use of former system models and properties represents a good starting point to the modeling of a new system, it might not be consistent enough to carry out uncertainty analysis. Designers and engineers responsible for the development of a new system must come up with a detailed uncertainty model to carry out the CPM. Design parameter uncertainty, external perturbation uncertainty and modeling uncertainty are three uncertainty categories tackled as example in the Case Studies. The probabilistic analysis tools of ModelCenter propose a large choice of PDF to propagate the input variations upwards in the analytical tree.

- Statistical analysis tools: The diversity of the DOE and sensitivity analysis tools on ModelCenter ensures a good monitoring of the KC along the life cycle of a product. The Case Studies provide a good overview of the useful graphs and tools to identify both critical parameters and irrelevant variables that can be neglected in the statistical analysis. The diversity of algorithms and sampling methods on ModelCenter suits for all kind of model complexity. A compromise must be found between estimation accuracy and computing time (Table 4-6). The question of computational complexity and possible remedies is tackled in Chapter 6, as it is the main issue of the optimization studies.

5 Deterministic design optimization of the aircraft

During the development process of a new complex system, the objective of the engineers is to maximize the technical performances of the system, while minimizing the development costs in the meantime. To support multi-objective optimization, a set of objective functions and configuration parameters must be defined in a first time.

For the next chapters, the system of interest is a new commercial aircraft in its design phase and the model built up in the Case Study 3 remain valid. Multi-objective optimization aims to adjust the design parameters to come up with the best alternative in terms of performances and costs. The optimization process follows the flowchart created in Chapter 3 (Figure 3-9).

While Chapter 5 describes the implementation of a deterministic optimization, the reliability-based optimization of Chapter 6 brings the reliability and the uncertainty propagation analysis into the optimization loop. The best design solutions will finally be compared and the results discussed.

5.1 Initial situation

The study relies on the descriptive and analytical models created in the previous chapter. Like in Case Study 3, for the sake of clarity, the model does not consider the uncertainty coming from the external perturbations and from the transfer functions. Table 5-1 specifies the fifteen design parameters inputs and their initial PDF properties before the optimization. All input parameters follow a Gaussian distribution, as it is the most common model to describe the variation of design parameters in manufacturing (Thornton 2003: 27). Their initial standard deviation is set to 4%. The requirement diagram remains the same than the one defined in Figure 4-21.

Table 5-1: PDF of input parameters before the optimization

Design Parameters i	Units	Distribution Type	$\mu_{i,ini}$	$\sigma_{i,ini}$ (in %)
BPR	Ø	Normal	9.13	4%
A_{Vtp}	m²	Normal	51	4%
A_{Htp}	m²	Normal	85	4%
l_{Fus}	m	Normal	5.69	4%
L_{Wing}	m	Normal	28	4%
c_{Tip}	m	Normal	0.35	4%
c_{Root}	m	Normal	13.70	4%
L_{Fus}	m	Normal	65.31	4%
h_{Fus}	m	Normal	6.42	4%
L_{Nac}	m	Normal	5.72	4%
l_{Nac}	m	Normal	4.01	4%
T_{SLS}	N	Normal	387000	4%
MC	Ø	Normal	1	4%
$V_{FuelBlock}$	m³	Normal	103	4%
Λ_{Sweep}	rad	Normal	0.56	4%

Chapters 5 and 6 remain consistent with the mathematical formalism introduced in the theoretical background (Part 2.4). Furthermore, the list of design parameters is denoted Ω (Eq. (5-1)) and the vector $\boldsymbol{x}$ represents the aircraft design and contains the set of mean and standard deviations of the different parameters belonging to Ω (Eq. (5-2)).

In this Case Study, four system performances are considered: the TOFL, the OWE, the range and the wingspan of the aircraft constitute the Δ set. For the sake of clarity in the equations, TOFL, OWE, the range and the wingspan will be noted L_{TO}, M_{OWE}, d_{Range} and b, respectively (Eq. (5-3)).

$$\Omega = \begin{Bmatrix} BPR, A_{Vtp}, A_{Htp}, l_{Fus}, L_{Fus}, h_{Fus}, c_{Tip}, c_{Root}, \\ L_{Wing}, L_{Nac}, l_{Nac}, T_{SLS}, MC, V_{FuelBlock}, \Lambda_{Sweep} \end{Bmatrix} \quad \textbf{Eq. (5-1)}$$

$$\boldsymbol{x} = (\mu_i, \sigma_i)_{i \in \Omega} \quad \textbf{Eq. (5-2)}$$

$$\Delta = \{L_{TO}, M_{OWE}, d_{max}, b\} \quad \textbf{Eq. (5-3)}$$

5.2 Problem definition

The implementation of a deterministic optimization requires a precise mathematical problem definition. This part focuses on the specification of the design space range, defines the objective functions and lists the constraints to meet the requirements. These three topics are the milestones to carry out a meaningful optimization (See Figure 3-9).

5.2.1 Design parameters

Table 5-1 lists the fifteen input parameters of the analytical model, which rule the main design concepts of the aircraft: the wings, the fuselage and the tails geometry as well as the engine bloc properties directly depends on these parameters.

Optimization requires defining a design space for each input variable. Thus, the mean value and standard deviation value of each design parameter must be bounded. In this deterministic optimization, each design variable's mean μ_i might take a value within the +/- 5% interval around its initial value before optimization $\mu_{i,ini}$ (Eq. (5-4), Eq. (5-5)). The standard deviation σ_i can evolve between 0.5 % and 4 % of the mean μ_i (Eq. (5-6), Eq. (5-7)).

$$\forall\, i \in \Omega, \quad \begin{cases} \mu_i^L = 0.95 \cdot \mu_{i,ini} & \textbf{Eq. (5-4)} \\ \mu_i^U = 1.05 \cdot \mu_{i,ini} & \textbf{Eq. (5-5)} \end{cases}$$

$$\forall\, i \in \Omega, \quad \begin{cases} \sigma_i^L = 0.005 \cdot \mu_i & \textbf{Eq. (5-6)} \\ \sigma_i^U = 0.04 \cdot \mu_i & \textbf{Eq. (5-7)} \end{cases}$$

Eq. (5-8) and Eq. (5-9) define the boundary conditions of the deterministic design optimization:

$$\forall\, i \in \Omega, \qquad \begin{cases} \mu_i^L \leq \mu_i \leq \mu_i^U & \textbf{Eq. (5-8)} \\ \sigma_i^L \leq \sigma_i \leq \sigma_i^U & \textbf{Eq. (5-9)} \end{cases}$$

5.2.2 Definition of objective function

Engineering and finance domains are often separated during the development process of a new aircraft (Markish and Willcox 2003). However, the simplification of data transfer between models and teams in the context of MBSE makes it possible to improve the MDO.

During the design phase, engineers seek both to maximize the performance of the new system and to reduce costs, which leads to conflicting objectives. Two objective functions are introduced in this part: a cost objective function and a performance objective function, assessing the level of technical performance of the system. These functions ensure the data-driven and holistic nature of the optimization.

A simple and coherent model is proposed. The objective is not to define the most accurate cost and performance models but to study their implementation within the framework of a RBDO on ModelCenter. Moreover, in order to homogenize the behavior of the two objective functions which do not have the same unit, they will be defined in such a way that 1 corresponds to the worst output and 0 to the best result.

5.2.2.1 Definition of performance objective function

Some performances commonly evaluated for a commercial aircraft are the range, the fuel consumption, the maximum number of passengers, the OWE and the Maximum Takeoff Weight (MTOW). The notions of Best in Class (BIC) and Worst in Class (WIC) are important while defining a performance model. They respectively refer to the highest and lowest current performance levels in the industry. The performance objective function can therefore base the evaluation of the design solution on the WIC and BIC performance values.

In addition, the performance objective function can consider the risk aversion of the customer in its definition (Rabin 2000). Krüger et al. (2015) define a utility function based on the customer's aspiration level, the uncertainty associated with its realisation and the risk aversion of the customer. The customer can be either risk seeking, either risk neutral or risk averse.

For the sake of simplicity, this Case Study does not address the risk aversion of the customer. The range, the TOFL, the OWE and the wingspan are the four performances considered in the analysis. For each of them, an aspiration level must be set. The optimization configuration intend to minimize the performance objective function, which values evolve within the interval $[0\,;1]$ (Part 5.2.2). BIC performance corresponds to the best performance in the industry, so the performance objective function will associate the value 0 to $p_{j,BIC}$. WIC performance corresponds to the worst performance

in industry so $p_{j,WIC}$ get equal to 0. The evolution of the performance objective function is set linear between these two points. Table 5-2 lists the BIC and WIC values for the four performances.

Table 5-2: BIC and WIC performance values for the range, the TOFL, the OWE and the wingspan

Perf. j / BIC/WIC	$Range$ (in km)	$TOFL$ (in m)	OWE (in kg)	b (in m)
$p_{j,BIC}$	15 400	1 600	135 500	57.0
$p_{j,WIC}$	10 800	2 350	148 500	66.5

Figure 5-1 maps the performance objective function evolution between $p_{j,BIC}$ and $p_{j,WIC}$, and Eq. (5-10) represents the final performance objective function for the optimization. Weight factors are introduced to set up the relative importance between the different performances. Sum of weights factors must equal 1 to ensure a total performance function included between 0 and 1 (Eq. (5-11)).

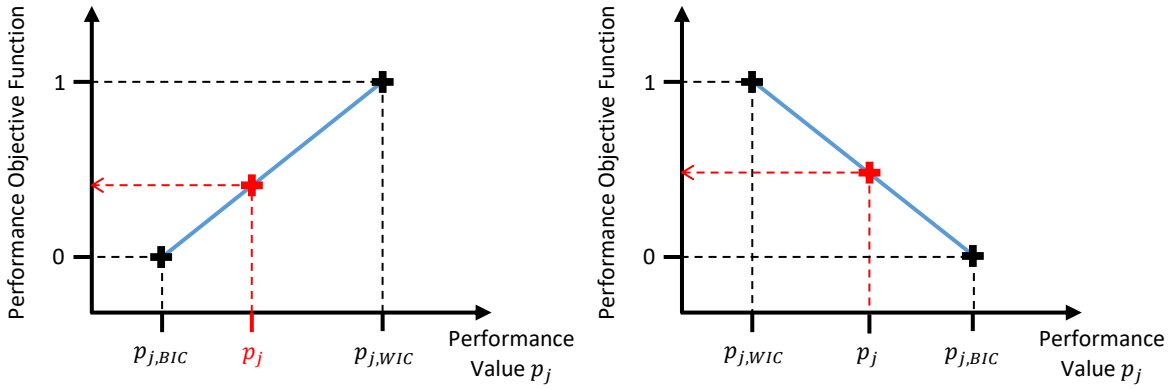

Figure 5-1: Representation of the Performance Objective Function depending on the Best in Class and Worst in Class values

$$f_{Perf}(\boldsymbol{x}) = \sum_{j \in \Delta} w_j \cdot \left(\frac{p_{j,BIC} - p_j}{p_{j,BIC} - p_{j,WIC}} \right) \qquad \textbf{Eq. (5-10)}$$

$$s.t. \sum_{j \in \Delta} w_j = 1 \qquad \textbf{Eq. (5-11)}$$

$f_{Perf}(\boldsymbol{x})$ is the global performance objective function and p_j represents the value of the performance j. w_j is the weight factor associated to the performance j.

In order to carry out a quantitative and objective analysis, it is necessary to avoid weighting the performances subjectively. Keane and Nair (2005) describes the consistent eigenvalue method relying on multiple pairwise comparisons between the different performances (Keane and Nair 2005: 166–7). While the range and the OWE are considered as the most important performances in the Case Study, the wingspan value has not so much influence on the customer opinion. Appendix B.3 describes in detail the different steps of the calculation to come up with the following weighting configuration, which verifies Eq. (5-11):

$$\begin{pmatrix} w_{d_{Range}} \\ w_{M_{OWE}} \\ w_{L_{TO}} \\ w_b \end{pmatrix} = \begin{pmatrix} 0.4 \\ 0.3 \\ 0.2 \\ 0.1 \end{pmatrix} \qquad \textbf{Eq. (5-12)}$$

5.2.2.2 Definition of cost objective function

The definition of cost estimation models for aircrafts is necessary to guide and test preliminary aircraft design. In the literature, costs are split up into two main categories: Direct Operating Costs (DOC) and Indirect Operating Costs (Oliveira 2015). The latter are rather hard to estimate given their high reliance on the customer buying the aircraft. DOC and DOC_{sys} are the two most used operating cost models. They cover aircraft depreciation, fuel consumption, maintenance and storage costs (Westphal and Scholz 1997; Scholz 1998). These models are very complex and regressions exist in order to link the component masses and the MTOW of the aircraft to the DOC (Ali and Al-Shamma 2014). Although some papers introduce models to bridge the gap between design parameters and aircraft costs (Urdu 2015; Zijp 2014), there is no global cost model taking the component level properties as inputs in the literature (Scholz 2017). The impact of manufacturing uncertainty on the aircraft's operating costs is also difficult to quantify.

Other cost categories applicable to the system are rework costs, development costs and production costs. Manufacturing and assembly uncertainty lead to defect parts, which need a rework or a replacement. The Taguchi cost of poor quality model quantifies the occurring rework costs (Thornton 2003) and therefore considers the influence of manufacturing and assembly uncertainty on the global system costs (Tsou 2007; Saravi et al. 2013). Wu and Wang (2012) seek to extend tolerancing and variation analysis by considering PLC costs and not only manufacturing costs.

Since the case study does not pretend to come up with a revolutionary cost model and data about product specifications is hardly available in this early design stage, a simple cost function is set up. The goal is mainly to confront the performance optimization under uncertainty to the reduction of development costs. The initial design configuration of the system before optimization serves as basis for the definition of the cost model.

The cost objective function considers that any modification of parameter from its initial value will lead to additional development costs. It will be supposed that the costs will linearly increase with a shift of an input mean from its initial value and exponentially increase with a reduction of an input standard deviation (Eq. (5-13)). Figure 5-2 schematizes the impact of a mean shift or a standard deviation decrease on the cost objective function.

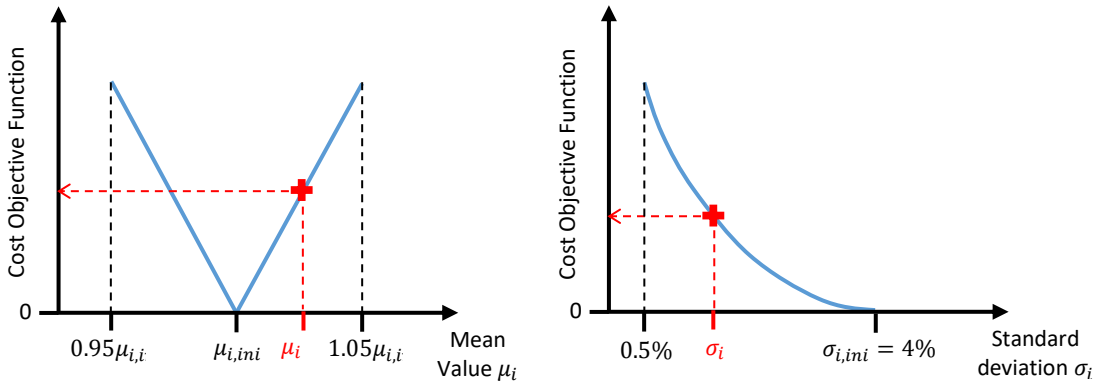

Figure 5-2: Projections of the Cost Objective Function to see the dependence with the mean value and the standard deviation of each input parameter

$$C(\boldsymbol{x}) = \sum_{i \in \Omega} \left[\frac{\left|\mu_i - \mu_{i,ini}\right|}{\mu_{i,ini}} \cdot c_i + \frac{\left(\sigma_{i,ini} - \sigma_i\right)}{\sigma_i} \cdot q_i \right] \qquad \textbf{Eq. (5-13)}$$

Cost factors c_i and q_i reflect the relative contribution of the input parameters on the development costs.

The cost factors may be different for each design parameter. However, for the sake of model simplicity, the design parameters are organized into categories: nacelle, tails, wings, engine and fuselage. Cost factors are considered to be the same within a category. A relative weighting is established between the categories, considering that modifications of the fuselage and the engine parameters lead to more additional costs than the other parameters due to their technical complexity and their importance in the aircraft design. Table 5-3 illustrates the cost factors set up.

Cost Objective Function of Eq. (5-13) requires a normalization to have the same order of magnitude as the Performance Objective Function. A full fractional DOE provides the maximum output of the Cost Function defined in Eq. (5-13). Eq. (5-14) uses this result to normalize the cost function, which is now included between 0 and 1 like the Performance Function.

$$f_{Cost}(\boldsymbol{x}) = \frac{C(\boldsymbol{x})}{\max C} \qquad \textbf{Eq. (5-14)}$$

Table 5-3: Set-up of cost factors for the design parameters, gathered into component categories

	Input parameter i	Cost factor c_i	Cost factor q_i
Nacelle parameters	L_{Nac}	20	0.50
	l_{Nac}	20	0.50
Tails parameters	A_{Htp}	50	1.00
	A_{Vtp}	50	1.00
Wings parameters	L_{Wing}	70	1.20
	c_{Tip}	70	1.20
	c_{Root}	70	1.20
	$V_{FuelBlock}$	70	1.20
	Λ_{Sweep}	70	1.20
Engine parameters	BPR	100	1.50
	T_{SLS}	100	1.50
	MC	100	1.50
Fuselage parameters	l_{Fus}	200	1.30
	L_{Fus}	200	1.30
	h_{Fus}	200	1.30

5.2.3 Constraints

Finally, the optimization tool requires a set of constraints arising from the requirement diagram to ensure that the solutions meet all the requirements.

To remain consistent with the formalism introduced in Chapter 2, $\boldsymbol{g}$ represents the constraint vector of the optimization Eq. (5-15). $\boldsymbol{g}$ contains four elements; each of them evaluates the feasibility of the design regarding the different performance thresholds (Eq. (5-16)).

$$\boldsymbol{g}(\boldsymbol{x}) \leq \mathbf{0} \qquad \textbf{Eq. (5-15)}$$

$$\boldsymbol{g}(\boldsymbol{x}) = \begin{pmatrix} L_{TO} - 2200 \\ M_{OWE} - 146000 \\ 11500 - d_{Range} \\ b - 65 \end{pmatrix} \qquad \textbf{Eq. (5-16)}$$

5.3 Deterministic design optimization

Since the design space, the constraints and the objective functions are defined, the optimistic tool can be implemented on ModelCenter.

This type of optimization neither considers the reliability of the performances nor the uncertainty propagation coming from the design parameter variations. However, this optimization screens the design space and may teach some knowledge about the best solutions without uncertainty consideration and the parameters that have no influence on the objectives. This deterministic optimization also addresses the configuration of the optimization workflow on ModelCenter and thus facilitates the RBDO

implementation in Chapter 6. The results will be compared later with the optimal designs of the RBDO and show the trade-off between objective function minimization and reliability-based constraints satisfaction.

5.3.1 Workflow configuration

For each optimization run, analytical models placed inside the optimization loop assess the technical performances of the aircraft and the objective values for the given input design. The descriptive models and analytical scripts created in the previous chapter to compute the range, the OWE, the TOFL and the wingspan of the system remain valid in this Case Study. MagicDraw Plug-In creates and import the workflow related to the constraints blocks on Cameo. The analytic chain is integrated to the optimization loop to assess the performances.

An Excel file supports the cost model defined by Eq. (5-14). The Excel Plugin integrates the analytical model to the workflow. The linkage with the other models is done manually so the Excel file can compute the cost objective function for each run of the optimization loop.

Finally, Scripts components ensure the normalization of the cost objective function, and compute the performance objective function based on the results of the simulation.

Deterministic optimization does not need to execute a probabilistic analysis for each input design tested as this type of optimization does not address the reliability of the requirements fulfilment. Figure 5-3 illustrates the final workflow of the deterministic optimization on ModelCenter.

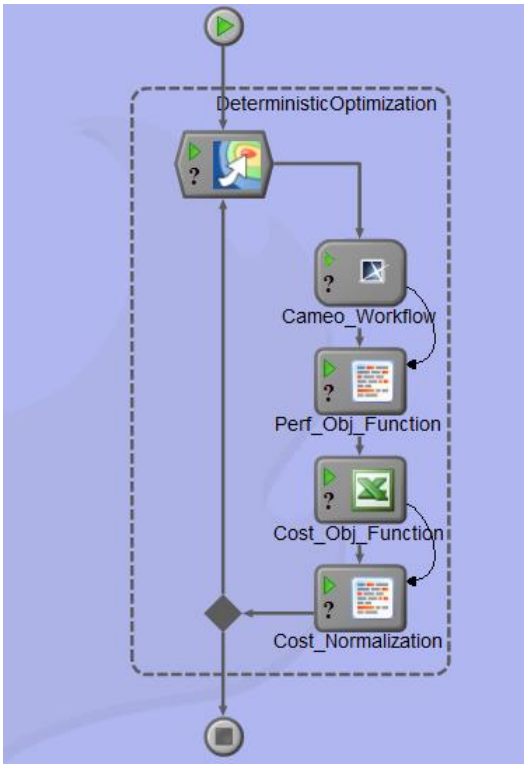

Figure 5-3: Workflow of the deterministic design optimization implemented on ModelCenter

5.3.2 Optimization tool configuration

The complexity of the workflow is quite low. A run inside the optimization loop requires around sixty function evaluations, which are all scripts or Excel files, and are therefore quickly executed. The first run of the optimization is a bit longer, because of the execution of Cameo in the background.

The analytical model do not need any improvement to reduce the complexity or enhance the computational performance. According to the comparison done in Part 3.6.2, and since the model speed is not an issue, almost all algorithms proposed by ModelCenter are suitable to perform the optimization.

Population based algorithm afford to carry out multiple-objective optimization by determining the Pareto-front of the problem. Evolutionary Algorithms like NSGA-II, Darwin and DAKOTA Multi-objective Genetic Algorithm achieve this process efficiently. Finally, NSGA-II is selected to perform the deterministic optimization on ModelCenter. The user can configure the different parameters of the algorithm, like the size of the population, the crossover probability and the stopping criteria of the optimization. Deb et al. (2002) detail all the features of this multi-objective genetic algorithm.

Figure 5-4 describes the configuration of NSGA-II used in this Case Study. The population size is numerous in order to get a precise screening of the design space. The thresholds regarding convergence criteria, number of function evaluations and number of generations are suited to obtain a precise Pareto-front: the optimization is stopped as soon as five generations in a row fail overcoming the convergence threshold, which is set to a low value.

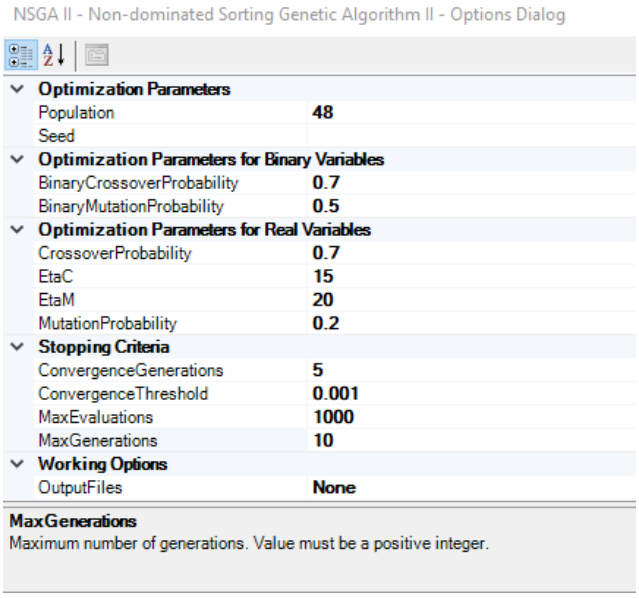

Figure 5-4: Configuration of the NSGA-II algorithm to perform the deterministic optimization

The following system formalizes the multi-objective deterministic design optimization implemented in the optimization tool of ModelCenter:

$$\min_{\boldsymbol{x}} f_{Perf}(\boldsymbol{x}) \qquad \textbf{Eq. (5-17)}$$

$$\min_{\boldsymbol{x}} f_{Cost}(\boldsymbol{x}) \qquad \textbf{Eq. (5-18)}$$

$$s.t. \quad \boldsymbol{g}(\boldsymbol{x}) \leq \mathbf{0} \qquad \textbf{Eq. (5-19)}$$

$$\mu_i^L \leq \mu_i \leq \mu_i^U \quad \forall\, i \in \Omega \qquad \textbf{Eq. (5-20)}$$

$$\sigma_i^L \leq \sigma_i \leq \sigma_i^U \quad \forall\, i \in \Omega \qquad \textbf{Eq. (5-21)}$$

5.3.3 Results of the deterministic design optimization

Figure 5-5 displays the evolution of the Pareto-front of the NSGA-II optimization over the generations. The front progresses toward lower values of both performance and cost objective functions. The stopping criteria of five generations without sufficient improvements is reached for the generation 40.

While the Pareto-front explores the best design solutions without any relative weighting between the performance and the cost objective functions, this decision is actually only postponed. Engineers will have to define a hierarchy between the objectives to choose a design solution of the Pareto-front.

The area in the upper left corner of the Pareto-front corresponds to the lowest values of the cost function. In this zone, the cost function minimization is preferred to the performance function optimization. Furthermore, the area at the bottom right of the Pareto front corresponds to the lowest values of the performance function. In this area, the optimization of the performance function is favored over the optimization of the cost function.

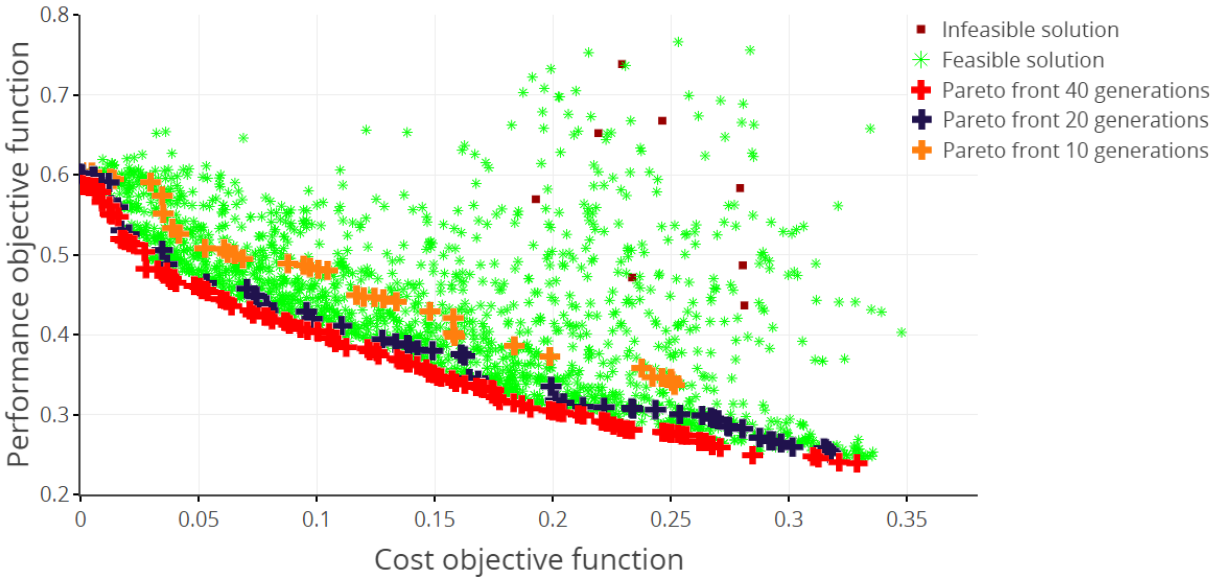

Figure 5-5: Evolution of the Pareto-front over the population's generations during the computation of a multi-objective NSGA-II optimization algorithm

Pareto-front solutions may draw interesting conclusions about the optimal designs and are worth a further analysis. Thus, the design points evaluated in the deterministic optimization are colored according to the value taken by a given parameter. Figure 5-6 and Figure 5-7 report two interesting cases to gain knowledge about the aircraft optimal design.

Figure 5-6 colors the design points according to their value for $\mu_{c_{Root}}$. All designs located close to the Pareto-front have a root chord mean value very close to the initial mean value before optimization $\mu_{c_{Root},ini}$. $\mu_{c_{Root}}$ is similar for all best design solutions. Therefore, the final design of this parameter does not depend on the relative importance between the objectives. Additional analysis draw the same conclusions for the mean values of the tip chord, the vertical tail area and the SLS Thrust.

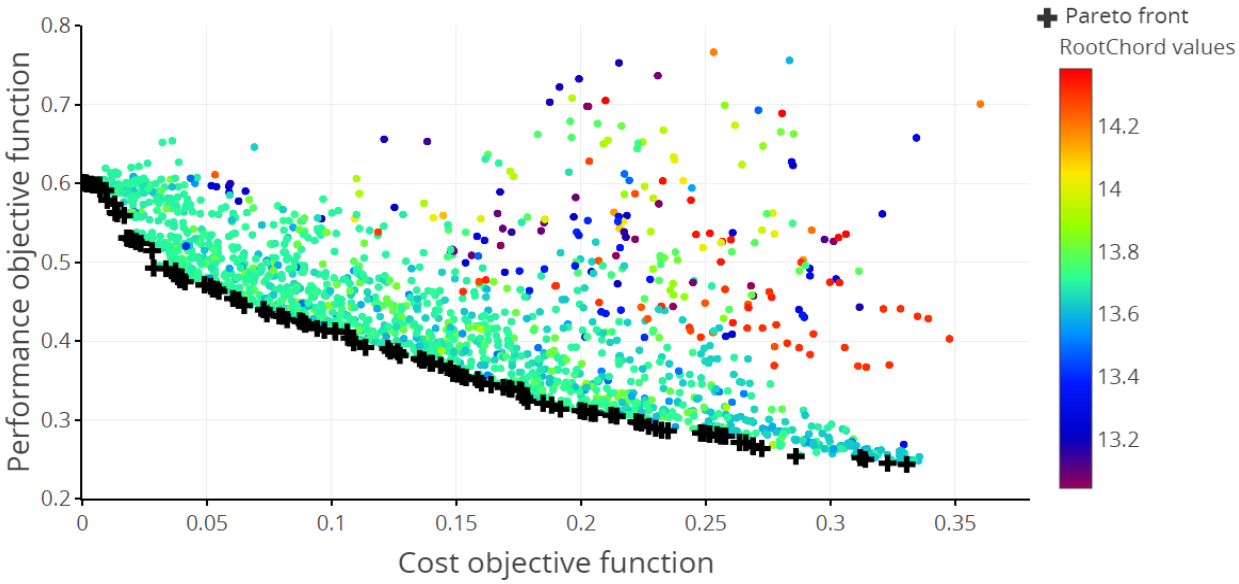

Figure 5-6: Design solutions and Pareto-front of the multi-objective NSGA-II deterministic design optimization, colored by c_{Root} mean values

Figure 5-7 colors the design points depending on the BPR mean value. This time, two distinct areas stand out for the design points close to the Pareto-front. On the one hand, when the cost function minimization is preferred to the performance function reduction, μ_{BPR} is close to its initial configuration before optimization $\mu_{BPR,ini}$. On the other hand, for the design points close to the bottom right part of the Pareto front, μ_{BPR} values are all located into the upper part of the design space interval. In this situation, the relative weighting between the objective functions has a real impact on the optimal design configuration of the aircraft. Similar analysis draw the same conclusions for the fuselage and the nacelle geometrical properties.

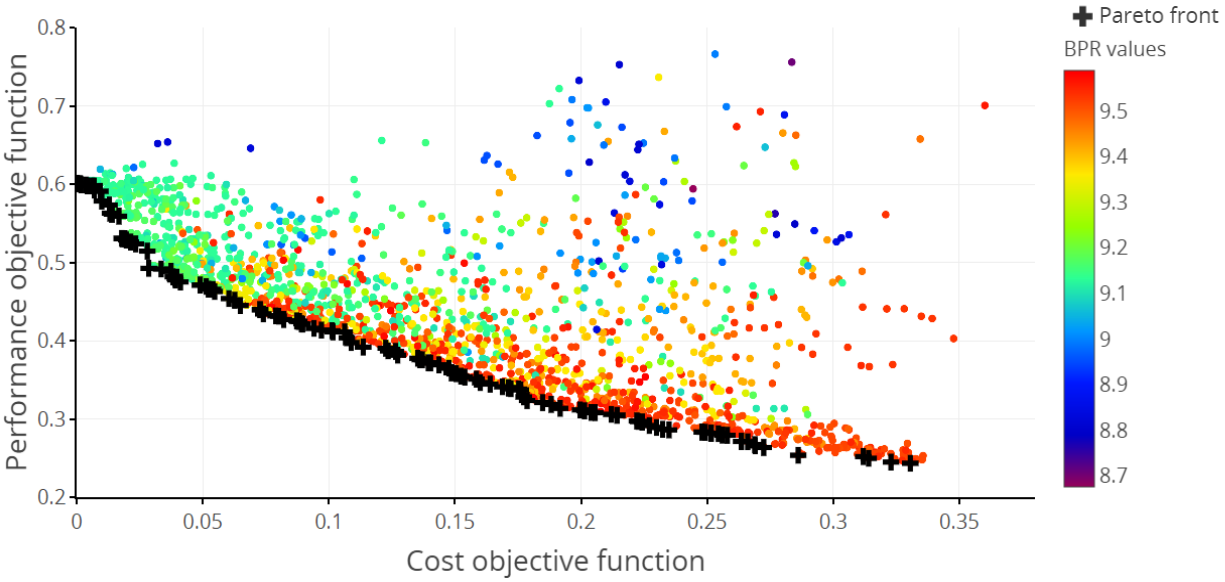

Figure 5-7: Design solutions and Pareto-front of the multi-objective NSGA-II deterministic design optimization, colored by BPR mean values

5.3.4 Conclusion

In conclusion, the collaborative sotware environment defined in Chapter 3 supports deterministic design optimization. The variety of optimization algorithms and the wide variety of configuration parameters enable a precise fitting of the optimization tool to the problem.

This chapter draws insights into optimal deterministic design of the new aircraft and sets up useful tools from the perspective of the RBDO implementation in the next chapter:

- Definition of the performance and cost objective functions driving the design optimization
- Set up of the optimization tool on ModelCenter (algorithm configuration, creation of scripts and excel models to compute the objective functions)
- Implementation of a multi-objective optimization: Since the deterministic design optimization do not require running any probabilistic analysis, the complexity level of the simulation is quite low. This characteristic affords to evaluate the performance of a multi-objective GA. The complexity of the RBDO process could limit the use of this type of multi-objective algorithms in Chapter 6.
- The Pareto-front of the deterministic optimization brings information about the optimal design of the system, even if reliability-based constraints may make some solutions infeasible and therefore shift the Pareto-front to higher objective values. The front provides relevant results regarding the effect of the relative

weighting between objectives on the optimal design configuration. While some parameters remain similar for the different solutions of the front, several inputs vary considerably depending on the preference established for the objectives. This observation shows the importance of the weight assignment when the multi-objective problem is too complex and is therefore converted into a single objective optimization.

6 Reliability-based design optimization of the aircraft

This chapter tackles the uncertainty propagation into the analytical model during the optimization of the aircraft design. The deterministic optimization provides a Pareto-front of the best design solutions (see Part 5.3.3), but these configurations may not reach the reliability threshold for all the performances. While the design solutions of the Pareto-front ensure the best results for the objective functions, a small variation of any input parameter may lead to critical performance degradation indeed. It is interesting to analyze the effects of the reliability-based constraints on the optimal design and to evaluate the ability of ModelCenter to perform RBDO.

6.1 System of equations

The set of equations defining the design space and the objective functions of the RBDO remains similar to the one defined in Part 5.2 for the deterministic optimization. Eq. (5-4), Eq. (5-6) and Eq. (5-8) describe the design space of the RBDO and Eq. (5-10) and Eq. (5-13) refer to the objective functions definition.

Since reliability plays a central part in the RBDO, the set of constraints defined for the deterministic optimization (Eq. (5-15) and Eq. (5-16)) is no more applicable. To remain consistent with the formalism of Chapter 2 concerning the optimization, an inequation gathers all reliability-based constraints (Eq. (6-1)). The definition of constraint vector $\boldsymbol{g}$ evolves from deterministic design optimization and considers the reliability of the system associated to the input vector $\boldsymbol{x}$ (Eq. (6-2)). The reliability vector $\boldsymbol{R}$ contains four parameters: $R_{L_{TO}}$, $R_{M_{OWE}}$, $R_{d_{Range}}$ and R_b denote the reliability threshold associated to the four system requirements (Eq. (6-3)). These parameters must be set up before each optimization, according to the reliability level the engineers are willing to reach.

$$\boldsymbol{g}(\boldsymbol{x}) \leq \boldsymbol{R} \qquad \textbf{Eq. (6-1)}$$

$$\boldsymbol{g}(\boldsymbol{x}) = \begin{pmatrix} R_{L_{TO} \leq 2200}(\boldsymbol{x}) \\ R_{M_{OWE} \leq 146000}(\boldsymbol{x}) \\ R_{d_{Range} \geq 11500}(\boldsymbol{x}) \\ R_{b \leq 65}(\boldsymbol{x}) \end{pmatrix} \qquad \textbf{Eq. (6-2)}$$

$$\boldsymbol{R} = \begin{pmatrix} R_{L_{TO}} \\ R_{M_{OWE}} \\ R_{d_{Range}} \\ R_b \end{pmatrix} \qquad \textbf{Eq. (6-3)}$$

6.2 Analytical model complexity problematic

The workflow of Figure 5-3 in Part 5.3.1 serves as a basis for the RBDO workflow. However, the RBDO process needs to run a probabilistic analysis for each run of the optimization loop to evaluate the reliability. The execution of the Cameo Workflow inside the Probabilistic Analysis loop requires around fifty function evaluations. The complexity of the RBDO process gets exponential. The critical steps of the UMDO process identified in Figure 3-9 must therefore be tailored to the specific system complexity.

6.2.1 Model simplification

ModelCenter provides a Response Surface Modeling (RSM) toolkit to face the complexity of long running models. A surface model approximates the analysis code and executes the workflow much quicker (He and Fang 2011). This tool is essential to perform RBDO that may require thousands of evaluations.

The RSM component is comparable to a black box linking input and output parameters. Two types of RSM are available on ModelCenter: Design Explorer Kriging and Polynomial approximation. While Polynomial RSM are easy to create and are the first choice for capturing overall trends in the data, Design Explorer Kriging interpolates the data and often provides better approximations for complex systems (Phoenix Integration 2018).

ModelCenter RSM Toolkit recommends which DOE to implement depending on the type of RSM chosen and on the complexity of the system. The Adjusted Coefficient of Determination R^2 and the root mean square error characterize the created RSM. It is therefore possible to monitor the accuracy of the RSM component.

6.2.2 Problem dimensionality reduction

The number of design parameters is an important factor in an optimization. The design space growths with the number of design parameters and the search for optimal designs may therefore take longer.

A screening DOE, based on LHS method or fractional factorial design for instance, can be implemented in order to gain in knowledge about the design space (Khan 2013: 407) and to identify the KC. The analysis of the DOE results enables the refinement of the design space interval of some variables. In addition, design parameters that significantly influence neither objective functions nor constraint functions can be set to a constant value, thus decreasing the dimensionality of the design space (Narayanan and Khoh 2008: 1078).

6.2.3 Selection of suited analysis algorithms

RBDO requires the execution of a probabilistic analysis inside the optimization loop to estimate the reliability of the design. The configuration of the optimization tool as well as the probabilistic analysis tool on ModelCenter must be suited to the workflow complexity in order to provide results in a reasonable time:

- Probabilistic analysis tool: As described earlier in Part 4.4.3 regarding the choice of the probabilistic analysis tool, there is a tradeoff between estimation accuracy and computation time. Monte-Carlo emphasizes the accuracy of the result but requires many runs, while NESSUS methods requires less runs but can lead to approximations in the reliability estimation. Implementing NESSUS methods at the expense of Monte Carlo thus considerably reduces the number of function evaluations for the probabilistic analysis.

- Optimization algorithm: As described in Part 3.6.2, various types of algorithms are available on ModelCenter to perform an optimization. The conversion from a multi-objective optimization problem into a single objective optimization problem focuses the search for the optimal design on a specific area of the global Pareto-front and reduces the number of function evaluations to identify the optimal designs.

6.2.4 Computational performance enhancement

In addition to reducing the complexity and the dimensionality of the optimization problem, computational performance enhancement allows to face the high number of function evaluations in an UMDO. ModelCenter offers different solutions to reduce the computation time of the solving process:

- Parallel Computing: Some probabilistic analysis methods as well as optimization algorithms allow parallel computing. Property configurations can be modified for these components to allow runs in parallel, disabled in the default setting (Figure 6-1). Many simulations are carried out at the same time on different cores, reducing the total computing time of the optimization.

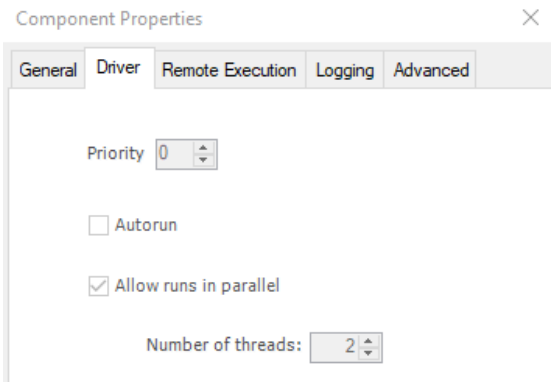

Figure 6-1: Modification of the component properties to allow parallel computing on ModelCenter

- Virtual Machine: Analysis Server enables the connection between a local ModelCenter workflow and wrappers located on a server. This feature provides an alternative to the computational limitations of the computer by running programs on a Virtual Machine (Figure 6-2). The combination of the previous point and of this configuration exploits the computing power of parallel server cores and reduces the computing time of the workflow.

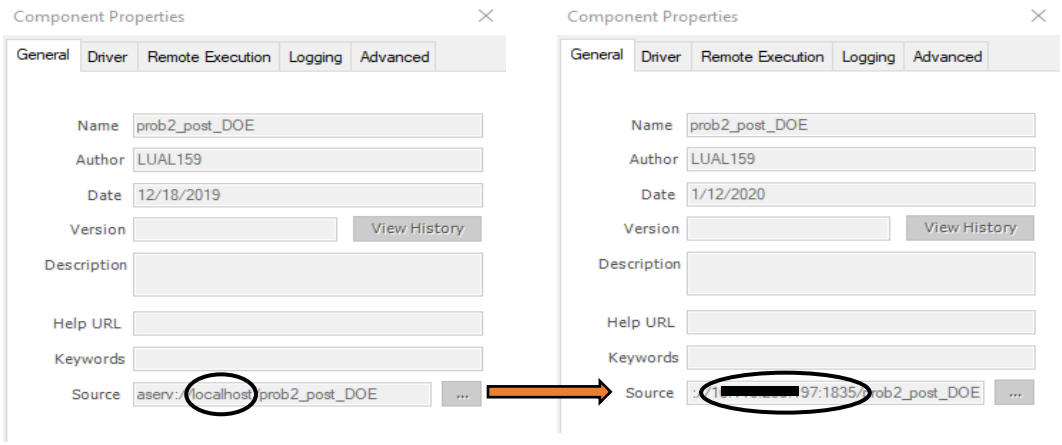

Figure 6-2: Modification of the source location to execute the simulation on a Virtual Machine

6.3 Screening of the design space

The initial set of design parameters and their design interval range for RBDO is the same as for deterministic optimization (See Part 5.2.1) and therefore contains 30 variables. The objective of the design space screening is to reduce the problem's dimensionality by identifying irrelevant parameters that do not influence the outputs, and to narrow the design space interval of some input parameters.

6.3.1 Workflow configuration

A RSM is applied to approximate the Cameo Workflow component assessing the performances of the aircraft (see Figure 5-3). Four regression equations replace the fifty initial scripts to calculate the range, the OWE, the wingspan and the TOFL of the aircraft under study. The best solution between the Design Explorer Kriging and the Stepwise Regression is selected. R^2 highlights the quality of the regression and affords to quantify the uncertainty coming from the model approximation. Figure 6-3 shows the RSM results for evaluating the wingspan, the OWE, the range and the TOFL.

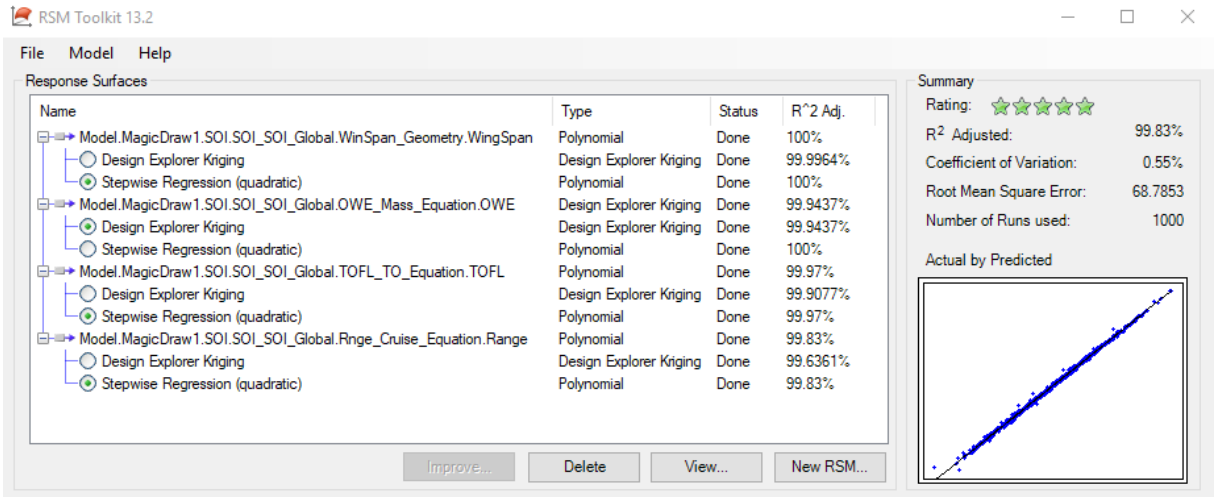

Figure 6-3: Results of the RSM to approximate the wingspan, the range, the OWE and the TOFL

A Probabilistic Analysis component is then added to the ModelCenter workflow to evaluate the reliability of the different performances. After running some tests, it appears that the computing time to perform the Probabilistic Analysis whatever the type of method chosen is quite long. The GUI of the probabilistic analysis, which automatically opens when the probabilistic analysis runs, limits the computation speed. To solve this issue, the probabilistic analysis component is exported to a new ModelCenter process and forms a second workflow. Some assembly components ensure the connection between the variables of both workflows and therefore the traceability of the model. The second workflow is saved on the localhost and executed through Analysis Server. Figure 6-4 illustrates the ModelCenter workflows to perform the RBDO.

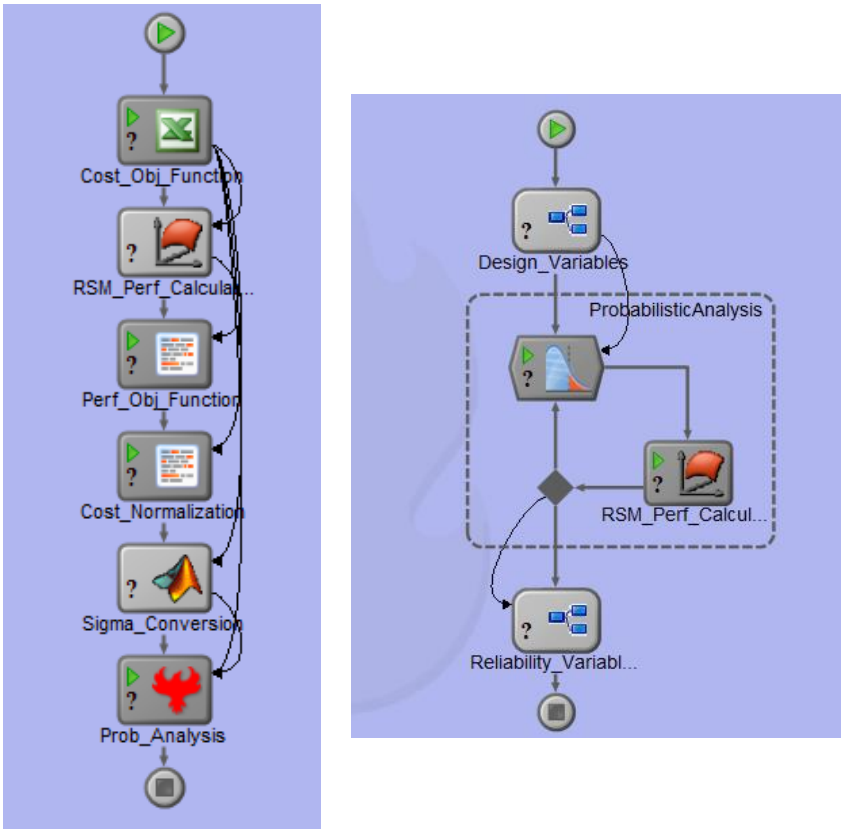

Figure 6-4: Workflow of the screening DOE (left) and of the probabilistic analysis (right) on ModelCenter

6.3.2 Set-up of the screening DOE

The dimensionality of the system is high, as they are 30 design parameters that can evolve inside their specific design interval range (Eq. (5-4) and Eq. (5-6)). In addition, exporting the probabilistic analysis to another ModelCenter process significantly reduces the execution time of a Monte Carlo analysis with 10 000 runs. Thus, taking into account the importance of accurate estimation in the context of a RBDO, Monte Carlo analysis is preferred to NESSUS analytic methods.

The chosen DOE also computes 5 000 runs based on Design Explorer Orthogonal Array + LHS sampling methods. Full fractional DOE requires too many design evaluations here.

6.3.3 Results

The DOE aims to identify the critical and irrelevant parameters and refine the design space interval of some design parameters. This section focuses on the study of three design parameters, $\mu_{L_{Fus}}$, $\mu_{L_{Wing}}$ and $\mu_{V_{FuelBlock}}$, to provide an overview of the analysis tools of ModelCenter to achieve the objectives.

Figure 6-5 represents the design tested during the screening DOE colored in function of $\mu_{L_{Fus}}$ values. All the design points located on or near the Pareto-front of the multi-objective problem have a low $\mu_{L_{Fus}}$ value. The design space interval of this design parameter is therefore narrowed, the lower part of the initial design interval range will be further investigated in the optimization analysis and the upper part dropped because leading to bad results.

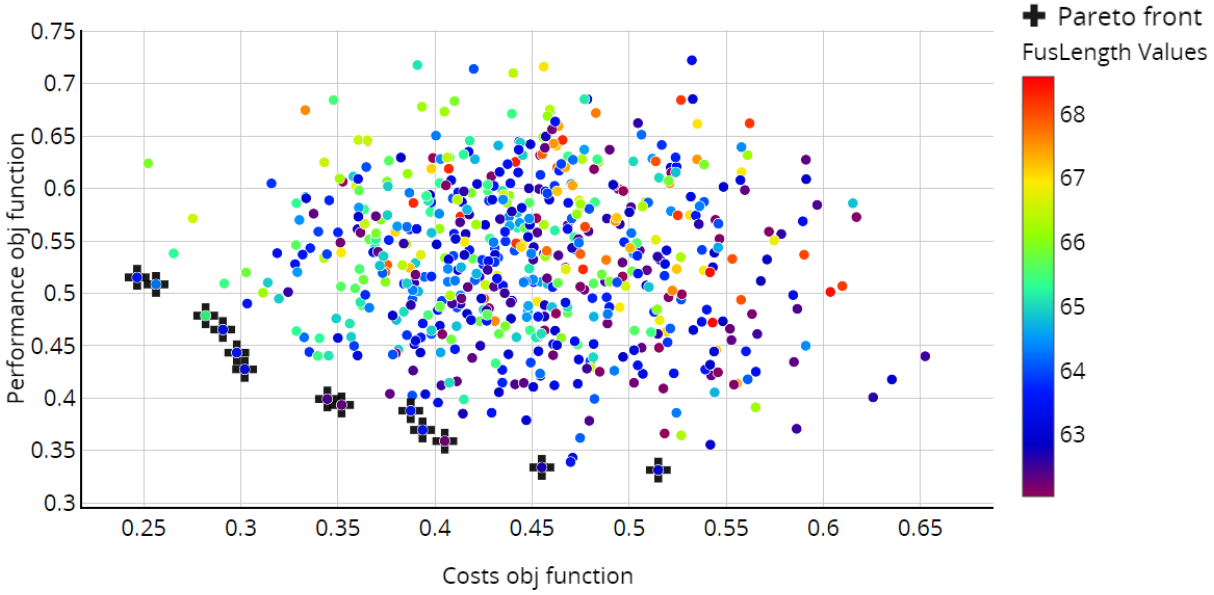

Figure 6-5: Representation of the simulated design points and of the Pareto front after a DOE screening, colored by $\mu_{L_{Fus}}$ values

The sensitivity analysis histograms and the Prediction Profiler XY graphs make stand out the critical and irrelevant parameters of the problem. Figure 6-6 highlights the sensitivity analysis results regarding $\mu_{L_{Wing}}$. The parameter is critical for four out of the six outputs considered in the study. The greater the value of $\mu_{L_{Wing}}$, the more reliable are the range and the TOFL performances. However, the increase of $\mu_{L_{Wing}}$ also leads to a reduction of the system reliability regarding the OWE and wingspan requirements.

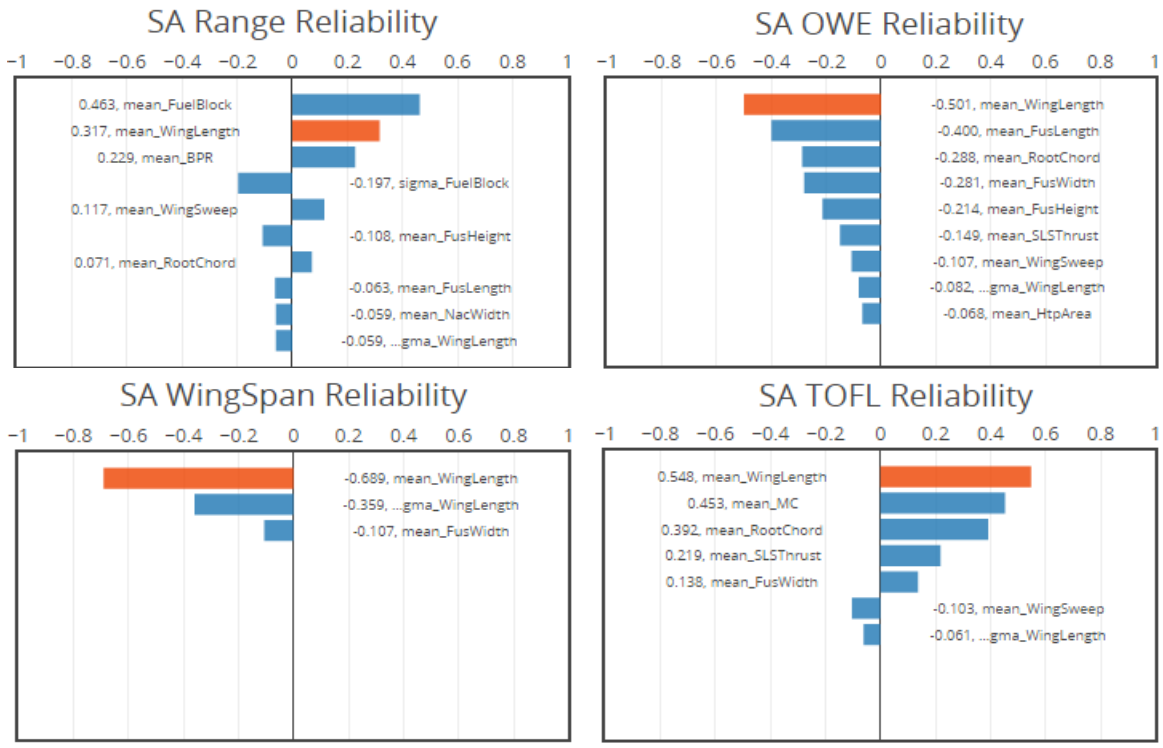

Figure 6-6: Sensitivity Analysis obtained thanks to the DOE screening, highlighting the results regarding $\mu_{L_{Wing}}$

Prediction Profiler of Figure 6-7 confirms this analysis; the curves represent the evolution of the outputs in function of $\mu_{L_{Wing}}$ when all other design parameters are set to their initial configuration value before optimization (Table 5-1). In this trade-off situation, it is impossible to draw clear conclusions concerning the best range to focus on for $\mu_{L_{Wing}}$ during the optimization.

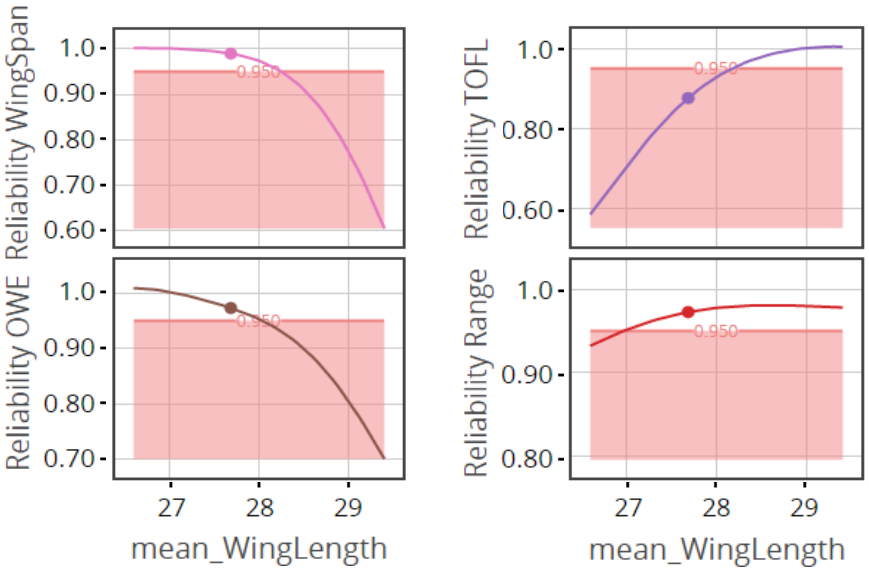

Figure 6-7: Prediction Profiler XY depicting the dependence between $\mu_{L_{Wing}}$ and the reliability of wingspan, OWE, TOFL and range while the other design parameters remain equal to their initial configuration

Figure 6-8 shows that $\mu_{V_{FuelBlock}}$ is the most critical parameter regarding both performance objective function and range reliability. The greater the value of $\mu_{V_{FuelBlock}}$, the better the performance function output and the range reliability. Prediction Profiler XY of Figure 6-9 confirms this result as well as the irrelevance of $\mu_{V_{FuelBlock}}$ for other ouputs like the cost objective function. As higher values of $\mu_{V_{FuelBlock}}$ lead to better results for the aircraft design, the design space interval of the design variable is narrowed to the upper values of the variable.

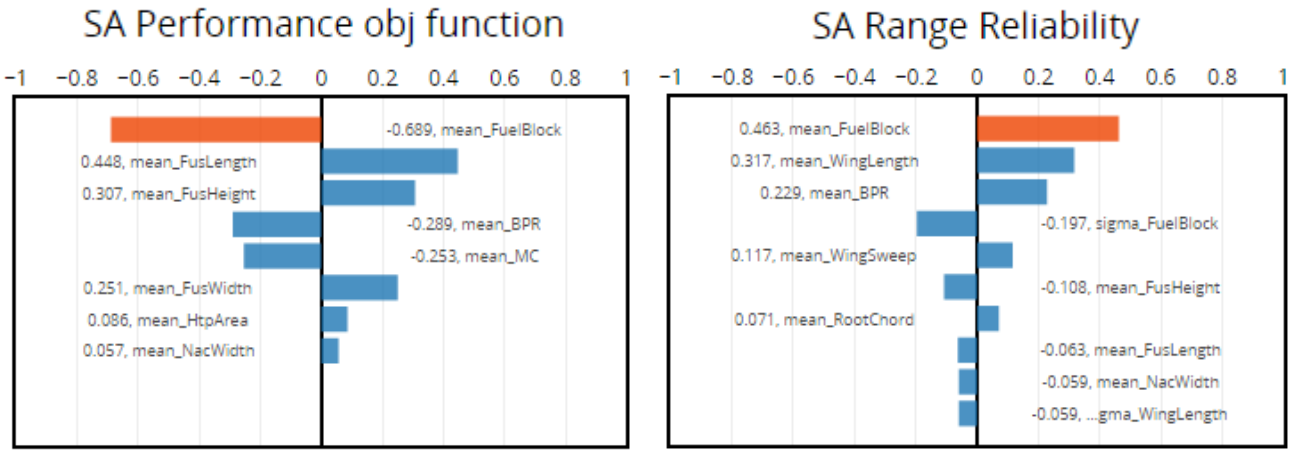

Figure 6-8: Sensitivity Analysis obtained thanks to the DOE screening, highlighting the results regarding $\mu_{V_{FuelBlock}}$

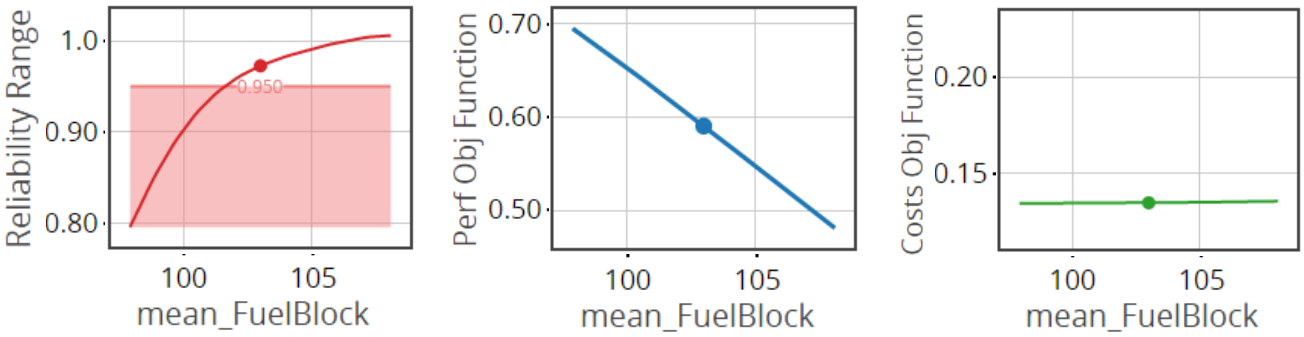

Figure 6-9: Prediction Profiler XY depicting the dependence between $\mu_{V_{FuelBlock}}$ and the outputs

Finally, this DOE helps reducing the problem dimensionality. Parameters that have no influence on both performance reliabilities and objective functions are set to a constant value. Furthermore, some analysis drive to the refinement of the design space interval of the rest of the design parameters, like for $\mu_{V_{FuelBlock}}$.

A second DOE is performed to even more reduce the problem dimensionality and refine the design space. Table 6-1 summarizes the evolution of the design space of the design parameters thanks to the two DOE. Out of the 30 initial design parameters, 15 are set constant for the RBDO, and the design space of 13 other design parameters has been refined. The DOE also reduces the dimensionality of the RBDO problem by 50%.

Table 6-1: Reduction of the design space after DOE screening. The orange boxes refer to design parameters for which the space interval is narrowed and the green boxes highlight design parameters that will be set constant for the RBDO.

	Initial Design Space		*Design Space after Screening*		*Initial Design Space*		*Design Space after Screening*	
Design Parameters	μ_i^L	μ_i^U	μ_i^L	μ_i^U	σ_i^L	σ_i^U	σ_i^L	σ_i^U
BPR	8.67	9.59	9.13	9.59	0.5%	4%	4%	4%
A_{Vtp}	48.45	53.55	51	51	0.5%	4%	4%	4%
A_{Htp}	80.75	89.25	83	83	0.5%	4%	3%	3%
l_{Fus}	5.41	5.97	5.41	5.69	0.5%	4%	3%	3%
L_{Wing}	26.60	29.40	26.60	29.40	0.5%	4%	1%	3.5%
c_{Tip}	0.33	0.37	0.35	0.35	0.5%	4%	4%	4%
c_{Root}	13.02	14.39	13.70	14.39	0.5%	4%	3%	3%
L_{Fus}	62.04	68.58	62.04	64	0.5%	4%	3%	3%
h_{Fus}	6.10	6.74	6.10	6.30	0.5%	4%	4%	4%
L_{Nac}	5.43	6.01	5.72	5.72	0.5%	4%	4%	4%
l_{Nac}	3.81	4.21	4.01	4.01	0.5%	4%	4%	4%
T_{SLS}	367650	406350	367650	406350	0.5%	4%	2%	4%
MC	0.95	1.05	1	1.05	0.5%	4%	2%	4%
$V_{FuelBlock}$	97.85	108.15	106	108.15	0.5%	4%	2%	4%
Λ_{Sweep}	0.53	0.59	0.53	0.56	0.5%	4%	2%	4%

6.4 Reliability-based design optimization (RBDO)

6.4.1 Workflow configuration

Figure 6-10 illustrates the workflow of the RBDO. The only difference with the DOE workflow (Figure 6-4) is the addition of the optimization tool. The probabilistic analysis is still located on a different workflow, in order to perform the analysis without opening the GUI and reduce the computing speed.

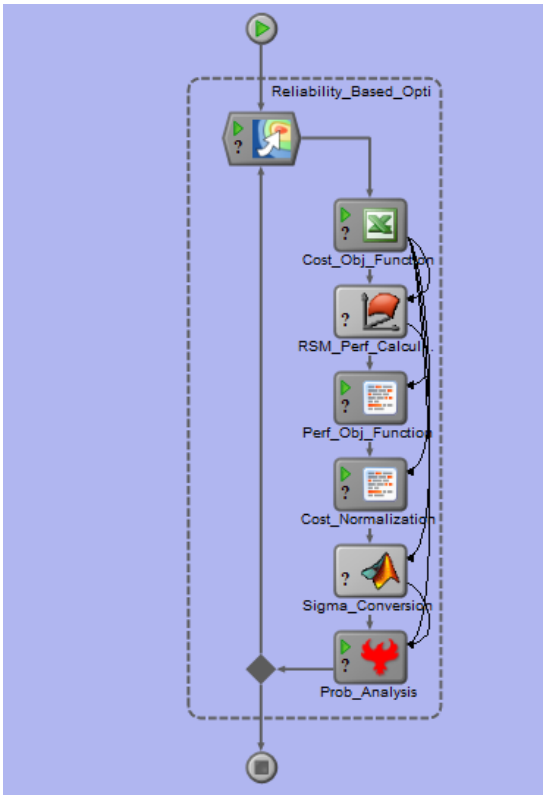

Figure 6-10: Workflow of the RBDO on ModelCenter

6.4.2 Optimization parameters

Despite the reduction of the problem dimensionality, the RBDO simulation complexity remains quite high. The multi-objective GA DAKOTA OPT ++ and NSGA-II take too long to determine the Pareto-front. Design Explorer, hybrid optimization algorithm described in Part 3.6.2, requires less time to find the solution and will support the RBDO. However, the algorithm converts the multi-objective function into a single objective one.

Eq. (6-4) formalizes the single objective function by summing up the performance and the cost objective functions defined in Eq. (5-10) and Eq. (5-13) and introducing weight factors:

$$f(\boldsymbol{x}) = w_{Perf} \cdot f_{Perf}(\boldsymbol{x}) + w_{Cost} \cdot f_{Cost}(\boldsymbol{x}) \qquad \textbf{Eq. (6-4)}$$

w_{Perf} and w_{Cost} are the weight factors of the performance and cost objective functions, respectively.

The different weight configurations will generate various design solutions. The final choice of the performance and costs weight factors may require diverse weight pair tests to get good results.

The following system formalizes the single objective RBDO implemented in the optimization tool of ModelCenter:

$$\min_{\boldsymbol{x}} \; f(\boldsymbol{x}) \qquad \text{Eq. (6-5)}$$

$$s.t. \;\; \boldsymbol{g}(\boldsymbol{x}) \leq \boldsymbol{R} \qquad \text{Eq. (6-6)}$$

$$\mu_i^L \leq \mu_i \leq \mu_i^U \quad \forall\, i \in \Omega \qquad \text{Eq. (6-7)}$$

$$\sigma_i^L \leq \sigma_i \leq \sigma_i^U \quad \forall\, i \in \Omega \qquad \text{Eq. (6-8)}$$

6.4.3 Results RBDO with different weight factors

The optimization tool runs with three different input configurations of the weighting pairs. The reliability thresholds $R_{d_{TO}}, R_{M_{OWE}}, R_b$ and $R_{d_{Range}}$ defined in Eq. (6-3) are set equal to 0.97 for the three optimizations. Configurations A and C focuses on the performance objective function minimization and on the costs objective function, respectively. Configuration B sets equal weights for the performance and the costs function.

To better understand the difference between a multi-objective optimization and a conversion into a single objective problem, Figure 6-11 illustrates all the design points tested during the optimizations with Configurations A, B and C. The single objective optimization algorithm focuses on a particular part of the multi-objective Pareto-front. The searched area depends on the weights configuration. Configuration A, B and C focus on the bottom left, on the middle and on the bottom right parts of the Pareto front, respectively.

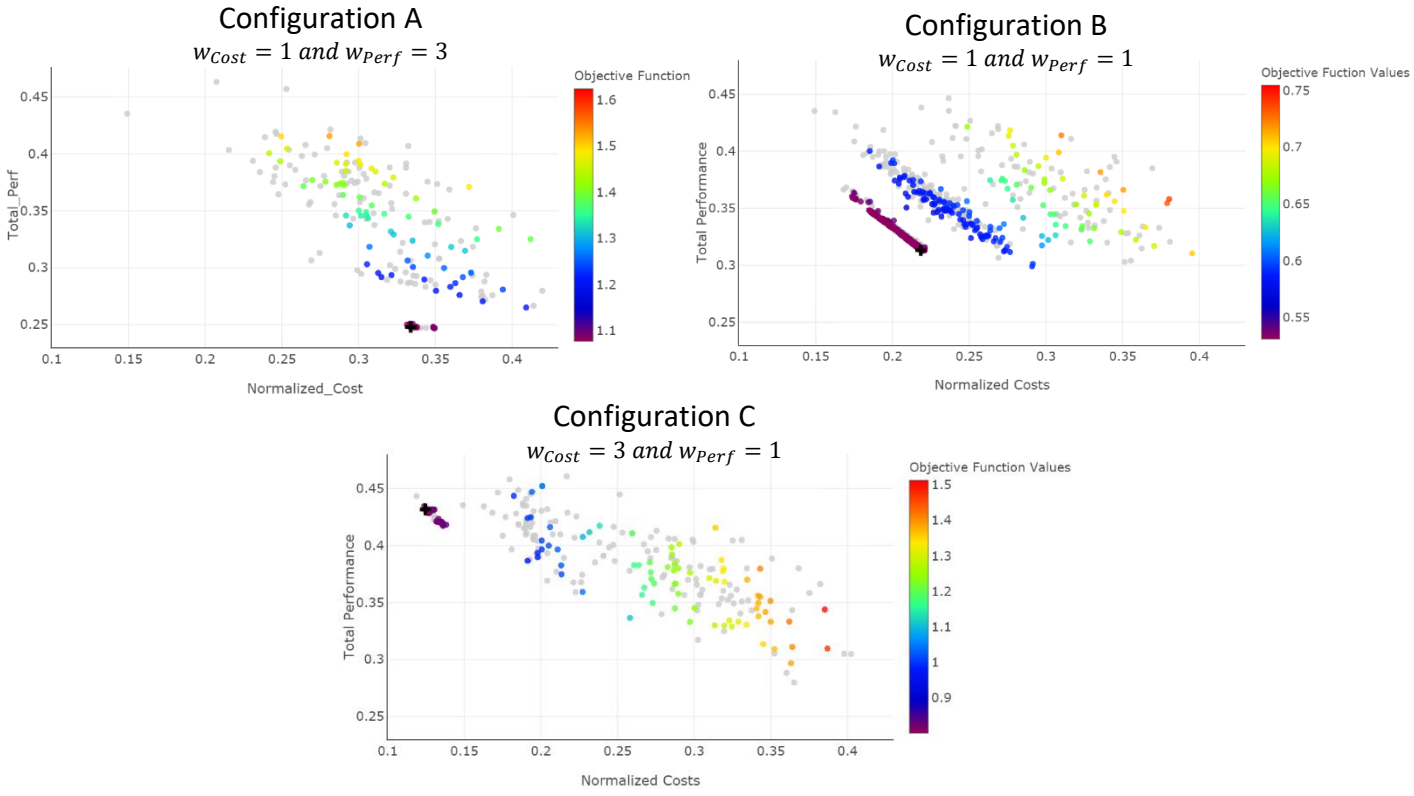

Figure 6-11: 2D Scatter Plot representing the outputs of the cost and performance objective functions for RBDO with different weight factor configurations

Table 6-2 reports the output results for each of the three Configurations A, B and C. The greater the relative weighting of an objective function, the better the output of the optimization regarding this objective function. Configuration A leads to the the optimal costs results, while Configuration C enhance the performances of the aircraft. Configuration B, which equally weights both objective functions, offers a good compromise between Configurations A and C.

Table 6-2: Comparison of the RBDO results with Configurations A, B and C

RBDO input configuration	w_{Cost}	w_{Perf}	f_{Cost}	f_{Perf}	$TOFL$ (m)	$Range$ (km)	OWE (kg)	b (m)
Configuration A	1	3	0.360	0.283	1932	14291	139380	61.3
Configuration B	1	1	0.219	0.313	1903	14189	141060	61.7
Configuration C	3	1	0.188	0.435	1966	13709	141966	61.5

Furthermore, Table 6-3 shows the best design solution of each optimization configuration. Design parameters which final value evolves between the different configurations are highlighted. It concerns eight variables among the fifteen selected parameters that can vary in the optimization: μ_{BPR}, $\mu_{l_{Fus}}$, $\mu_{L_{Wing}}$, $\mu_{L_{Fus}}$, $\mu_{h_{Fus}}$, μ_{MC}, $\sigma_{L_{Wing}}$ and $\sigma_{T_{SLS}}$. Therefore, the optimal design of the aircraft strongly depends on the relative weighting between the performance and the cost objective functions.

For the seven other design parameters, the best design solution does not depend on the weighting configuration. This information facilitates the design process, since no subjective decision concerning the weight assignment is needed to come up with the optimal value for these variables. They may however vary depending on the values of the reliability thresholds.

Finally, the relative weighting of the objectives directly affects the area of the Pareto-front in which the algorithm seeks for optimal solution and influences indirectly the final design configuration. In reality, the decision about objectives weighting depends on the business model of the company. For instance, a low cost company would rather minimize the development costs than enhance the performance of the aircraft and therefore choose Configuration C. Configuration B explores a larger area of the Pareto-front and offers a good compromise between the cost minimization and the performance optimization. This weighting configuration is selected for the rest of the study.

Since the weighting configuration is set, Part 6.4.4 will focus on the influence of the reliability thresholds on the optimal design solution.

Table 6-3: Comparison of the reliability-based optimal designs for Configurations A, B and C. Red highlighting represents the parameters which final value evolves depending on the weight Configuration.

Design Parameters	Configuration A RBDO 97% $w_{Cost} = 1$ $w_{Perf} = 3$	Configuration B RBDO 97% $w_{Cost} = 1$ $w_{Perf} = 1$	Configuration C RBDO 97% $w_{Cost} = 3$ $w_{Perf} = 1$
μ_{BPR}	9.59	9.59	9.13
$\mu_{l_{Fus}}$	5.41	5.69	5.69
$\mu_{L_{Wing}}$	27.96	28	27.89
$\mu_{c_{Root}}$	13.70	13.70	13.70
$\mu_{L_{Fus}}$	62.04	62.04	64
$\mu_{h_{Fus}}$	6.10	6.30	6.30
$\mu_{T_{SLS}}$	386849	387000	387000
μ_{MC}	1.05	1.05	1.02
$\mu_{V_{FuelBlock}}$	108.15	108.15	108.15
$\mu_{\Lambda_{Sweep}}$	0.56	0.56	0.56
$\sigma_{L_{Wing}}$	3.50%	3.12%	2.38%
$\sigma_{T_{SLS}}$	3.99%	4%	3.55%
σ_{MC}	4%	4%	3.98%
$\sigma_{V_{FuelBlock}}$	4%	4%	4%
$\sigma_{\Lambda_{Sweep}}$	4%	3.97%	4%

6.4.4 Results RBDO with different reliability thresholds

RBDO adds reliability-based constraints to the classic deterministic optimization set of equations (Eq. (6-1)). The initial set up of the thresholds $R_{L_{TO}}$, $R_{M_{OWE}}$, R_b and $R_{d_{Range}}$ emphasizes the level of reliability the company is willing to achieve. This part deals with the evolution of the RBDO results depending on the reliability thresholds configuration and compares the final designs obtained by running deterministic and RBDO.

Design Explorer algorithm achieves the different RBDO and equally weights the performance and costs objectives, as decided in Part 6.4.3. The reliability thresholds $R_{L_{TO}}$, $R_{M_{OWE}}$, R_b and $R_{d_{Range}}$ are set equal and four optimizations are run for reliability thresholds equal to 0.95, 0.97, 0.99 and 0.999. In the meantime, a single objective deterministic optimization with the same weight configuration as the RBDO is performed, in order to analyze the tradeoff between optimal deterministic and optimal reliable solutions. Table 7-6 in Appendix B.4 regroups the results of these different optimizations.

Table 6-4 represents the design parameters which final value differs between the different optimizations. The initial configuration of the design parameters before the optimization serves as a reference to compare the design modifications. Out of the 15 selected design parameters for the optimization, only three change between the initial configuration and the deterministic optimal design: μ_{BPR}, $\mu_{FuelBlock}$ and $\mu_{FusLength}$. Regarding the RBDO results, the higher the reliability threshold, the more the number of design parameters which configuration evolves from their initial value. The cost model explains these results: each design parameter modification from its initial value leads to additional costs.

Table 6-4: Representation of the design parameters, which value evolves between the initial configuration and the deterministic and reliable optimal designs

Design Parameters	Initial Configuration	Deterministic design opti. $w_{Cost} = 1$ $w_{Perf} = 1$	RBDO 95% $w_{Cost} = 1$ $w_{Perf} = 1$	RBDO 97% $w_{Cost} = 1$ $w_{Perf} = 1$	RBDO 99% $w_{Cost} = 1$ $w_{Perf} = 1$	RBDO 99.9% $w_{Cost} = 1$ $w_{Perf} = 1$
μ_{BPR}	9.13	9.59	9.59	9.59	9.59	9.59
$\mu_{V_{FuelBlock}}$	103	108.15	108.15	108.15	108.15	108.15
$\mu_{L_{Fus}}$	65.31	62.09	62.04	62.04	62.04	62.04
$\mu_{A_{Htp}}$	85	85	83	83	83	83
$\sigma_{A_{Htp}}$	4%	4%	3%	3%	3%	3%
$\sigma_{l_{Fus}}$	4%	4%	3%	3%	3%	3%
$\sigma_{c_{Root}}$	4%	4%	3%	3%	3%	3%
$\sigma_{L_{Fus}}$	4%	4%	3%	3%	3%	3%
$\mu_{h_{Fus}}$	6.42	6.42	6.30	6.30	6.30	6.30
μ_{MC}	1	1	1.05	1.05	1.05	1.05
$\sigma_{L_{Wing}}$	4%	4%	3.50%	3.12%	2.59%	1.45%
$\sigma_{T_{SLS}}$	4%	4%	4%	4%	3.89%	2.13%
σ_{MC}	4%	4%	4%	4%	3.99%	2.79%
$\mu_{L_{Wing}}$	28	28	27.99	28	28	27.69

The deterministic solution that minimizes the costs does not meet the reliability-based constraints and additional costs occurs to meet the thresholds (Figure 6-12). The costs increase by 52% between the deterministic optimal result and the best design of the 95% RBDO. While the costs are stable between the 95% and 99% RBDO, the shift of the reliability threshold to 0.999 increases the result by 14%. This threshold requires great changes of the initial design configuration to meet the requirements. Furthermore, the performance function value remains stable for the optimal solution of the deterministic optimization and of the different RBDO. However, the increase of the

costs objective function to obtain designs that are more reliable leads to the raise of the single objective function results.

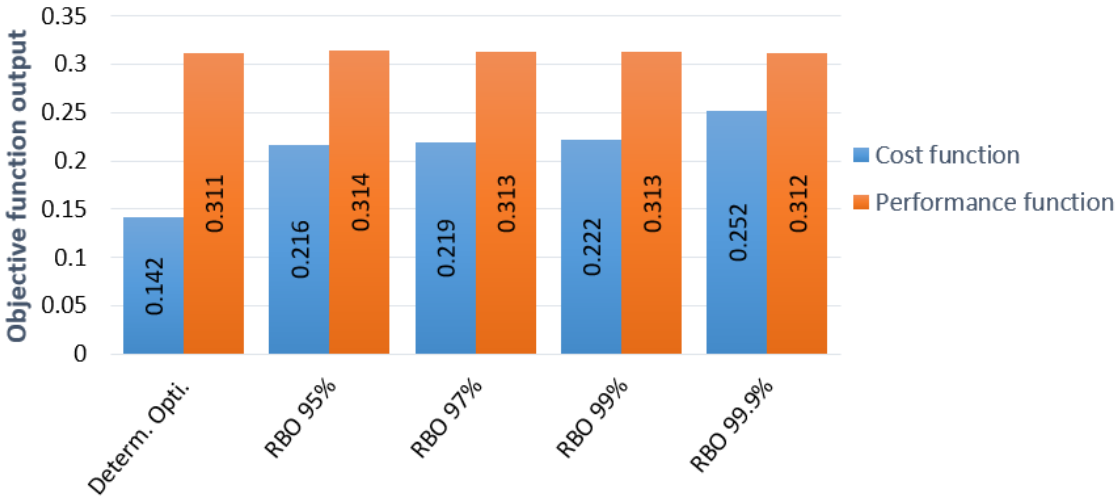

Figure 6-12: Representation of the optimal results regarding the performance and the cost objectives for the deterministic optimization and the different RBDO

Reliability-based constraints restrict the solution space of the problem. The best designs get infeasible, as they do not reach the required reliability level for the aircraft performances. The Pareto front of the RBDO moves towards greater performance and costs objective function values when the reliability thresholds tops up (Figure 6-13).

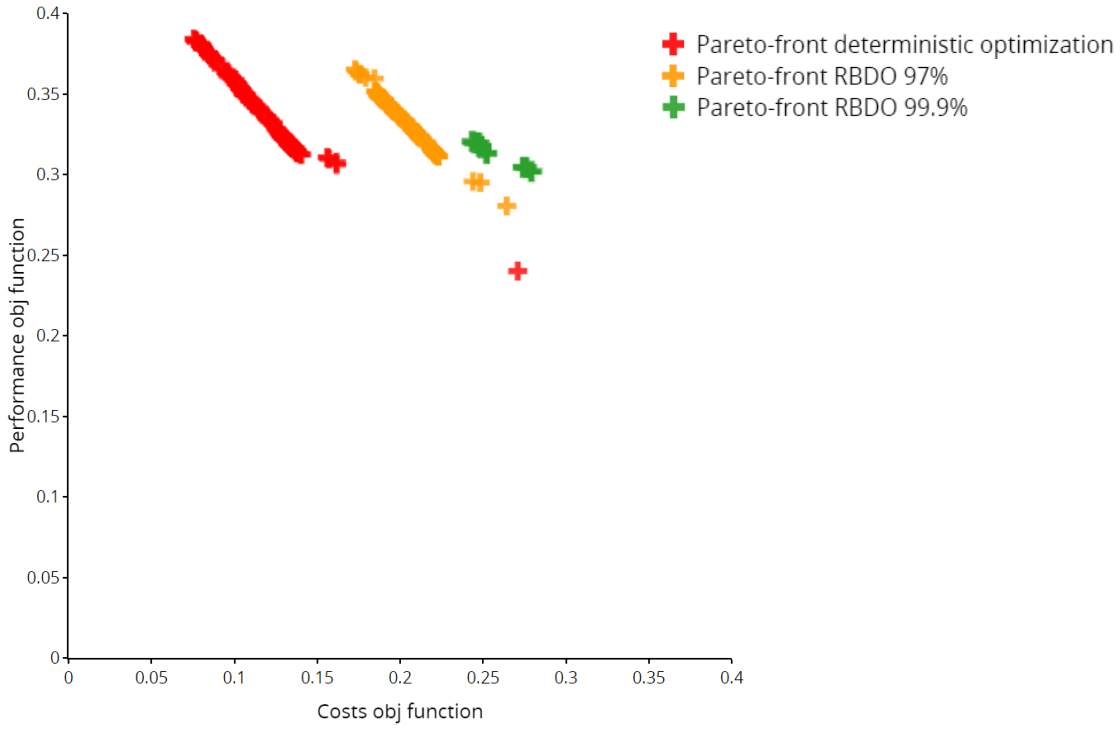

Figure 6-13: Evolution of the Pareto-front for increasing reliability thresholds

The reduction of the solution space due to the reliability-based constraints affects the process to identify the optimal solution. The initial population of the Design Explorer

optimization algorithm does not contain any valid design solution for the 99% reliability threshold configuration (Figure 6-14). Only 30 designs out of the 1600 tested for the 99.9% RBDO satisfy all reliability-based constraints.

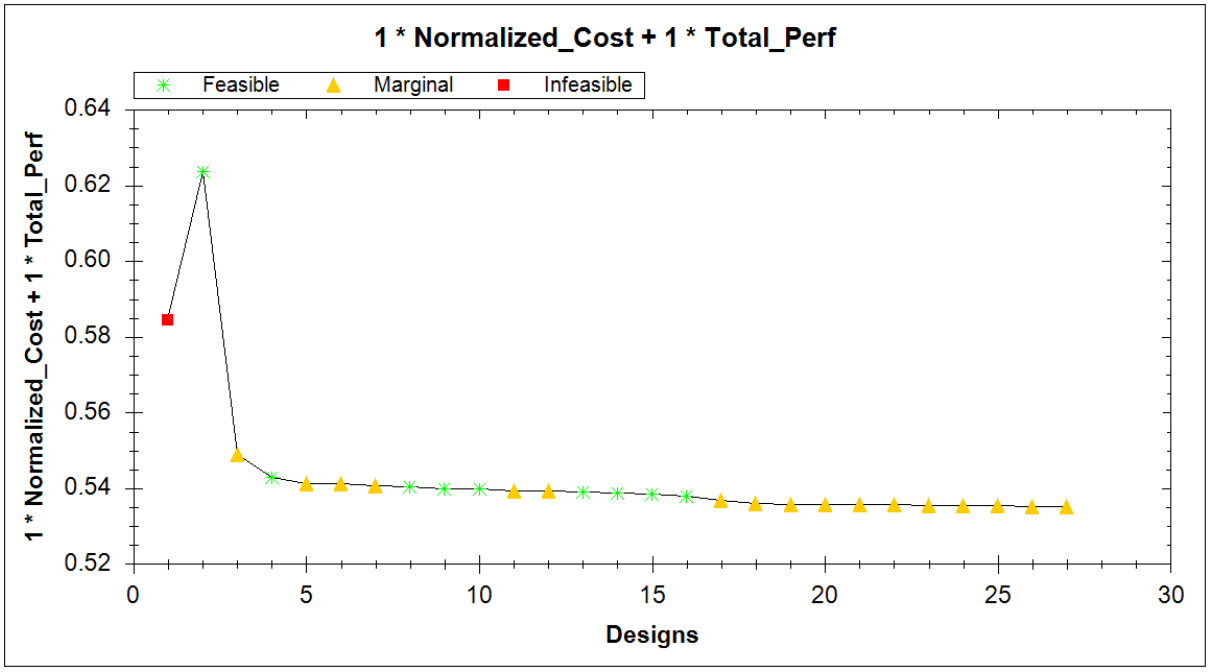

Figure 6-14: Evolution of the optimal design solution throughout the 99% RBDO process

When reliability thresholds get close to 1, the main part of the design tested is infeasible (Figure 6-15), the optimization algorithm requires more runs to compute the best design solution. The refinement of the design space of the problem around the optimal design points may improve the rate of the feasible solutions and improve the quality of the Pareto-front.

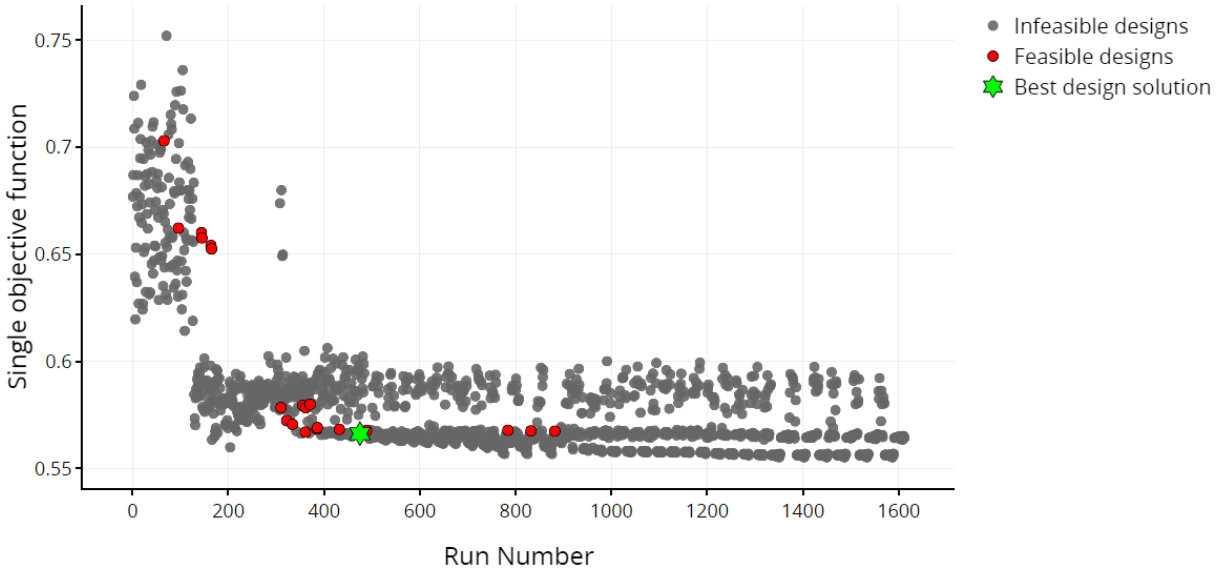

Figure 6-15: Representation of the design configurations tested during the 99.9% RBDO process

6.4.5 Validation of RBDO results

In order to validate the results of the RBDO, Monte Carlo algorithm samples 1000 design points for the different optimal design configurations. This probabilistic analysis aims to ensure that the optimal results satisfy the reliability-based constraints and to highlight the evolution of the performance probability distribution when the reliability of the aircraft increases.

OWE and TOFL requirement constraints are responsible for the most part of the infeasible solutions in the initial configuration. Figure 6-16 illustrates the improvement of the OWE and TOFL performances between the initial design configuration and the 99.9% reliable optimal design. The comparison shows a shift of the results away from the constraint thresholds for both OWE and TOFL values. The mean of both performances is reduced and the deviation decreases in the meantime. The RBDO manages limiting the rate of infeasible designs.

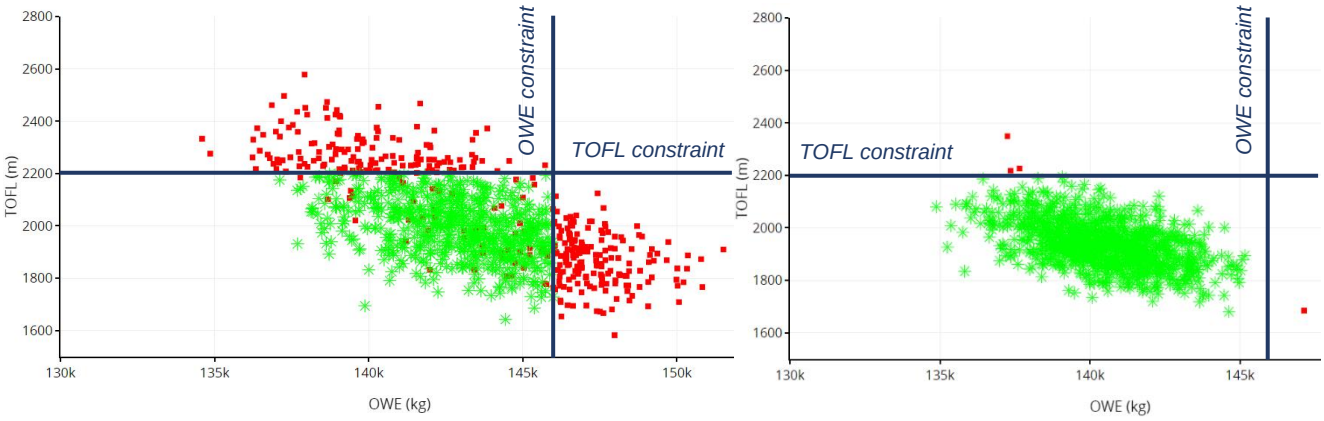

Figure 6-16: 2D Scatter Plot of the TOFL and the OWE after a Monte Carlo analysis with 1000 runs based on the initial design parameters configuration (left) and on the optimal set of design parameters obtained with the 99.9% RBDO

Histograms of Figure 6-17 illustrate the evolution of the OWE distribution associated to the initial, the optimal deterministic and the optimal reliable design configurations. While the deterministic optimization enhances the deterministic performance of OWE by shifting down the mean, the standard deviation remains similar to the one obtain with the initial configuration. This mean shifting away from the OWE constraint threshold increases the reliability of the performance. The RBDO aims to reduce the rate of infeasible designs while keeping the best system performances. Reliability-based optimal designs narrow the deviation of the OWE performance and keep the mean close to the one of the deterministic optimal configuration. This combination of mean shifting and standard deviation reduction of OWE ensures the 99.9% reliability of the system regarding OWE requirement.

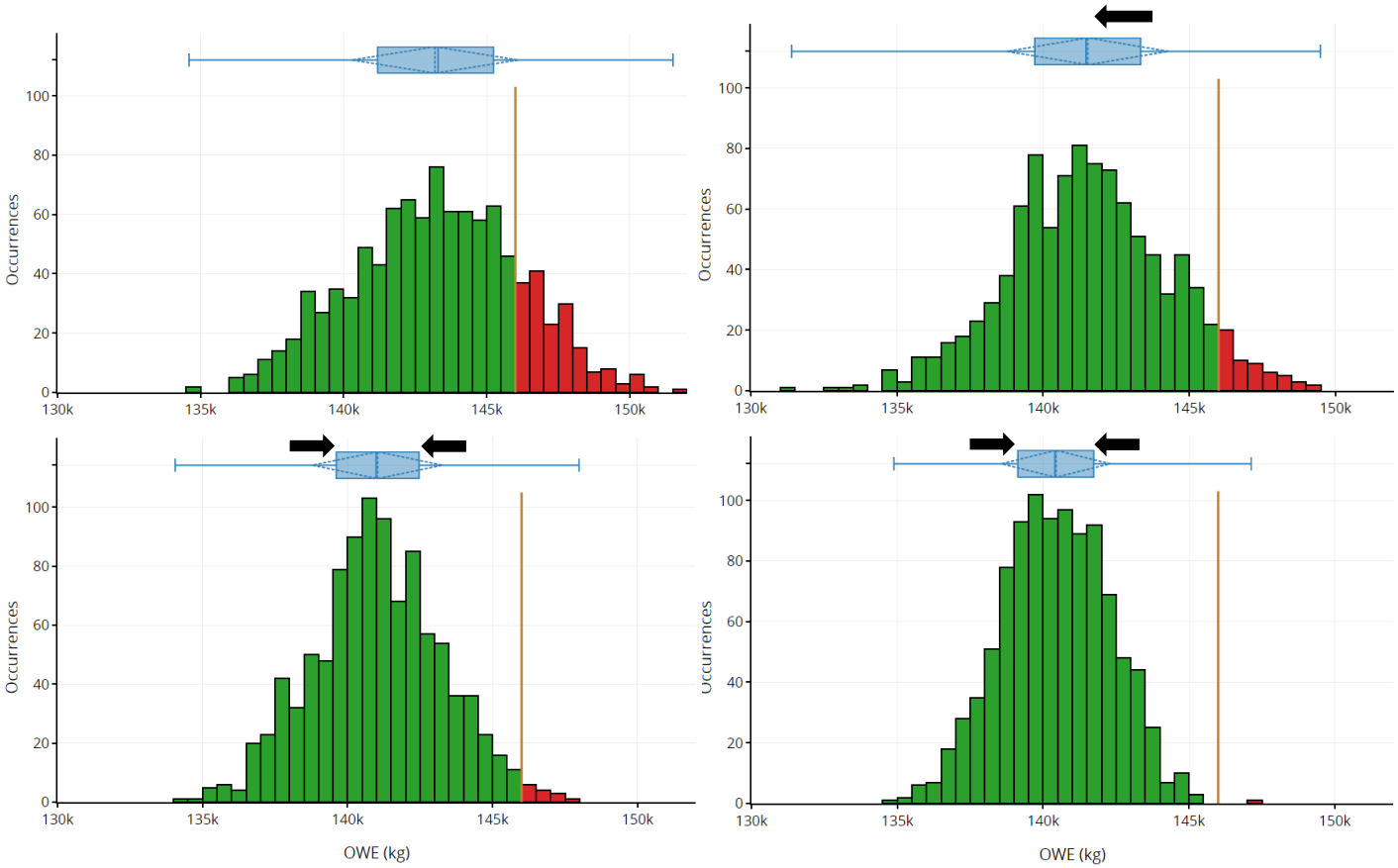

Figure 6-17: Evolution of the OWE distribution obtained after running a Monte Carlo analysis with 1000 runs and the following design configurations: initial design (top-left), deterministic optimal design (top-right), 97% reliable optimal design (bottom-left) and 99.9% reliable design (bottom-right)

6.5 Improvements and integration perspectives

Model Center provides useful tools to implement RBDO by identifying the critical parameters and propagating the uncertainty across the system. The model complexity requires model approximations to perform the studies. However, solutions to enhance the computing performance exist and are the key stones of the extrapolation of the uncertainty propagation tracking to systems that are more complex.

6.5.1 Case Study improvements

The parallelization of probabilistic and optimization runs works, as well as the connection to powerful servers to execute the simulations. Although the local machine still hosts the simulation workflow and limits the computational speed, the implementation of these measures to enhance the computational performance may improve the quality of the optimization.

The following list draws up some improvement ideas for the Case Study of Chapter 6:

- Instead of replacing the Cameo workflow by a RSM component (Part 6.3.1), keep the direct connection between Cameo and ModelCenter and compare the optimization results. This analysis allows assessing the quality of the RSM and the consequences of the approximation on the optimal design results.

- Run a multi-objective optimization algorithm to get rid of the weight factors of the performance and the costs objective functions. The assignment of weight factors reduces the solution space of the optimization by setting up a hierarchy between the objectives. Analyze the evolution of the global Pareto-front for increasing reliability thresholds.

- Improve the cost model function by including the rework costs (Taguchi), the maintenance costs, the production costs and the operating costs of the aircraft. Get access to precise cost models of Airbus commercial aircrafts. Consider the risk aversion of the customer in the performance objective function.

- Break down the architecture tree of the system into lower sub-system levels. Implement a use case based on a dynamic system model.

- Since Phoenix Integration released a new version of the Cameo-ModelCenter plugin called ModelCenter MBSE and replacing MBSE Pak, integrate the new plugin in the collaborative software environment model (Figure 3-10). List the modifications of the modeling process induced by this new Plug-In and evaluate the traceability of variables with this new software connection.

- Evaluate the potential fuel consumption reduction during the flights through a better understanding of the uncertainty propagation coming from the aircraft manufacturing. Project the potential operating costs savings per flight.

6.5.2 Integration perspectives

The integration perspectives of the RBDO process to more complex aeronautical systems address four different topics:

- System and uncertainty modeling: Conclusions of Part 4.5 remain valid in the case of a RBDO process based on the Cameo – ModelCenter connection. As the number of function evaluations to compute the system performances is a major parameter in the optimization process, it seems interesting to analyze the processing time of complex equations coded on CAD or fluid dynamics software. RSM offers an approximation solution if the performance calculation workflow lasts too long to assess the outputs, but breaks down the Cameo – ModelCenter connection.

- Screening DOE: This step is essential in order to lower the dimensionality of the optimization problem for complex aircraft systems. ModelCenter provides many

useful tools to screen the design space and identify the critical parameters (See Part 6.3.3).

- Probabilistic analysis: Each run of the optimization requires the execution of a probabilistic analysis to evaluate the reliability of the system. The wrapping of the probabilistic analysis into another ModelCenter workflow enhances the computation speed and reduce the computing time of Monte Carlo analysis. NESSUS analytic methods offer a good alternative to shorten the number of function evaluations.

- Optimization analysis: ModelCenter provides useful tools to run both deterministic and reliable, single and multi-objective optimizations. Computing time depends directly on the number of design parameters, the size of the design space, the complexity of the performance calculation workflow and the computational resources of the machine and the servers. It is impossible to come up with a global best design configuration of the optimization tool. A compromise must be found between the number of design parameters to conserve after the screening DOE, their design interval range configuration and the type of optimization to perform.

In conclusion, the integration perspectives of the RBDO pattern on ModelCenter depends on many parameters. Parallelization of the simulation runs as well as computing on powerful servers are key stones of the integration to more complex systems. The implementation of the UMDO guideline for a complex aircraft model containing several thousands of input parameters may provide a more precise idea of ModelCenter abilities to perform optimizations under uncertainty.

7 Conclusion

7.1 Summary

In the context of recent changes in Systems Engineering with the development of MBSE, this thesis addresses the setting up and the evaluation of a collaborative software environment to support uncertainty management for complex aeronautical systems.

First, a CPM flowchart based on the software used by Airbus is developed, in order to identify and assess the critical parameters, variation of which affects the top level performances of a complex system. Cameo Systems Modeler supports the structure modeling, while ModelCenter pulls together analytics models from different software into a unique simulation workflow. Analysis Server and MBSE Pak participate in bridging the gap between descriptive and analytics models.

In a second step, several case studies aim evaluating the ability to carry out a CPM within the collaborative software environment. A basic commercial aircraft model serves as an example. ModelCenter ensures the modularity and the flexibility of the modeling process and enables performing multi-level simulations. Knowledge transfer from similar projects helps facing the lack of data about a system in early steps of the design process. Uncertainty modeling is a key stone of the CPM. Engineers must therefore provide a precise and data-driven model to come up with meaningful SA results. Uncertainty coming from manufacturing, modeling approximation and external noise factors have been tackled in the thesis. The diversity of SA tools and the user-friendly visualization of results on ModelCenter deliver insights about the uncertainty propagation across the system levels. Design parameters that lead to performance and cost variations are identified and mitigation strategies derive directly from the analysis. These results guide the work of designers and engineers who can focus their work on improving the accuracy of the model or the design of specific components. The systematic CPM throughout the design process of a new system shows good results and can contribute to lead-time reduction by a better understanding of the system uncertainty.

Then, optimization has been performed on the commercial aircraft model with a deterministic and a reliability-based approach. The built up optimization framework combines the SA tools of ModelCenter, such as DOE and probabilistic analysis. RBDO introduces reliability-based constraints that strongly reduce the solution space and make the deterministic optimal design infeasible. Gradient-based and genetic algorithms such as NSGA-II have been compared. While multi-objective optimization algorithms require a great number of runs to determine the Pareto-front, alternatives convert the problem into a single objective optimization and reduce the computing time. This solution requires assigning weights to the objectives, which must be done cautiously as it focuses the search for optimal design on a part of the global multi-objective Pareto-front. The results show that the introduction of reliability-based constraints strongly modifies the optimal design of the aircraft.

Although uncertainty-based optimization enables coming up with reliable and robust design solutions, the process requires more function evaluations and therefore increases the complexity of the simulation. ModelCenter proposes a variety of solutions to face this major issue. While RSM and DOE screening reduce the complexity and the dimensionality of the problem, Analysis Server can enhance the computational performance by executing the simulation on virtual machines.

Finally, the collaborative and adaptive software environment revolving around Cameo and ModelCenter handles the uncertainty management of complex systems from the early steps of the design process. The SA, DOE and optimization tools of ModelCenter help guiding the work of engineers during the design phase and contribute to the development of a reliable and robust design.

7.2 Discussion and outlook

The Case Studies afford to evaluate the implementation of a CPM on Cameo Systems Modeler and ModelCenter. However, the complexity of the parameters involved in multidisciplinary optimization under uncertainty makes it difficult to extrapolate a general flowchart. For each system, engineers must strike a balance between accuracy of the results and computing time. With a view to integrating the design under uncertainty method into more complex systems at Airbus, it seems important to carry out a RBDO on a system with thousands of variables and complex analytics models, closer to real cases. This implementation would enable to test ModelCenter's complexity reduction methods and the parallelization of simulations on Airbus servers.

Furthermore, the cost model requires further development as it is a central element in the multidisciplinary design optimization. New cost model can consider the risk aversion of the customer and integrate costs occuring during the whole life cycle of a commercial aircraft. This model enhancement might be difficult, as there is no data-driven model linking design uncertainties to the operating costs of an aircraft yet.

Finally, MBSE Pak has been recently replaced by ModelCenter MBSE. According to Phoenix Integration, this new tool improves the traceability of variables and requirements along the modeling process of complex system. ModelCenter MBSE must be integrated into the collaborative software environment tackled in the thesis.

A References

Abdullah, M. B. (1990), 'On a Robust Correlation Coefficient', *Journal of the Royal Statistical Society. Series D (The Statistician)*, 39/4: 455–460.

Akoglu, H. (2018), 'User's guide to correlation coefficients', *Turkish Journal of Emergency Medicine*, 18.

Alam, F. M., McNaught, K. R., and Ringrose, T. J. (2004), 'Using Morris' Randomized Oat Design as a Factor Screening Method for Developing Simulation Metamodels', in , *2004 Winter Simulation Conference* (IEEE), 949–57.

Ali, R., and Al-Shamma, O. (2014), 'A Comparative Study of Cost Estimation Models used for Preliminary Aircraft Design', *Global Journal of Researches in Engineering*, Volume XIV/Issue IV.

Archer, G., Saltelli, A., and Sobol, I. (1997), 'Sensitivity measures, ANOVA-like techniques and the use of bootstrap', *Journal of Statistical Computation and Simulation - J STAT COMPUT SIM*, 58: 99–120.

Ba, S., and Joseph, V. R. (2011), 'Multi-Layer Designs for Computer Experiments', *Journal of the American Statistical Association*, 106: 1139–1149.

Balaji, S., and Sundararajan Murugaiyan, M. (2012), 'WATERFALL Vs V-MODEL Vs AGILE: A COMPARATIVE STUDY ON SDLC', *International Journal of Information Technology and Business Management*, 2.

Barton, R. R. (1999), *Graphical Methods for the Design of Experiments* (Lecture Notes in Statistics, 143, New York, NY: Springer New York; Imprint; Springer).

Beihoff, B., Oster, C., Friedenthal, S. et al. (2014), *A World in Motion – Systems Engineering Vision 2025*.

Bilal, N. (2016), 'Implementation of Sobol's Method of Global Sensitivity Analysis to a Compressor Simulation', in , *22nd International Compressor Engineering Conference at Purdue 2014*. *West Lafayette, Indiana, USA, 14-17 July 2014* (Red Hook, NY: Curran).

Blitzstein, J. K., and Hwang, J. (2015), *Introduction to probability* (Chapman & Hall/CRC texts in statistical science series, Boca Raton: CRC Press).

Brevault, L., Balesdent, M., Bérend, N. et al. (2013), *Comparison of different global sensitivity analysis methods for aerospace vehicle optimal design*.

Bubevski, V. (2018), *Novel six sigma approaches to risk assessment and management* (Hershey PA: Business Science Reference an imprint of IGI Global).

Cao, Y., Liu, T., and Yang, J. (2018), 'A comprehensive review of tolerance analysis models', *The International Journal of Advanced Manufacturing Technology*, 97.

Choudri, A. (2004), 'Design for Six Sigma for Aerospace Applications', in , *Space 2004 Conference and Exhibit* (AIAA SPACE Forum: American Institute of Aeronautics and Astronautics).

DAKOTA (2017), *Dakota, A Multilevel Parallel Object-Oriented Framework for Design Optimization, Parameter Estimation, Uncertainty Quantification, and Sensitivity Analysis: Version 6.7 User's Manual*.

Deb, K., Pratap, A., Agarwal, S. et al. (2002), 'A fast and elitist multiobjective genetic algorithm: NSGA-II', *Evolutionary Computation, IEEE Transactions on*, 6: 182–197.

DeLaurentis, D., and Mavris, D. (1970), 'Uncertainty Modeling and Management in Multidisciplinary Analysis and Synthesis', 1970.

Dimov, I., Georgieva, R., Ostromsky, T. et al. (2013), 'Advanced algorithms for multidimensional sensitivity studies of large-scale air pollution models based on Sobol sequences', *Computers & Mathematics with Applications*, 65: 338–351.

Divahar, J. (2009), *Airfoil Analyzer* <https://ww2.mathworks.cn/matlabcentral/fileexchange/12889-airfoil-analyzer?s_tid=FX_rc3_behav>.

Du, W., Rong, m., Li, S. et al. (2012), 'Design of Product Key Characteristics Management System', *Advanced Materials Research*, 468-471: 835–838.

Du, X. (2002), 'Efficient Uncertainty Analysis Methods For Multidisciplinary Robust Design', *AIAA Journal*, 40.

Estable, S., Telaar, J., Lange, M. et al. (2017), 'Definition of an Automated Vehicle with Autonomous Fail-Safe Reaction Behavior to Capture and Deorbit Envisat', in T. Flohrer and F. Schmitz (eds.), *Proceedings of the 7th European Conference on Space Debris* (ESA Space Debris Office).

Estefan, J. (2008), 'Survey of Model-Based Systems Engineering (MBSE) Methodologies', *INCOSE MBSE Focus Group*, 25.

Feo, J. de, and Bar-El, Z. (2002), 'Creating strategic change more efficiently with a new Design for Six Sigma process', *Journal of Change Management*, 3/1: 60–80.

Flohrer, T., and Schmitz, F. (2017) (eds.), *Proceedings of the 7th European Conference on Space Debris* (ESA Space Debris Office).

Friedenthal, S. (2015), *A practical guide to SysML*: *The systems modeling language* (Third edition).

Friedenthal, S., Griego, R., and Sampson, M. (2009), 'INCOSE Model Based Systems Engineering (MBSE) Initiative', 2009.

Han, Y.-Y., Gong, D.-w., Sun, X.-Y. et al. (2014), 'An improved NSGA-II algorithm for multi-objective lot-streaming flow shop scheduling problem', *International Journal of Production Research*, 52.

He, Z., and Fang, J. (2011), 'Comparative study of response surface designs with errors-in-variables model', *Transactions of Tianjin University*, 17/2: 146 <https://doi.org/10.1007/s12209-011-1605-5>.

Hirsch, C., Wunsch, D., Szumbarski, J. et al. (2019) (eds.), *Uncertainty Management for Robust Industrial Design in Aeronautics*: *Findings and Best Practice collected during UMRIDA, a Collaborative Research Project (2013- 2016) funded by the European Union* (Notes on numerical fluid mechanics and multidisciplinary design, volume 140, Cham, Switzerland: Springer).

Idriss, D., Beaurepaire, P., Homri, L. et al. (2018), 'Tolerance Analysis - Key Characteristics Identification by Sensitivity Methods', *Procedia CIRP*, 75: 33–38 <http://www.sciencedirect.com/science/article/pii/S221282711830489X>.

INCOSE (2014), 'A World in Motion, Systems Engineering Vision 2025', 2014.

Jin, Y., and Branke, J. (2005), 'Evolutionary Optimization in Uncertain Environments---A Survey', *IEEE Transactions on Evolutionary Computation*, 9: 303–317.

Keane, A. J., and Nair, P. B. (2005), *Computational approaches for aerospace design*: *The pursuit of excellence* (Chichester, England, Hoboken, N.J: Wiley).

Khan, R. M. (2013), *Problem Solving and Data Analysis Using Minitab*: *A Clear and Easy Guide to Six SIGMA Methodology* (West Sussex: John Wiley & Sons).

Koch, P. N., Yang, R.-J., and Gu, L. (2004), 'Design for six sigma through robust optimization', *Structural and Multidisciplinary Optimization*, 26/3: 235–248 <https://doi.org/10.1007/s00158-003-0337-0>.

Krüger, S., Strunz, R., and Herrmann, J. (2015), *A liquid rocket engine conceptual design tradeoff methodology using an a priori articulation of preference information with epistemic uncertainties*.

Lamboni, M., Iooss, B., Popelin, A.-L. et al. (2012), 'Derivative-based global sensitivity measures: General links with Sobol' indices and numerical tests', *Mathematics and Computers in Simulation*, 87.

Lemieux, C. (2009), *Monte carlo and quasi-monte carlo sampling* (Springer Series in Statistics, New York: Springer).

Levy, S., and Steinberg, D. M. (2010), 'Computer experiments: a review', *AStA Advances in Statistical Analysis*, 94/4: 311–324 <https://doi.org/10.1007/s10182-010-0147-9>.

Lupan, R., Bacivarof, I. C., Kobi, A. et al. (2005), 'A Relationship Between Six Sigma and ISO 9000:2000', *Quality Engineering*, 17/4: 719–725.

Maass, E., and McNair, P. D. (2010), *Applying design for Six Sigma to software and hardware systems* (Print. digitally on demand, paperback version of an original hardcover book, Upper Saddle River, NJ [u.a.]: Prentice Hall).

Mackertich, N., and Kraus, P. (2012), *Using Critical Parameter Management to Manage, Analyze & Report Technical Product Performance*.

Mackertich, N., Kraus, P., Mittelstaedt, K. et al. (2017), *IEEE Computer Society/Software Engineering Institute Watts S. Humphrey Software Process Achievement Award 2016: Raytheon Integrated Defense Systems*.

Markish, J., and Willcox, K. (2003), 'Value-Based Multidisciplinary Techniques for Commercial Aircraft System Design', *Aiaa Journal - AIAA J*, 41: 2004–2012.

Mckay, M., Beckman, R., and Conover, W. (1979), 'A Comparison of Three Methods for Selecting Vales of Input Variables in the Analysis of Output From a Computer Code', *Technometrics*, 21: 239–245.

Morio, J. (2011), 'Global and local sensitivity analysis methods for a physical system', *European Journal of Physics*, 32: 1577.

Narania, S., Eshahawi, T., Gindy, N. et al. (2008), *Risk mitigation framework for a robust design process*.

Narayanan, H., and Khoh, S. (2008), *Deploying Design for Six Sigma (TM) in New Product Development*.

NDIA (2011), *Final Report Model Based Engineering Subcommittee*.

Oliveira, J. M. (2015), 'Development of Operating Cost Models for the Preliminary Design Optimization of an Aircraft', Master Thesis (Lisboa, Técnico Lisboa).

Padmanabhan, D., Agarwal, H., Renaud, J. et al. (2006), 'A study using Monte Carlo Simulation for failure probability calculation in Reliability-Based Optimization', *Optimization and Engineering*, 7: 297–316.

Phoenix Integration (2018), *Book of Knowledge ModelCenter 13.1*.

Rabin, M. (2000), 'Risk Aversion and Expected-Utility Theory: A Calibration Theorem', *Econometrica*, 68/5: 1281–1292 <www.jstor.org/stable/2999450>.

Ramos, A. L., Ferreira, J., and Barcelo, J. (2012), 'Model-Based Systems Engineering: An Emerging Approach for Modern Systems', *Systems, Man, and Cybernetics, Part C: Applications and Reviews, IEEE Transactions on*, 42: 101–111.

Rohatgi, V. K., and Saleh, A. K. M. E. (2015), *An introduction to probability and statistics* (Wiley series in probability and statistics; Third edition, Hoboken New Jersey: Wiley).

Romand, O. (2017), 'Model Based Systems Engineering for on-orbit servicing system analysis', Master Thesis (Toulouse, Institut Supérieur de l'Aéronautique et de l'Espace SUPAERO).

Saaty, T. L. (1990), 'How to make a decision: The analytic hierarchy process', *European Journal of Operational Research*, 48/1: 9–26 <https://econpapers.repec.org/RePEc:eee:ejores:v:48:y:1990:i:1:p:9-26>.

Saravi, M., Newnes, L., Mileham, A. et al. (2013), 'Using Taguchi method to optimise performance and product cost at the conceptual stage of design', *Proceedings of the Institution of Mechanical Engineers, Part B: Journal of Engineering Manufacture*, 227: 1360–1372.

Scholz, D. (1998), 'DOCsys-A Method to Evaluate Aircraft Systems', *Bewertung von Flugzeugen (Workshop: DGLR Fachausschuß S2-Luftfahrtsysteme, München, 26./27)*, 1998.

—— (2017), *Cost Evaluation of Aircraft Systems,* Lecture HAW Hamburg, 2017 (Hamburg).

Shahin, A. (2008), 'Design for Six Sigma (DFSS): Lessons learned from world-class companies', *International Journal of Six Sigma and Competitive Advantage*, 4.

Simmons, J., Ragon, S., and Davenport, T. (2018), *Trade Space Exploration of MBSE and MBE Integrated Workflows,* NIST 2018 MBE Summit, 3 Apr (Gaithersburg).

Southwest Research Institute (2012), 'NESSUS Theoretical Manual', 2012.

Squillero, G., and Burelli, P. (2016) (eds.), *Applications of evolutionary computation*: *19th European conference, EvoApplications 2016, Porto, Portugal, March 30 - April 1, 2016, proceedings* (LNCS Sublibrary: SL1 - Theoretical Computer Science and General Issues, 9597-9598; 1st ed. 2016, [Switzerland]: Springer).

Stein, M. (1987), 'Large Sample Properties of Simulations Using Latin Hypercube Sampling', *Technometrics*, 29/2: 143–151.

Teich, J. (2001), *Pareto-Front Exploration with Uncertain Objectives* (1993).

Thornton, A. C. (2003), *Variation risk management*: *Focusing quality improvements in product development and production / Anna C. Thornton* (New York, Chichester: Wiley) <http://www.loc.gov/catdir/bios/wiley046/2003017776.html>.

Tsou, J.-C. (2007), 'Economic order quantity model and Taguchi's cost of poor quality', *Applied Mathematical Modelling - APPL MATH MODEL*, 31: 283–291.

Urdu, M. (2015), 'Aircraft maintenance cost modelling considering the influence of design parameters', Master Thesis (Delft, Delft University of Technology).

Vaneman, W. (2016), *The system of systems engineering and integration "Vee" model*.

Vrinat, M. (2007), 'Driving Product Development with Critical Parameters. Cognition delivers Active Requirements Management for the Full Product Lifecycle', 2007.

Westphal, R., and Scholz, D. (1997), 'A Method for Predicting Direct Operating Costs During Aircraft System Design', *Cost Engineering*, 39.

Whitney, D. E. (2004), *Mechanical assemblies*: *Their design, manufacture, and role in product development / Daniel E. Whitney* (Oxford series on advanced manufacturing, New York, Oxford: Oxford University Press).

Wu, J., and Wang, Y. (2012), 'Applying Life Cycle Six Sigma in Tolerance Design Methodology', *Advanced Materials Research*, 443-444: 881–887.

Xu, W., Hou, Y., Hung, Y. et al. (2010), 'Comparison of Spearman's rho and Kendall's tau in Normal and Contaminated Normal Models', *Signal Processing*, 93.

Yao, W., Chen, X., Luo, W. et al. (2011), 'Review of uncertainty-based multidisciplinary design optimization methods for aerospace vehicles', *Progress in Aerospace Sciences*, 47/6: 450–479.

Ye, C.-J., and Huang, M.-X. (2015), 'Multi-Objective Optimal Power Flow Considering Transient Stability Based on Parallel NSGA-II', *Power Systems, IEEE Transactions on*, 30: 857–866.

Zaman, K., Mcdonald, M., and Mahadevan, S. (2011), 'Probabilistic Framework for Uncertainty Propagation With Both Probabilistic and Interval Variables', *Journal of Mechanical Design*, 133.

Zang, T., Hemsch, M., Hilburger, M. et al. (2002), 'Needs and Opportunities for Uncertainty-Based Multidisciplinary Design Methods for Aerospace Vehicles', 2002.

Zijp, S.O.L. (2014), 'Development of a Life Cycle Cost Model for Conventional and Unconventional Aircraft', Master Thesis (Delft, Delft University of Technology).

B Appendices

B.1 Probability Density Functions implemented in the Case Studies

Probability Density Functions are a commonly used mathematical tool to express the uncertainty of manufacturing and assembly parameters.

Blitzstein and Hwang (2015) introduce the following formalism to define the PDF associated to a Uniform and a Normal distributions (Blitzstein and Hwang 2015: 201–11):

- Uniform distribution: The continuous random variable U follows a Uniform distribution on $[a, b]$ if its PDF is:

$$f(x) = \begin{cases} \frac{1}{b-a} & if\ a < x < b \\ 0 & otherwise \end{cases} \qquad \textbf{Eq. (7-1)}$$

- Normal distribution: The continuous random variable Z follows a standard Normal distribution if its PDF is:

$$\varphi(z) = \frac{1}{\sqrt{2\pi}}\, e^{-z^2/2}, \qquad -\infty < z < \infty \qquad \textbf{Eq. (7-2)}$$

B.2 Step by step CPM of Part 4.3

Chapter 4.3 carries out a step-by-step CPM throughough the design process of a new commercial aircraft. Following Tables describe the PDF of the input parameters and the composition of the KC list for each step of the process. Mitigation strategies to improve the TOFL reliability are presented too.

Table 7-1: Configuration of inputs PDF at Step 2 of the design process. Since Step 1, introduction of new input parameters and improvement of model accuracy. Reliability TOFL Step 2: 52.1%.

Steps 1->2	*Parameters*	*Distrib type*	*Nominal*	*Deviation*	*Lower bound*	*Upper bound*	*Remarks*	*Previous KC status*	*New KC status*
Design parameters	c_{Root}	Normal	13.7	5%			New design parameter		
	c_{Tip}	Normal	0.35	5%			New design parameter		
	L_{Wing}	Normal	23.32	5%			New design parameter		
	l_{Fus}	Normal	5.69	5%			New design parameter		
	BPR	Normal	9.13	3%			Deviation: 5% -> 3%		
	MC	Normal	1	3%			Deviation: 5% -> 3%		
	T_{SLS}	Normal	387000	3%			Deviation: 5% -> 3%		
Equation uncertainties	U_{TOFL}	Uniform			0.93	1.07	Bound: 30% -> 14%		
	$U_{c_{z,TO}}$	Uniform			0.94	1.06	New equation uncertainty		
	$U_{T_{TO}}$	Uniform			0.97	1.03	Bound: 20% -> 6%		
	$U_{Ma_{TO}}$	Uniform			0.97	1.03	New equation uncertainty		
	$U_{A_{Wing}}$	Uniform			0.99	1.01	New equation uncertainty		

Table 7-2: Configuration of inputs PDF at Step 3 of the design process. Since Step 2, focus on the wings design, increase of WingLength and RootChord, improvement of model accuracy. Reliability TOFL Step 3: 65.6%.

Steps 2->3	*Parameters*	*Distrib type*	*Nominal*	*Deviation*	*Lower bound*	*Upper bound*	*Remarks*	*Previous KC status*	*New KC status*
Design parameters	c_{Root}	Normal	13.9	4%			Nom: 13.7 -> 13.9 | Dev: 5% -> 4%		
	c_{Tip}	Normal	0.35	4%			Dev: 5% -> 4%		
	L_{Wing}	Normal	23.7	4%			Nom: 23.32 -> 23.7 | Dev: 5% -> 4%		
	l_{Fus}	Normal	5.69	4%			Dev: 5% -> 4%		
Equation uncertainties	U_{TOFL}	Uniform			0.97	1.03	Bound: 14% -> 6%		
	$U_{c_{z,TO}}$	Uniform			0.97	1.03	Bound: 12% -> 6%		
	$U_{T_{TO}}$	Uniform			0.98	1.02	Bound: 6% -> 4%		
	$U_{Ma_{TO}}$	Uniform			0.98	1.02	Bound: 6% -> 4%		

Table 7-3: Configuration of inputs PDF at Step 4 of the design process. Since Step 3, focus on the engine parameters and improvement of model accuracy. Reliability TOFL Step 4: 88.1%.

Steps 3->4	*Parameters*	*Distrib type*	*Nominal*	*Deviation*	*Lower bound*	*Upper bound*	*Remarks*	*Previous KC status*	*New KC status*
Design parameters	c_{Root}	Normal	13.9	2%			Dev: 4% -> 2%		
	L_{Wing}	Normal	23.7	2%			Dev: 4% -> 2%		
	l_{Fus}	Normal	5.69	2%			Dev: 4% -> 2%		
	MC	Normal	1.03	2%			Nom: 1.00 -> 1.03 | Dev: 3% -> 2%		
	T_{SLS}	Normal	395000	2%			Nom: 387000 -> 395000 | Dev: 3% -> 2%		
Equation uncertainties	$U_{T_{TO}}$	Uniform			0.99	1.01	Bound: 4% -> 2%		
	$U_{Ma_{TO}}$	Uniform			0.99	1.01	Bound: 4% -> 2%		

Table 7-4: Configuration of inputs PDF at Step 5 of the design process. Since Step 4, increase of the wing size and of the engine power. Reliability TOFL Step 5: 97.2%.

Steps 4->5	*Parameters*	*Distrib type*	*Nominal*	*Deviation*	*Lower bound*	*Upper bound*	*Remarks*	*Previous KC status*	*New KC status*
Design parameters	c_{Root}	Normal	14.0	1%			Nom: 13.9 -> 14.0 | Dev: 2% -> 1%		
	L_{Wing}	Normal	24.0	1%			Nom: 23.7 -> 24.0 | Dev: 2% -> 1%		
	l_{Fus}	Normal	5.69	1%			Dev: 2% -> 1%		
	MC	Normal	1.04	1%			Nom: 1.03 -> 1.04 | Dev: 2% -> 1%		
	T_{SLS}	Normal	400000	1%			Nom: 395000 -> 400000 | Dev: 2% -> 1%		
Equation uncertainties	U_{TOFL}	Uniform			0.99	1.01	Bound: 6% -> 2%		

Table 7-5: Configuration of inputs PDF at Step 6 of the design process. Since Step 5, narrowing of design parameters variations. Reliability TOFL Step 6: 99.3%.

Steps 5->6	*Parameters*	*Distrib type*	*Nominal*	*Deviation*	*Lower bound*	*Upper bound*	*Remarks*	*Previous KC status*	*New KC status*
Design parameters	c_{Root}	Normal	14.0	0.5%			Dev: 1% -> 0.5%		
	L_{Wing}	Normal	24.0	0.5%			Dev: 1% -> 0.5%		
	l_{Fus}	Normal	5.69	0.5%			Dev: 1% -> 0.5%		
	MC	Normal	1.04	0.5%			Dev: 1% -> 0.5%		
	T_{SLS}	Normal	400000	0.5%			Dev: 1% -> 0.5%		
Equation uncertainties	$U_{C_{z,TO}}$	Uniform			0.99	1.01	Bound: 6% -> 2%		

B.3 Multi-objective weight assignment

In Part 5.2.2.1, the definition of the performance objective function of the aircraft requires the assessment of the performance weight factors. The eigenvalue method provides data-driven results; the different steps of the assessment are described below.

The preference ratio p_{ij} characterizes the relative importance between the performances i and j. If the performance i is 4 times as important as performance j, p_{ij} equals 4.

The preference matrix (**Eq. (5-12)**) regroups the results of the pairwise comparisons between the 4 performances. The successive lines and colums of $\boldsymbol{P}$ refer to the $Range$, the OWE, the $TOFL$ and the $WingSpan$ in that order.

$$\boldsymbol{P} = \begin{pmatrix} 1 & 4/3 & 2 & 4 \\ 3/4 & 1 & 3/2 & 3 \\ 1/2 & 2/3 & 1 & 2 \\ 1/4 & 1/3 & 1/2 & 1 \end{pmatrix} \qquad \textbf{Eq. (7-3)}$$

As $\boldsymbol{P}$ is self consistent, the largest eigenvalue, noted λ_{max}, equals the number of goals (Saaty 1990: 13).

Then, the objective is to determine an eigenvector $\boldsymbol{w} = (w_1 \quad w_2 \quad w_3 \quad w_4)^T$ associated to the eigenvalue $\lambda_{max} = 4$. $\boldsymbol{w}$ verifies the following equations:

$$\boldsymbol{P}\boldsymbol{w} = \lambda_{max}\boldsymbol{w} \qquad \textbf{Eq. (7-4)}$$

$$\Leftrightarrow \begin{pmatrix} -3w_1 & \frac{4}{3}w_2 & 2w_3 & 4w_4 \\ \frac{3}{4}w_1 & -3w_2 & \frac{3}{2}w_3 & 3w_4 \\ \frac{1}{2}w_1 & \frac{2}{3}w_2 & -3w_3 & 2w_4 \\ \frac{1}{4}w_1 & \frac{1}{3}w_2 & \frac{1}{2}w_3 & -3w_4 \end{pmatrix} = \begin{pmatrix} 0 \\ 0 \\ 0 \\ 0 \end{pmatrix} \qquad \textbf{Eq. (7-5)}$$

$$\Leftrightarrow \begin{pmatrix} -3w_1 & \frac{4}{3}w_2 & 2w_3 & 4w_4 \\ 0 & -\frac{8}{3}w_2 & 2w_3 & 4w_4 \\ 0 & 0 & -2w_3 & 4w_4 \\ 0 & 0 & 0 & w_4 \end{pmatrix} = \begin{pmatrix} 0 \\ 0 \\ 0 \\ 0 \end{pmatrix} \qquad \textbf{Eq. (7-6)}$$

$$\Leftrightarrow \begin{pmatrix} w_1 \\ w_2 \\ w_3 \\ w_4 \end{pmatrix} = w_4 \begin{pmatrix} 4 \\ 3 \\ 2 \\ 1 \end{pmatrix} \qquad \textbf{Eq. (7-7)}$$

In order to satify Eq. (5-11), w_4 is set to 0.1 and the final weight vector is:

$$\begin{pmatrix} w_1 \\ w_2 \\ w_3 \\ w_4 \end{pmatrix} = \begin{pmatrix} 0.4 \\ 0.3 \\ 0.2 \\ 0.1 \end{pmatrix} \qquad \textbf{Eq. (7-8)}$$

B.4 Results Reliability-Based Design Optimization of Part 6.4

Following Table 7-6 contains the results of the different optimizations performed in Chapter 6. The multi-objective optimization problem is converted into a single objective function, the weight factors of the performance and of the cost objectives are set equal to 1.

Table 7-6: Results of the different design optimizations of Chapter 6 and comparison with the initial design parameters configuration. Orange highlighting makes stand out parameters which value in the optimal design differs from the initial configuration.

	Initial Configuration	Deterministic opti. design $w_{Cost}=1$ $w_{Perf}=1$	RBDO 95% $w_{Cost}=1$ $w_{Perf}=1$	RBDO 97% $w_{Cost}=1$ $w_{Perf}=1$	RBDO 99% $w_{Cost}=1$ $w_{Perf}=1$	RBDO 99.9% $w_{Cost}=1$ $w_{Perf}=1$
Objective Functions						
$Single\ objective\ function\ f(\boldsymbol{x})$	0.601	0.453	0.530	0.532	0.535	0.564
$Cost\ Function\ f_{Cost}(\boldsymbol{x})$	0	0.142	0.216	0.219	0.222	0.252
$Performance\ Function\ f_{Perf}(\boldsymbol{x})$	0.601	0.311	0.314	0.313	0.313	0.312
Reliabilities						
$R_{L_{TO}\leq 2200}$	0.858	0.874	0.984	0.988	0.990	0.999
$R_{d_{Range}\geq 11500}$	0.948	0.999	0.999	0.999	0.999	0.999
$R_{M_{OWE}\leq 146000}$	0.827	0.945	0.950	0.983	0.990	0.999
$R_{b\leq 64}$	0.925	0.923	0.973	0.970	0.991	1.000
Design Parameters						
μ_{BPR}	9.13	9.59	9.59	9.59	9.59	9.59
$\mu_{l_{Fus}}$	5.69	5.69	5.69	5.69	5.69	5.68
$\mu_{L_{Wing}}$	28	28	27.99	28	28	27.69
$\mu_{c_{Root}}$	13.70	13.70	13.70	13.70	13.70	13.70
$\mu_{L_{Fus}}$	65.31	62.09	62.04	62.04	62.04	62.04
$\mu_{h_{Fus}}$	6.42	6.42	6.30	6.30	6.30	6.30
$\mu_{T_{SLS}}$	387000	387000	386849	387000	387000	386924
μ_{MC}	1	1	1.05	1.05	1.05	1.05
$\mu_{V_{FuelBlock}}$	103	108.15	108.15	108.15	108.15	108.15
$\mu_{\Lambda_{Sweep}}$	0.56	0.56	0.56	0.56	0.56	0.56
$\mu_{A_{Htp}}$	85	85	83	83	83	83
$\sigma_{L_{Wing}}$	4%	4%	3.50%	3.12%	2.59%	1.45%
$\sigma_{T_{SLS}}$	4%	4%	4%	4%	3.89%	2.13%
σ_{MC}	4%	4%	4%	4%	3.99%	2.79%
$\sigma_{V_{FuelBlock}}$	4%	4%	4%	4%	4%	3.99%
$\sigma_{\Lambda_{Sweep}}$	4%	4%	4%	3.97%	3.98%	3.98%
$\sigma_{A_{Htp}}$	4%	4%	3%	3%	3%	3%
$\sigma_{l_{Fus}}$	4%	4%	3%	3%	3%	3%
$\sigma_{c_{Root}}$	4%	4%	3%	3%	3%	3%
$\sigma_{L_{Fus}}$	4%	4%	3%	3%	3%	3%

C Declaration on oath and privacy statement

I will not pass on any information, documents and findings that are considered confidential to third parties after my work at the chair.

I also agree that my Master's thesis may be made available by the Institute of Astronautics on request to interested persons and that the Institute of Astronautics may make unrestricted use of the results contained therein as well as of the developments and programs resulting from them.

I also declare that I have produced this work without any external help and that I have only used the sources and aids listed in the bibliography.

Garching, January 24, 2020

Signature